Title
Genome-Free Viral Capsids for Targeted Drug Delivery to Breast Cancer

Author
Wu, Wesley

Publication Date
2012

Peer reviewed|Thesis/dissertation

Genome-Free Viral Capsids for Targeted Drug Delivery to Breast Cancer

By

Wesley Wu

A dissertation submitted in partial satisfaction of the

requirements for the degree of

Doctor of Philosophy

in

Chemistry

in the

Graduate Division

of the

University of California, Berkeley

Committee in charge:

Professor Matthew B. Francis, Chair
Professor Michelle C. Chang
Professor Britt A. Glaunsinger

Fall 2012

Genome-Free Viral Capsids for Targeted
Drug Delivery to Breast Cancer

by Wesley Wu

Abstract

Genome-Free Viral Capsids for Targeted Drug Delivery to Breast Cancer

by

Wesley Wu

Doctor of Philosophy in Chemistry

University of California, Berkeley

Professor Matthew B. Francis, Chair

A targeted drug delivery vehicle based on the bacteriophage MS2 viral capsid was constructed using site-selective bioconjugation reactions. A palladium-catalyzed tyrosine allylation reaction was evaluated for interior modification of intact MS2 capsids with water-insoluble drug molecules. Ultimately, a tri-functional linker was synthesized and used to attach multiple copies of the chemotherapeutic agent taxol to the interior surface of an MS2 mutant containing a uniquely modifiable cysteine. This virus-based vehicle was able to deliver and release taxol to breast cancer cells *in vitro* and effect cytotoxicity at comparable levels to that of the drug alone. We next utilized a sodium periodate mediated oxidative coupling reaction to attach multiple types of targeting groups to the exterior of the MS2 capsids. Targeting groups we evaluated include short peptides, DNA aptamers, and engineered proteins. The most effective of these targeting groups proved to be a class of engineered binding proteins called designed ankyrin repeat proteins (DARPins). MS2 capsids modified with αHER2 DARPins were found to preferentially bind *in vitro* to several breast cancer cell lines overexpressing HER2.

To my parents: For always believing in me, for your unconditional and unbounded love and support, and for always allowing me to find my way.

To my "family" here at Berkeley: For living life together, for opening your lives, and for bearing with me through thick and thin; we are in eternal partnership.

Table of Contents

Acknowledgements

Looking back at the years here in Berkeley, there are innumerable people who have entered my life here in grad school and have helped bring me through this time. Without these people, this work, this degree would not have been possible. Support has come in all forms, academic and professional, to personal and emotional, to just the simple daily presence of many of these people. It is a testament to the fact that none of us is ever truly alone and independent in this world.

I would first like to thank the educators who taught me about chemistry and science, but more importantly shared their passion for seeking truth in this way. First to my high school chemistry and biology teachers, Mr. Lorah and Mrs. Herbes – these two managed to make science both fun and challenging while driving us students to excel. To Prof. D. Tyler McQuade, my second semester organic chemistry professor at Cornell who made organic chemistry exciting, who opened my eyes to the vast possibilities in this discipline. To Prof. Dave Collum for taking me on as an undergraduate researcher in his lab, and Dr. Mohsen Khalili, who took me on as a summer intern at DuPont – they both gave me these chances to experience research first-hand, even though nothing I did really worked that well. These experiences did, however, show me the excitement possible in research and made me hope for the chance that something would someday work.

Moving on to Berkeley and the Francis Group, I would like to highlight the support and guidance that I have received from my advisor, Matt Francis. Matt, thank you for taking me into the group that first year even after Dirk had told me you were full (3 students! Ha!). Thank you for giving me the chance to work on the MS2 project and letting me take it where it has ended up. Most of all, thank you for your never-ending optimism and encouragement. Thank you for teaching me to have confidence in my work and giving me the courage to take pride in it, and share that with others. Thank you for always gently pushing me to do the things that I needed to get done. You taught me not just how to do experiments, but helped me mature into a more complete scientist and person.

Next are all the members of the Francis Group I have overlapped with. The first class is Jacob, Tilley, Tara, Andrew, Ravi, Amanda, and Josh. Jacob is probably the hardest working guy I have ever met and I was lucky enough to learn so many things from him during my first year in the group, from running a column, to culturing MS2, to fixing the LCMS. Jacob was the first guy to try and put taxol in MS2 and really got our group's work with MS2 to a point where those of us following him could start throwing stuff on and see what would happen. Tilley was the guy I could always go to for synthetic advice as well as with questions about getting his reaction to work on MS2. Josh always had a kind word for me after every discouraging, lousy presentation I gave my first year in grad school. Andrew helped me quite a bit with dyes and proteins and just being one of the more fun, friendly presences in the lab. The next class had Jesse, Pat, and Dante. Jesse and I shared the Cornell connection and helped me quite a bit with a variety of synthetic challenges. Pat and I had quite a few long days through the years dealing with the LCMS and the group computers, and he was the first one to teach me about HPLC and columns etc. His talks were always able to get me excited again about photovoltaics. Dante also gave me quite a bit of help with synthesis and the oxidative coupling reaction and was from New Jersey.

Next up are Aaron, Rebekah, and Rebecca. Aaron and I shared the 4th floor outpost my first year here (along with Jacob), and he was always the one I could go to for help if Jacob was being moody. Aaron taught me how to run my first gel, explained oxime formation to me, and really got me to think about my project with his questions, among many many other things. He was also my GSI for chem271, so I could always go to him for help with homework too. Aaron always had interesting ideas for our projects and always brought a lot of fun into things he did. After the outpost, we were together in 743 for a few years, where you were finally free to play your preferred music (no more of Jacob's Emerson Drive), I'll always remember walking in on you "dancing to your thesis" one of those nights. Rebekah was the first person who I heard give group meeting in the Francis group, and I still remember being thoroughly confused why everything with TMV was in ratios of 17:1. Her work is also what got me thinking quite a bit about dyes quenching in our viruses, and I'll always remember her running reactions in her bench drawer. Rebecca was my bench/desk neighbor in 743 for a year and we managed to share our sink without much issue. Rebecca thought of and helped me a lot with most of the antibody experiments and also was my much-needed color consultant for my GRS figures. Sean and Nick were next. Sean was always just chill and calming with his Texas drawl. Nick seemed kind of outrageous at times, but deep down is a very serious scientist and we had a lot of things shared in dealing with MS2 and water-insoluble things.

Now comes my class, Zac, Gary, Sonny, Kanna, and Michel. For whatever reason, Matt tried to have "first-years" night with us that year at Triple Rock. Anyway, I owe Zac a lot for his MS2 mutants that solved quite a few of my problems and I could always go to him for help with molecular biology and reagents. Gary's project was the closest to mine in the group, so we shared quite a bit of complaining about MS2 expression, purification, and modification and actually being able to target anything, from in a dish to in an animal. Sonny was the happiest member of our lab, just always happy, and his ideas with the possibilities of bioconjugation and cell patterning were amazing and came from reading stacks and stacks of books that were always on his desk. He also helped me quite a bit with using Bertozzi group resources and teaching me how to keep cells alive. Kanna, I was always impressed with his ability to find the perfect words to express his point. Michel was the lab fixer, always taking things apart and putting them back together, building useful things, as well as always wearing interesting shirts from Goodwill – I'm not quite sure when he did his actual work. He also helped me quite a bit with dealing with proteins and dyes and random molecular biology questions.

Leah and Chris were the next two to join the group. Leah replaced Rebecca on the PLP project and also as my bench/desk neighbor. Leah was always hard at work with her libraries but always able to also handle all of the other random things that Matt wanted done in the group. She taught me quite a bit about PLP modification of proteins, peptide synthesis, and helping me make my presentations look better. More than that, she was always an encouraging presence, with random snacks and emails and just her words. Chris was the most appropriate person to continue on the imaging projects from Jacob and Dante, and I was always impressed with his hard work and perseverance in dealing with all the issues in such a long-term and involved project.

The next class was another huge one, with Troy, Kristen, Allie, Amy, Mike, and Dan. Kristen was the next member to join 743 and we had our share of music wars that I was mostly oblivious

to. Her project always seemed to involve gigantic columns and there was that sodium reaction that caused quite some excitement. We shared the Cornell connection, having horrifically messy benches, as well as both having really bad allergies. Allie was the next to join 743, and she is really one of the most impressive scientists I have met. We talked quite a bit about our MS2 projects over the years and was always willing to discuss just about anything, always asking about how life was going, always taking on responsibility for things and really making our lab a better place to work. Amy's work for her project has always been impressive, just the lengths taken to make things work with all the different cells, and it is always awesome to hear about her project. Dan and Mike were fellow softball players, Dan was always digging my throws from third base out of the dirt, and Mike captaining our team the last few years. Troy, we kind of lost track of you once you moved downstairs, but you're always good for an acerbic joke or two.

As for the younger ones, there seem to be very many of you that I haven't been able to get to know too well. Stacy and I shared a love for cute animal pictures which regularly provided entertainment in the midst of grad school. Kareem, it's great to see your hard work finally paying off and the project starting to take off. Jeff and I shared usage of the biosep column for most of the past few years and I'm always amazed that you managed to get MS2 reassembled. Jelly and I were the most concerned with actual therapeutics in the group, and we were the two always trying to kill cells, though not always successfully. Katherine thanks for all the baked goods you brought in. Abby, your sheer enthusiasm and loudness is something that will always be welcome in a group. Jake – good luck with the LCMS! Jim, take care of the hood and bench, and go Giants, Knicks, and Yankees. Kanwal, Ioana, and Richard, best of luck in the group!

The number of postdocs in our group suddenly jumped this year, probably for the betterment of the group. Praveena was from a different group era though, and was the only one for quite a while. Praveena and I shared quite a bit of grief over expressing pAF19 MS2 and she was always someone I could discuss confusing research things with. I'm glad that things really took off at the end. Michelle, I'm amazed that someone actually came into the group and got the cell culture room going, AND animal imaging to happen. We could always talk about NJ and whatever NY sports team was playing at the time. Some school will be getting a great scientist as well. Adel and Henrik, I've been mostly out of the lab since you've joined the group, but I can tell you guys know your chemistry and will bring some much needed expertise to our group.

As for the non-grad students, I had to pleasure to work with only one undergraduate student in my time in graduate school, but she was a good one. Even though she was a pre-med, Kathy Wai was extremely dedicated to our work despite her ridiculously busy schedule. I'm glad that we could work together for a few years – thanks for making lots of MS2, DARPins, taxol linker, etc, which really helped to make my life easier. Seeing you juggle the many obligations in your program makes me sure you will make a great doctor. Cezar, Chona, Adele thanks for taking care of a lot of things for me and the group. I seemed to regularly have some kind of paperwork missing or late, and you guys were really patient and accommodating in solving whatever issues arose.

I also want to thank the many people outside of chemistry that have made life as a grad student in Berkeley such a wonderful time. Most importantly are the members of ISM/IGSM, the campus grad student fellowship I was a part of my entire time in Berkeley. There are too many names to name, but your presence in my life has made grad school beyond just tolerable, but a time in my

life that I will look back with great fondness. To my mentors and the older ones, especially Chul and Sharon, Jisup, Karen and Shufei, thank you for just taking care of me these years, for spurring me on, for teaching me, and really helping me to grow. We have been able to experience so much together, many good times and a bit of the tougher times of life together, and I am thankful for your faithfulness and dedication to me. To the many guys that I lived together with, whether it be at the Dwight apartments, Cedar House, or MLK, I never would have thought of packing in as many guys as we did in these places, but you guys are what make each day livable even if things aren't working out in school or life, and remind me every day of what really matters in life. Thanks especially to Caleb, Travis, Kevin, Josiah, and Howard. I'm thankful we could go through grad school together. We had a lot of late nights, long days, working on all sorts of things or sometimes just doing not much. These are times I will treasure forever. To the newer guys, I look forward to sharing life with you all in the coming years.

Lastly, I would like to thank the people who have been with me the longest, my family. First are Aunt Janice and Uncle James, you were always my "California" relatives, and thank you for always opening your home to me over breaks though I think I only ever got to go down one time. Thanks for coming to my graduation and keeping me in the loop with all things family. Next are Aunt Gloria and Uncle Gary, and my cousin Chris. You always stopped by to visit when you were in the area, always treating me to meals and just making sure we were doing ok.

Dad and Cindy, thank you for welcoming me back to Jersey all the time and just making my breaks relaxing and stress-free, and times of refreshing from school. Dad, in my whole life, you were always around for me, every soccer and baseball game, every concert, every evening just to shoot around or relax. You never missed anything, and I see now how rare that is in this day and age. You always pushed me to excel, but I always knew that right under that, the reality was that you just wanted me to be happy. Cindy, I think you are a gift from heaven to our family, and I'm still amazed how you came into our lives the end of my first year in grad school. I'm thankful that even though we haven't lived together for longer than 2 weeks at a time, we have been able to get to know each other rather well these past few years. Thank you for making our home such a warm and welcome place the past few years, for taking care of us every day. Lastly, Mom, you followed me out to Berkeley and it was always an encouragement to be able to just drop by your place for a home-cooked meal and to hear what was on your mind. I'm glad that we have been able to live close by these past few years. Thanks for always looking out for me and wanting the best for me. Your idealism about life, your pursuit of the truth in this world, and your determination to do what is right and loving even if it comes at personal cost is an inspiration to me every day. I love you all and am so blessed to have you in my life.

Reflecting back on the years in grad school, it has been a challenging time, with a lot of work and struggle, as well as success and joy. But it has been a time really made perfect by the people in my life, and I am eternally grateful for your presence in my life - I would have it no other way.

"5 LORD, you have assigned me my portion and my cup;
you have made my lot secure.
6 The boundary lines have fallen for me in pleasant places;
surely I have a delightful inheritance."

Psalm 16:5-6 (NIV84)

Chapter 1: Toward targeted cancer treatment using macromolecules

1.1 Modern methods for cancer chemotherapy.

The past half-century has seen great advances in the treatments for cancer, leading to overall increased life expectancies. For several categories of tumors, modern treatments have led to high expected remission rates for what had been generally thought of as incurable diseases.[1] Up to 20 years ago, most chemotherapy treatments were through small molecule natural products, such as methotrexate, vinca alkaloids, taxanes, anthracyclines, and Pt-based chemotherapeutics[2] (Figure 1-1). These drugs, still in use today, are effective in their ability to kill cancerous cells, and most often effect cell death through non-specific targeting of rapidly dividing cells. Since cancer cells are typically characterized by their rapid proliferation, they are preferentially affected by these types of drugs.

The past 20 years has seen the dawn of the age of targeted therapies that take advantage of modern understanding of cellular and molecular biology and genetics.[3] These therapies seek to target certain receptors, enzymes, or constituent proteins that are present in higher abundance in cancer cells, and also which may be involved in a disregulated process that may be associated with carcinogenesis. Prime examples include imatinib[4] and trastuzumab[5] (Figure 1-2a). Imatinib is the first approved example of a rationally designed targeted therapy that works by inhibiting a specific receptor tyrosine kinase, *Bcr-Abl*, found in higher abundance in certain cancer cells and is currently used in the treatment of chronic myelogenous leukemia. Trastuzumab is the first example of a humanized monocolonal antibody approved by the FDA for the treatment of cancer. Its target is HER2, an orphan receptor that is found overexpressed in ~30% of breast cancers.

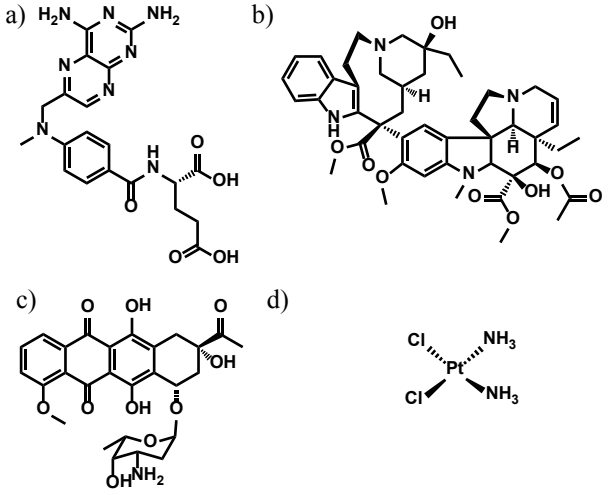

Figure 1-1. Representative chemotherapeutic agents. a) Methotrexate b) Vinblastine c) Daunorubicin d) cis-platin

In parallel with these advances in targeted cancer treatment has been the advent of drug carrier systems for the targeted delivery of cancer drugs to tumor tissues.[6] These strategies seek to bring known chemotherapeutics primarily to the tissues of interest in order to reduce adverse side effects on healthy cells. In contrast to the therapies listed above, delivery systems usually seek

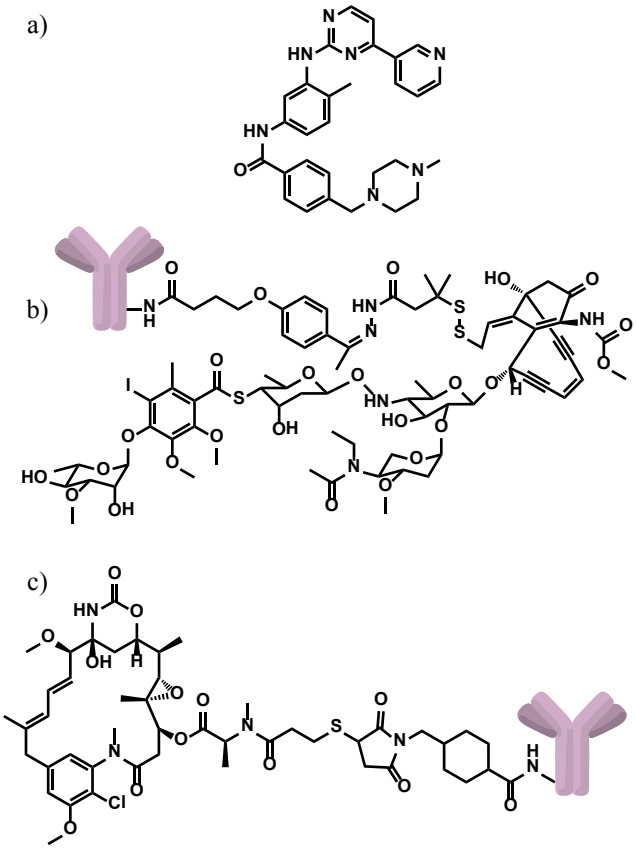

Figure 1-2. Representative modern chemotherapeutics. a) Imatinib (Gleevec) b) Gemtuzumab Ozogamicin (Mylotarg) c) Trastuzumab emtansine (Herceptin-DM1)

to decouple the targeting aspects and the cytotoxic effects of the treatment, as evidenced by the common usage of already approved small molecule drugs in tandem with novel targeting modalities. The current state of the art in targeted delivery are antibody-drug-conjugates (ADC's), which attach a small molecule drug to a targeting monoclonal antibody. Though the first example of these systems approved for human treatment ultimately failed in the clinic (Mylotarg –a calicheamycin/αCD33mAb conjugate),[7] several alternative systems are currently undergoing the FDA approval process, most prominently Herceptin-DM1 (Figure 1-2 b-c).[8]

1.2 Macromolecules for chemotherapeutic delivery.

Drugs used in chemotherapy predominantly act by targeting the mechanisms of cell division, and to an extent, preferentially affect cancer cells because of their unusually high proliferation rates. Unfortunately, many healthy cells are also affected by these treatments, resulting in side effects that cause substantial discomfort for the patient. Emerging methods seek to focus the delivery of drugs on cancer tissue by targeting specific characteristics found in solid tumors.[9] As a promising subset of these approaches, macromolecular drug delivery seeks to attach many small molecule drugs and targeting groups to large structures.[10] Many of these delivery vehicles experience prolonged circulation time because of their increased size,[11] as well as a degree of passive targeting through the enhanced permeation and retention effect, arising from unique characteristics of tumor vasculature.[12] As an additional benefit, macromolecules are large enough to display mul-

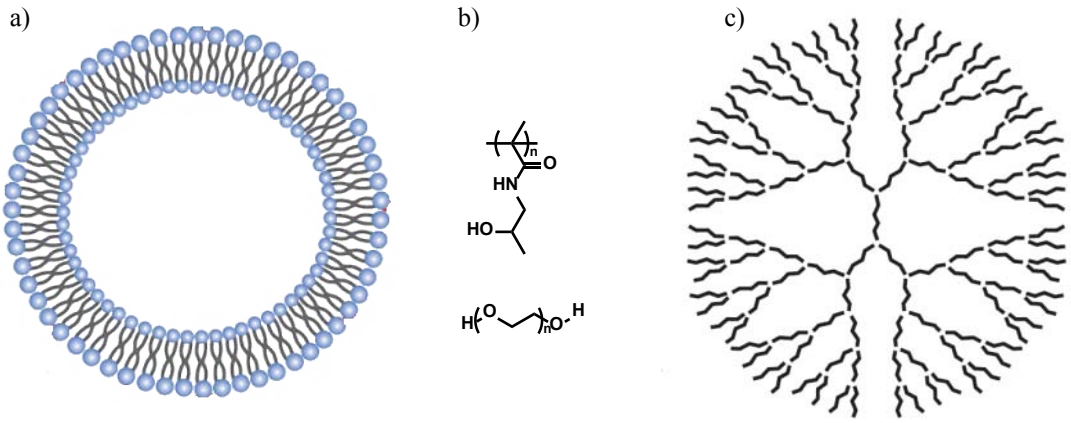

Figure 1-3. Representative macromolecular drug delivery scaffolds. Shown are (a) a liposome, (b) polymers such as *N*-(2-Hydroxypropyl)methacrylamide (HMPA) and Polyethylene glycol (PEG), and (c) a dendrimer

tiple copies of active targeting ligands to enhance binding avidity,[13] and can also provide multiple cargo attachment sites to increase the amount of payload that can be delivered.

Benefits of macromolecular based delivery include larger cargo loadings, enhanced pharmacokinetic and solubility profiles, passive targeting through the EPR effect, and the potential to take advantage of avidity affects by the attachment of multiple copies of active targeting moieties to the system. Many macromolecules are currently in use or being studied for use as drug carriers (Figure 1-3). Polymer therapeutics are based on a wide variety of materials, such as polyethylene glycol (PEG)[14] or hydroxypropyl methacrylate,[15] allowing carriers with a wide range of delivery behaviors to be designed. Dendritic polymers also offer these properties, with the added advantage of controlled polydispersity and globular shape.[16] Liposomal[17] and micellular[18] systems feature high cargo loadings, but can be difficult to store and can suffer from irregular release and distribution profiles. Inorganic nanoparticles[19] and carbon nanotubes[20] both feature unique properties as delivery vehicles, but must undergo thorough testing to evaluate their biocompatibility. Protein based systems, such as the recent usage of serum albumin,[21] are inherently biocompatible, but most current systems do not exhibit any form of active targeting. As a notable exception, thermophilic heat shock protein cages have been modified to house up to 24 doxorubicin molecules and display targeting peptide inserts on their exterior surface.[22]

1.3 MS2 as a drug delivery vehicle.

Our choice of viral capsid, the protein coat of bacteriophage MS2, exemplifies many of the advantageous characteristics provided by viral protein assemblies as drug delivery vehicles. MS2 is an *E. coli* infecting bacteriophage that possesses icosahedral symmetry with a crystal structure available at 2.8 Å resolution (Figure 1-4).[23] Structurally, it is a T=3 icosahedron that is composed of 180 identical coat protein monomers that self-assemble to form a hollow, spherical capsid.[24] The intact capsid is 27 nm wide, and has 32 pores, each 2 nm in diameter, located at the symmetry axes. These holes in the exterior allow access to the interior surface of the structure for cargo attachment. Monomers of MS2 are composed of a beta-hairpin, five anti-parallel beta sheets, two alpha helices, and four more amino acids at the C-terminus, with a total mass of 13.7

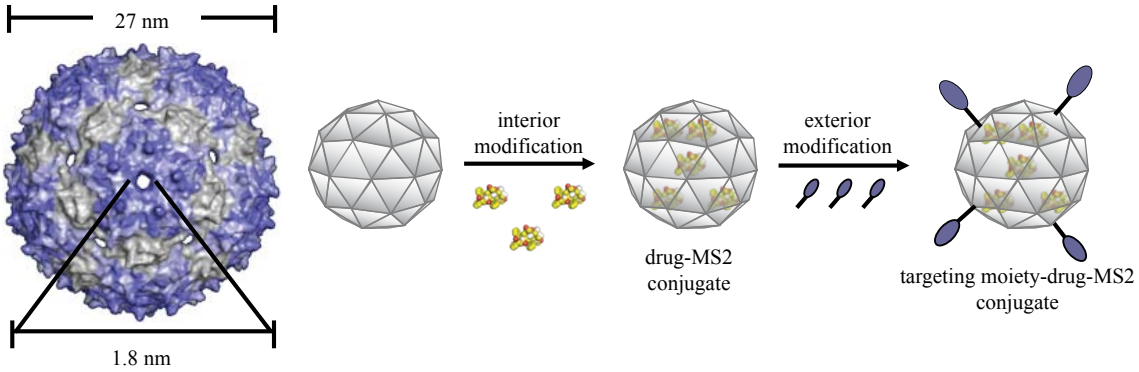

Figure 1-4. A representation of the MS2 capsid constructed from the monomer crystal structure, showing capsid dimensions and pore location. Empty capsids can be first modified on the interior surface to load the desired cargo, followed by exterior modification to introduce targeting groups.

kDa. Of the four tyrosine residues, the only solvent exposed residue is located on the "interior" surface. These MS2 monomers self-assemble into capsid structures upon recombinant expression in *E. coli*[25] or upon viral infection and propagation in *E. coli*.[26] The capsid structure is stable to a variety of physiologically relevant conditions, including a pH range of 3-11 and temperature up to ~50 °C. The hollow capsids provide a stable, entirely proteinacious, monodisperse, and biologically compatible nanoparticle scaffold to develop as a biomedical delivery vehicle.

Several other viral capsid scaffolds have been elaborated as novel materials. Most notable are work done on the cowpea mosaic virus (CPMV) by the Finn group,[27] as well as work with cowpea chlorotic mottle virus (CCMV) by the Douglas and Young groups.[28] Both these viruses are spherical and about the same diameter as MS2. Through both covalent and non-covalent modification, a variety of molecules have been attached to these viral capsids, using chemistry such as lysine acylation and subsequent copper catalyzed click chemistry.[29] In 2008, the Finn group was able to incorporate alkyne-containing unnatural amino acids into virus Qβ using bioorthogonal non canonical amino acid tagging (BONCAT) for site-specific modification.[30] Most recently, the red clover necrotic mottle virus (RCNMV) has been dual modified by non-covalent sequestration of doxorubicin and covalent lysine modification with targeting peptides.[31] One feature of MS2 that sets it apart from the alternative structures are the pores that allow facile interior modification, without pH dependent swelling of the capsid (as with CCMV), or complete capsid disassembly and reassembly. Notably, Qβ does contain pores similar to MS2, but inter-monomer disulfide bonds limit the options for chemical modification with cysteine-targeting reactions. Lastly, examples of dual-surface, site-specific modifications are few, including one example from our own group featuring the loading of MS2 particles with porphyrins on the interior and targeting aptamers to the exterior surface.[32] For a thorough overview of virus-based drug delivery, see the recent referenced review.[33]

1.4 Taxol as a drug of choice.

We chose taxol as our initial chemotherapeutic for several reasons. Taxol is a commonly used chemotherapy drug for the treatment of breast cancer (Figure 1-5). It was discovered in 1971 by Wani and Wall[34] from the bark of the Western Yew and has been the subject of various total syn-

thetic efforts.[35] It effects cell death via binding to polymerized microtubules and inhibiting depolymerization, a process that is important in cell division.[36] Therefore, rapidly dividing cells such as those found in cancerous tumors are particularly affected by this molecule. However, other rapidly dividing cells in the body are also affected by taxol treatment, such as immune cells and hair cells, leading to many of the side effects traditionally associated with cancer chemotherapy.

In addition taxol suffers from fairly low water solubility which limits the aggressiveness with which patients can be treated since it is difficult to administer high dosages of the drug. To increase water solubility of the drug, taxol is coadministered with Cremephor EL, a detergent that presents its own toxicity profile to the treatment as well as presenting practical problems because the detergent can leach chemicals out of traditionally used plastic tubing.[37] Because of the low overall solubility, even in the presence of detergent, the infusion of drug and detergent requires over 2 hours, adding to the burden of cancer treatment. Therefore, many efforts have been made to increase the solubility of taxol, through various prodrug and delivery strategies.[38]

Taxol presents an interesting chemical challenge because of this solubility profile. Like most proteins, the intact MS2 capsid is only soluble in aqueous solutions (up to 10% organic cosolvent).[39] In order to attach such an insoluble molecule to the intact capsid, we require a method to solubilize taxol while also imparting bioconjugation functionality to the molecule. Many strategies can be found in the literature of attempts to increase the solubility of taxol for use in the clinic while retaining its cytotoxicity effects. Most of these techniques target the 2'-OH group of taxol and use a charged functionality to increase water solubility.[25] The challenge for MS2 incorporation is not only to add water solubility, but also to impart bioconjugation functionality into the molecule.

Lastly, taxol is one of the larger molecules that we have attempted to attach to the interior of the capsid. Because access to the interior of the capsid is mediated by the 32 small pores, the large taxol molecule (853 g/mol) presents an interesting challenge to the limits of "small" molecules that can diffuse to access the interior surface. Using MS2 capsids as a drug delivery system requires both being able to load the drug molecule onto the interior of the capsid, as well as being able to release the drug from the capsid surface, and out of the interior.

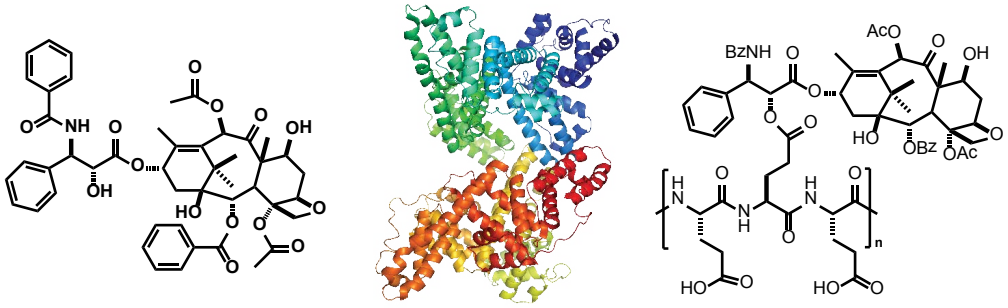

Figure 1-5. Taxol, human serum albumin, and paclitaxel polyglumex.

In the literature, delivery of taxol to cancer by protein-based systems is limited to a few cases. Abraxane is a formulation of taxol where the drug molecule is bound non-covalently to human serum albumin forming clusters of ~130 nm nanoparticles.[40] Paclitaxel Poliglumex (Opaxio,

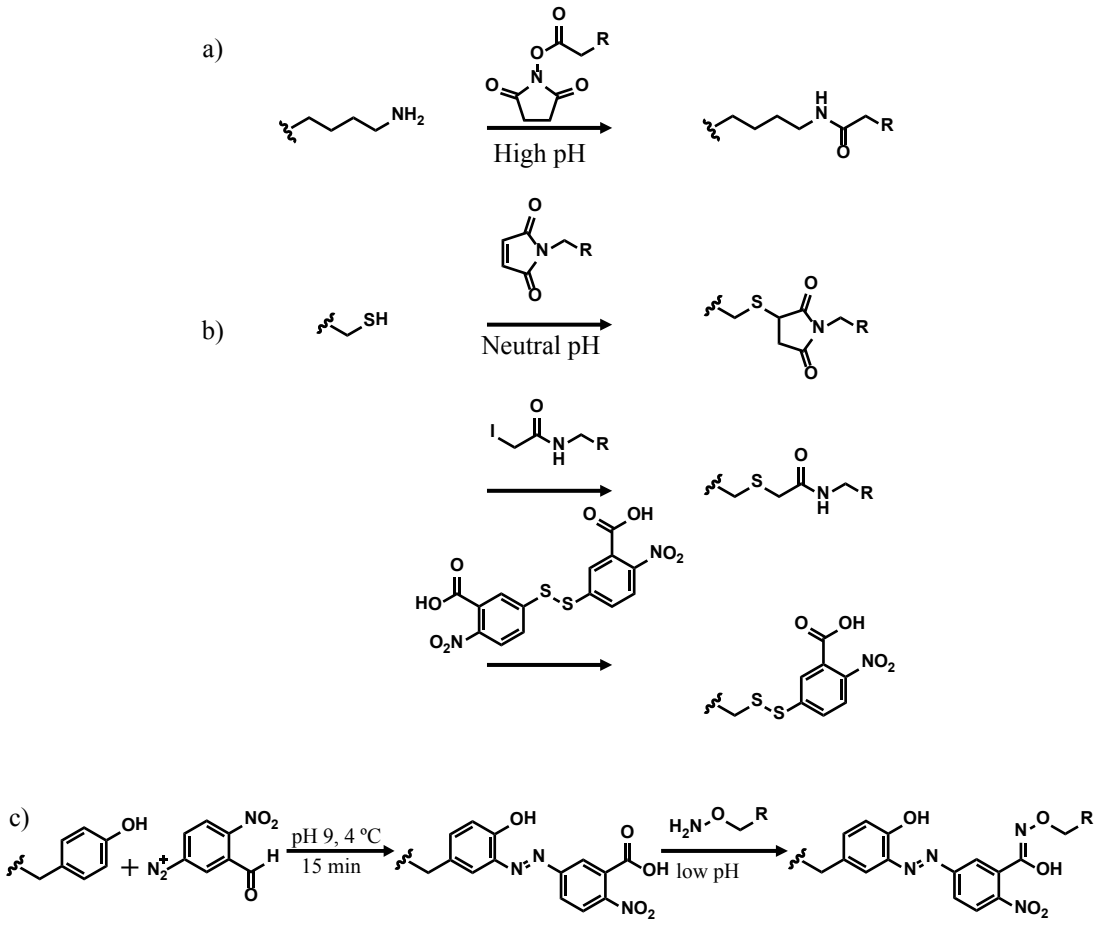

Figure 1-6. Bioconjugation strategies for MS2 modification. a) Lysine residues can be modified with NHS-ester reagents. b) Cysteine residues can be modified via alkylation with maleimides or iodoacetamides, and by disulfide exchange with disulfide reagents. c) A diazonium reaction for tyrosine modification developed in the Francis group. Aldehyde functionalized diazonium salts can be subsequently derivatized through oxime formation with various aminooxy functionalized cargoes.

formerly Xyotax) is a polymeric delivery system composed of taxol attached to a small polyglutamate polymer (Figure 1-5).[41] Both these systems greatly increase the water solubility of the drug, eliminating the need for a toxic detergent. They are also both biodegradable and non-toxic and feature prolonged half-life and drug release profiles. However neither of these systems features any form of active targeting.

1.5 Bioconjugation strategies for MS2 modification.

The intact capsid of MS2 has been addressed by several groups for bioconjugation purposes.[42] Most attempts at MS2 and other capsid derivitization have focused on traditional NHS-ester chemistry to modify the abundance of lysine residues found on the capsid surface. In the Francis group, we have used lysine chemistry as well for non-specific modification of the capsid exterior. Because of the desire to form well-defined interior/exterior dual-modified capsids however, lysine chemistry is restricted to use with very large molecules (PEG) that are not able to access the interior surface of the capsid. The traditional putative targets on the exterior of the MS2 capsid are K106 and K113, though K43, K57, K61, K66 are all surface accessible and see small levels

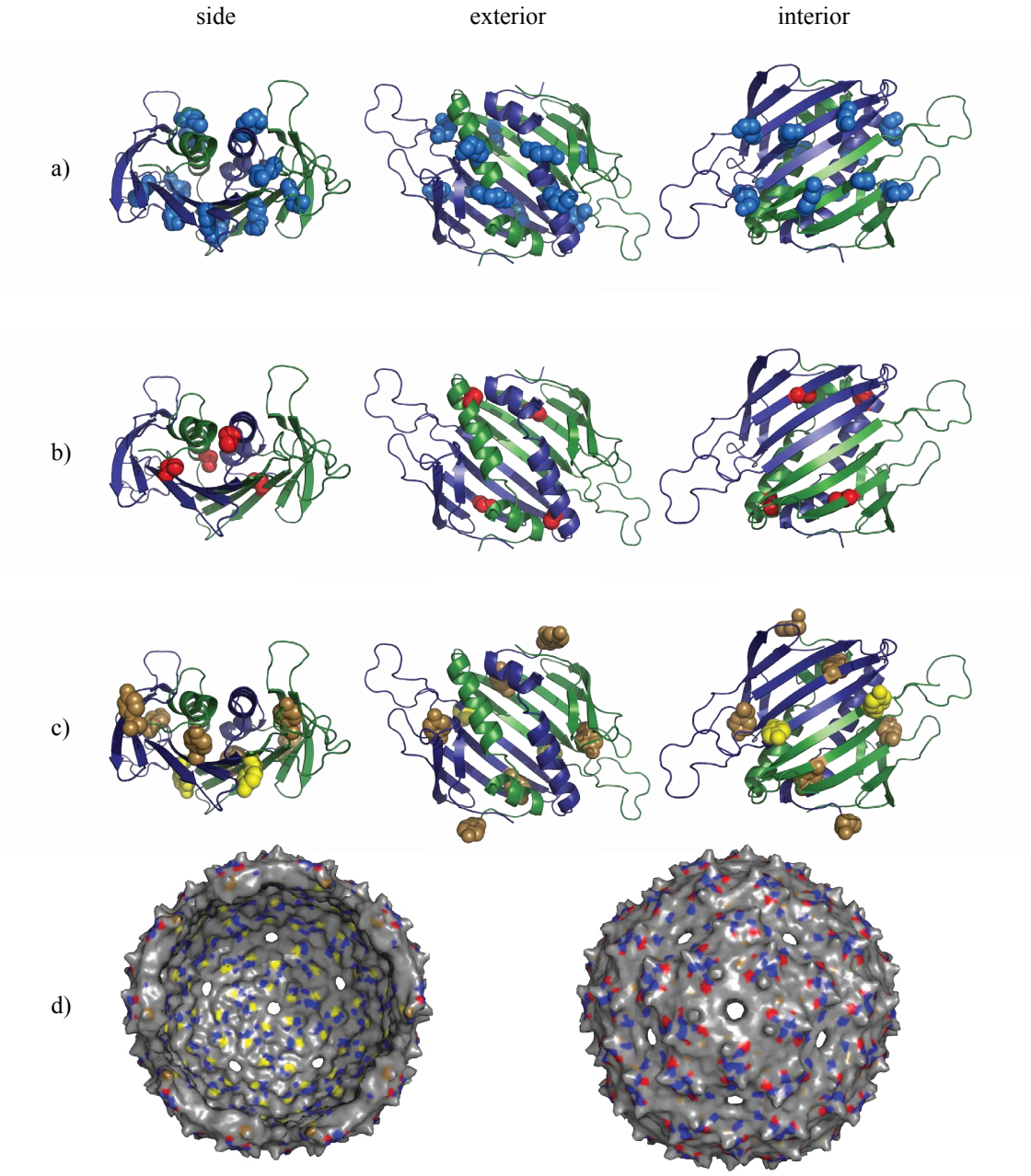

Figure 1-7. Structural representation of the MS2 coat protein, highlighting several amino acids amenable to chemical modification (PDB ID: 2MS2). Rows a-c show MS2 dimers from side, exterior, and interior perspectives, with the green and blue colors denoting MS2 monomers. In the side perspective, the top of the dimer is the exterior surface of the capsid while the bottom of the dimer is the interior surface of the capsid. a) Lysine residues on MS2 depicted in lighter blue (K43, K57, K61, K66, K106, K113). b) Cysteine residues depicted in red (C46, C101). c) Tyrosine residues shown in dark yellow (Y42, Y58, Y129), with Y85 highlighted in light yellow. d) Assembled half capsids are shown from the interior and exterior view, with the above amino acids colored as denoted previously.

of modification upon exposure to NHS-esters (Figure 1-7a).[43] The interior lysines of MS2 can also be modified by small molecule NHS esters that can access the interior surface (Figure 1-6a).

In order to increase specificity, former group members have attempted to utilize traditional cysteine chemistry to modify the capsid surface. MS2 has two exposed cysteines on the exterior surface C46 and C101 (Figure 1-7b), and previous work in the group has shown that these cysteines can be modified by small molecule maleimides, iodoacetamides, and disulfides that weigh less than 200 g/mol (Figure 1-6b)[44]. Attempts have been made to utilize this cysteine chemistry together with subsequent secondary bioconjugation reactions on the functionalities that have been added to the capsid exterior via cysteine modification.

Interior modification of the native capsid in the Francis group initially focused on the modification of Y85 using a diazonium coupling reaction. Low molecular weight diazo compounds containing highly electron withdrawing groups *para* to the diazo functionality are able to modify Y85 selectively to over 95% conversion despite the presence of three other tyrosine residues (Y42, Y58, Y129, Figure 1-7c).[45] Using a ketone- or aldehyde- functionalized diazo compound for the tyrosine modification allows for subsequent secondary bioconjugation via oxime formation (Figure 1-6c).[46] Using this technique, our group has been able to attach a variety of cargo molecules to the interior of the capsids, including various fluorescent dyes[47] and metal cages for MRI contrast applications.[48]

The two-step conjugation on the interior proceeds selectively at the single tyrosine at position 85 and provides moderate yields of modified capsid. However, the two-step process is fairly time consuming, involving two protein modification and purification steps as well as a lengthy oxime formation step. Another concern is the fact that aminooxy-functionalized molecules are still less commonly commercially available and more expensive than more traditional cysteine modification reagents. In addition, the diazonium reaction is relatively functional group intolerant, precluding the development of a one-step reaction, especially in the presence of functionally complex drug molecules. Therefore, we sought to target the interior tyrosine of MS2 using an alternative tyrosine modification reaction developed in the Francis group: work that will be detailed in Chapter 2.

To circumvent these issues, two efforts were undertaken by Zac Carrico, a fellow graduate student in the group. First was to create an interior cysteine mutant of MS2 in order to facilitate interior modification of the capsid using maleimide reagents.[49] Using the N87C mutant of the MS2 coat protein, maleimide reagents can be easily acquired and utilized for interior modification. Since most desired cargo is also larger than those that would modify the exterior cysteines, this maleimide coupling is almost always selective for the interior surface of the capsid. The other aspect of Zac's work was to develop an alternative strategy for exterior modification of the capsid. The culmination of his efforts was the development of a mutant of the MS2 coat protein containing an artificial amino acid, *para*-aminophenylalanine, on the exterior surface.[50] This pAF functionality can be reacted with phenylene diamines,[50] anisidines,[51] and aminophenols[52] in the presence of sodium periodate selectively and quickly to modify the exterior of the MS2 capsid. The N87C mutant will be utilized in Chapters 3 in the construction of taxol modified capsids, and in Chapters 4 and 5, T19pAF N87C dual mutants will be used for the construction of interior/exterior dual-modified MS2 capsids.

1.6 References.

1. Devita, V.T., Jr., Chu, E. A history of cancer chemotherapy. *Cancer Res.* **2008**, *68*, 8643-8653.
2. Chabner, B.A., Roberts, T.G. Timeline: Chemotherapy and the war on cancer. *Nat. Rev. Cancer* **2005**, *5*, 65-72.
3. Allen, T.M. Ligand-targeted therapeutics in anticancer therapy. *Nat. Rev. Cancer* **2002**, *2*, 750-763.
4. Deininger, M., Buchdunger, E., Druker, B.J. The development of imatinib as a therapeutic agent for chronic myeloid leukemia. *Blood* **2005**, *105*, 2640-2653.
5. Hudis, C.A. Trastuzumab – Mechanism of action and use in clinical practice. *New Engl. J. Med*. **2007**, *357*, 39-51.
6. Hughes, B. Antibody-drug conjugates for cancer: poised to deliver? *Nat. Rev. Drug Discovery* **2010**, *8,* 665-667.
7. Hamann, P.R., et al. Gemtuzumab Ozogamicin, a potent and selective anti-CD33 antibody-calicheamicin conjugate for treatment of acute myeloid leukemia. *Bioconjug. Chem.* **2002**, *13*, 47-58.
8. LoRusso, P.M., Weiss, D., Guardino, E., Girish, S., Sliwkowski, M.X. Trastuzumab Emtansine: A Unique Antibody-Drug Conjugate in Development for Human Epidermal Growth Factor Receptor 2–Positive Cancer. *Clin. Canc. Res.* **2011**, *17*, 6437-6447.
9. Kratz, F., Müller, I.A., Ryppa, C., Warnecke, A. Prodrug strategies in anticancer chemotherapy. *ChemMedChem* **2008**, *3*, 20-53.
10. a) Haag, R., Kratz, F. Polymer Therapeutics: Concepts and Applications. *Angew. Chem.* **2006**, *118*, 1218-1237; Haag, R., Kratz, F. *Angew. Chem., Int. Ed.* **2006**, *45*, 1198-1215; b) Peer, D., Karp, J.M., Hong, S., Farokhzad, O.C., Margalit, R., Langer, R. Nanocarriers as an emerging platform for cancer therapy. *Nat. Nanotechnol.* **2007**, *2*, 751-760.
11. a) Gabizon, A.A. Liposome circulation time and tumor targeting: implications for cancer chemotherapy. *Adv. Drug Delivery Rev.* **1995**, *16*, 285-294; b) Harris, J.M., Chess, R.B. Effect of pegylation on pharmaceuticals. *Nat. Rev. Drug Discovery* **2003**, *2*, 214-221.
12. Maeda, H., Wu, J., Sawa, T., Matsumura, Y., Hori, K. Tumor vascular permeability and the EPR effect in macromolecular therapeutics: a review. *J. Control. Release* **2000**, *65*, 271-284.
13. a) Hong, S., Leroueil, P.R., Majoros, I.J., Orr, B.G., Baker, J.R., Banaszak Holl, M.M. The Binding Avidity of A Nanoparticle-Based Multivalent Targeted Drug Delivery Platform. *Chem. Biol.* **2007**, *14*, 107-115; b) Joshi, A., Vance, D., Rai, P., Thiyagarajan, A., Kane, R.S. The design of polyvalent therapeutics. *Chem. Eur. J.* **2008**, *14*, 7738-7747.
14. a) Zalipsky, S., Gilon, C., Zilkha, A. Attachment of drugs to polyethylene glycols. *Eur. Polym. J.* **1983**, *19*, 1177-1183; b) Greenwald, R., Choe, Y.H, McGuire, J., Conover, C.D. Effective drug delivery by PEGylated drug conjugates. *Adv. Drug Delivery Rev.* **2003**, *55*, 217-250.
15. a) Duncan, R., Kopeckova-Rejmanova, P., Strohalm, J., Hume, I., Cable, H.C., Pohl, J., Lloyd, J.B., Kopecek, J. Anticancer agents coupled to N-(2-hydroxypropyl)methacrylamide

copolymers. I. Evaluation of daunomycin and puromycin conjugates in vitro. *Br. J. Cancer* **1987**, *55*, 165-174; b) Duncan, R., Seymour, L.W., Ulbrich, K., Kopecek, J. Soluble synthetic polymers for targeting and controlled release of anticancer agents, particularly anthracycline antibiotics. *J. Bioact. Compat. Pol.* **1988**, *3*, 4-15.

16. a) Ihre, H.R., Padilla De Jesús, O.L., Szoka, F.C., Fréchet, J.M.J. Polyester Dendritic Systems for Drug Delivery Applications: Design, Synthesis, and Characterization. *Bioconjug. Chem.* **2002**, *13*, 443-452; b) Padilla De Jesús, O.L., Ihre, H.R., Gagne, L., Fréchet, J.M.J, Szoka, F.C. Polyester Dendritic Systems for Drug Delivery Applications: In Vitro and In Vivo Evaluation. *Bioconjug. Chem.* **2002**, *13*, 453-461; c) Gillies, E.R., Fréchet, J.M.J. Designing Macromolecules for Therapeutic Applications: Polyester DendrimerPoly(ethylene oxide) "Bow-Tie" Hybrids with Tunable Molecular Weight and Architecture. *J. Am. Chem. Soc.* **2002**, *124*, 14137-14146; d) Wolinsky, J.B., Grinstaff, M.W. Therapeutic and diagnostic applications of dendrimers for cancer treatment. *Adv. Drug Delivery Rev.* **2008**, *60*, 1037-1055.
17. Torchilin, V.P. Recent advances with liposomes as pharmaceutical carriers. *Nat.Rev. Drug Discovery.* **2005**, *4*, 145-160.
18. a) Masayuki, Y., Mizue, M., Noriko, Y., Teruo, O., Yasuhisa, S., Kazunori, K., Shohei, I. Polymer micelles as novel drug carrier: Adriamycin-conjugated poly(ethylene glycol)-poly(aspartic acid) block copolymer. *J. Control. Release* **1990**, *11*, 269-278; b) Torchilin, V.P. Micellar nanocarriers: pharmaceutical perspectives. *Pharm. Res.* **2007**, *24*, 1-16.
19. a) Gibson, J.D., Khanal, B.P., Zubarev, E.R. Paclitaxel-Functionalized Gold Nanoparticles. *J. Am. Chem. Soc.* **2007**, *129*, 11653-11661.
20. a) Bianco, A., Kostarelos, K., Prato, M. Applications of carbon nanotubes in drug delivery. *Curr. Opin. Chem. Biol.* **2005**, *9*, 674-679; b) Liu, Z., Chen, K., Davis, C., Sherlock, S., Cao, Q., Chen, X., Dai, H. Drug delivery with carbon nanotubes for in vivo cancer treatment. *Cancer Res.* **2008**, *68*, 6652-6660.
21. a) Kratz, F. Albumin as a drug carrier: Design of prodrugs, drug conjugates and nanoparticles. *J. Control. Release* **2008**, *132*, 171-183; b) Hawkins, M.J., Soon-Shiong, P., Desai, N. Protein nanoparticles as drug carriers in clinical medicine. *Adv. Drug Delivery Rev.* **2008**, *60*, 876-885.
22. a) Flenniken, M.L., Willits, D.A., Harmsen, A.L., Liepold, L.O., Harmsen, A.G., Young, M.J., Douglas, T. Melanoma and Lymphocyte Cell-Specific Targeting Incorporated into a Heat Shock Protein Cage Architecture. *Chem. Biol.* **2006**, *13*, 161-170; b) Flenniken, M.L., Liepold, L.O., Crowley, B.E., Willits, D.A., Young, M.J., Douglas, T. Selective attachment and release of a chemotherapeutic agent from the interior of a protein cage architecture. *Chem. Comm.* **2005**, *2*, 447.
23. a) Valegard, K., Liljas, L., Fridborg, K., Unge, T. The three-dimensional structure of the bacterial virus MS2. *Nature* **1990**, *345*, 36-41; b) Valegard, K., Liljas, L., Fridborg, K., Unge, T. Structure determination of the bacteriophage MS2. *Acta Crystallogr. B* **1991**, *47*, 949-960. c) Golmohammadi, R., Valegard, K., Fridborg, K., Liljas, L. The refined structure of bacteriophage MS2. *J. Mol. Biol.* **1993**, *234*, 620-639.
24. Branden, C., Tooze, J. *Introduction to Protein Structure*, *2nd ed.* **1999** (Garland Publishing,

New York).

25. Ni, C.-Z., Syed, R., Kodandapani, R., Wickersham, J., Peabody, D.S., Ely, K.R. Crystal structure of the MS2 coat protein dimer: implications for RNA binding and virus assembly. *Structure* **1995**, *3*, 255-263.

26. Strauss, J., Sinsheimer, R. Purification and properties of bacteriophage MS2 and of its ribonucleic acid. *J. Mol. Biol.* **1963**, 43.

27. Wang, Q., Kaltgrad, E., Lin, T., Johnson, J.E., Finn, M.G. Natural supramolecular building blocks: Wild-type cowpea mosaic virus. *Chem. Biol.* **2002**, *9,* 805-811.

28. Liepold, L., Anderson, S., Willits, D., Oltrogge, L., Frank, J.A., Douglas, T., Young, M. Viral capsids as MRI contrast agents. *Magn. Reson. Med.* **2007**, *58*, 871-879.

29. Wang, Q., Chan, T.R., Hilgraf, R., Fokin, V.V., Sharpless, K.B., Finn, M.G. Bioconjugation by copper(I)-catalyzed azide-alyne [3+2] cycloaddition. *J. Am. Chem. Soc.* **2003**, *125*, 3192-3193.

30. Strable, E., Prasuhn, D.E., Jr., Udit, A.K., Brown, S., Link, A.J., Ngo, J.T., Lander, G., Quispe, J., Potter, C.S., Carragher, B., Tirrell, D.A., Finn, M.G. Unnatural amino acid incorporation into virus-like particles. *Bioconjug. Chem.* **2008**, *19*, 866-875.

31. Lockney, D.M., Guenther, R.N., Loo, L., Overton, W., Antonelli, R., Clark, J., Hu, M., Luft, C., Lommel, S.A., Franzen, S. The Red clover necrotic mosaic virus capsid as a multifunctional cell targeting plant viral nanoparticle. *Bioconjug. Chem.* **2011**, *22*, 67-73.

32. Stephanopoulos, N., Tong, G.J., Hsiao, S.C., Francis, M.B. Dual-surface modified virus capsids for targeted delivery of photodynamic agents to cancer cells. *ACS Nano* **2010**, *4*, 6014-20.

33. Ma, Y., Nolte, R.J.M., Cornelissen, J.L.M. Virus-based nanocarriers for drug delivery. *Adv. Drug Del. Rev.* **2012**, *64*, 811-825.

34. Wani, M.C., Taylor, H.L., Wall, M., Coggon, P., McPhail, A.T. Plant antitumor agents. VI. The isolation and structure of taxol, a novel antileukemic and antitumor agent from *Taxus brevifolia*. *J. Am. Chem. Soc.* **1971**, *93,* 2325-2327.

35. a) Holton, R.A., Somoza, C., Kim, H.B., Liang, F., Biediger, R.J., Boatman, P.D., Shindo, M., Smith, C.C., Kim, S. First total synthesis of taxol. 1. Functionalization of the B ring. *J. Am. Chem. Soc.* **1994**, *116,* 1597-1598; b) Holton, R.A., Kim, H.B., Somoza, C., Liang, F., Biediger, R.J., Boatman, P.D., Shindo, M., Smith, C.C., Kim, S. First total synthesis of taxol. 1. Completetion of the C and D rings. *J. Am. Chem. Soc.* **1994**, *116,* 1599-1600; c) Nicolaou, K.C., Yang, Z., Liu, J.J., Ueno, H., Nantermet, P.G., Guy, R.K., Claiborne, C.F., Renaud, J., Couladouros, E.A., Paulvannan, K., Sorensen, E.J. Total synthesis of taxol. *Nature* **1994**, *367*, 630-634.

36. Schiff, P.B., Fant, J., Horwitz, S.B. Promotion of microtubule assembly in vitro by taxol. *Nature,* **1979**, *277*, 665-667.

37. a) Sparreboom, A., Van Tellingen, O., Nooijen, W.J., Beijnen, J.H. Nonlinear pharmacokinetics of paclitaxel in mice results from the pharmaceutical vehicle Cremophor EL. *Cancer Res.* **1996**, *56*, 2112-2115; b) Singla, A., Garg, A., Aggarwal, D. Paclitaxel and its formulations. *Int. J. Pharm.* **2002**, *235*, 179-192.

38. Skwarczynski, M., Hayashi, Y., Kiso, Y. Paclitaxel Prodrugs: Toward Smarter Delivery of Anticancer Agents. *J. Med. Chem.* **2006**, *49*, 7253-7269.

39. Johnson, H.R., Hooker, J.M., Francis, M.B., Clark, D.S. Solubilization and stabilization of bacteriophage MS2 in organic solvents. *Biotechnol. Bioeng.* **2007**, *18*, 1140-1147.

40. Gradishar, W. J., et al. Phase III Trial of Nanoparticle Albumin-Bound Paclitaxel Compared With Polyethylated Castor Oil–Based Paclitaxel in Women With Breast Cancer. *J. Clin. Oncol.* **2005**, *23*, 7794-7803.

41. Singer, J.W. Paclitaxel poliglumex (XYOTAX, CT-2103): A macromolecular taxane. *J. Control. Release* **2005**, *109*, 120-126.

42. a) Wu. M., Brown, W.L., Stockley, P.G. Cell-specific delivery of bacteriophage-encapsidated Ricin A chain. *Bioconjug. Chem.* **1995**, *6*, 587-595; b) Peabody, D.S. A viral platform for chemical modification and multivalent display. *J. Nanobiotechnology* **2003**, *1*.

43. Kovacs, E.W., Hooker, J.M., Romanini, D.W., et al. Dual-Surface-Modified Bacteriophage MS2 as an Ideal Scaffold for a Viral Capsid-Based Drug Delivery System. *Bioconjug. Chem*. **2007**, *18*, 1140-1147.

44. Kovacs, E.W. The Covalent Modification of MS2 Viral Capsids for the Development of Drug Delivery Vehicles. Ph.D. dissertation, University of California, Berkeley, Berkeley, CA, 2006.

45. Hooker, J.M., Kovacs, E.W., Francis, M.B. Interior surface modification of bacteriophage MS2. *J. Am. Chem. Soc*. **2004**, *126,* 3718-3719.

46. Hooker, J.M., Datta, A., Botta, M., Raymond, K.N., Francis, M.B. Magnetic Resonance Contrast Agents from Viral Capsid Shells: A Comparison of Exterior and Interior Cargo Strategies. *Nano Lett*. **2007**, *7,* 2207-2210.

47. Tong, G.J., Hsiao, S.C., Carrico, Z.M., Francis, M.B. Viral Capsid DNA Aptamer Conjugates as Multivalent Cell-Targeting Vehicles. *J. Am. Chem. Soc.* **2009**, *131*, 11174-11178.

48. Datta, A., Hooker, J.M., Botta, M., Francis, M.B., Aime, S., Raymond, K.N. High Relaxivity Gadolinium Hydroxypyridonate-Viral Capsid Conjugates: Nanosized MRI Contrast Agents. *J. Am. Chem. Soc.* **2008**, *130*, 2546-2552.

49. Wu, W., Hsiao, S.C., Carrico, Z.M., Francis, M.B. Genome-Free Viral Capsids as Multivalent Carriers for Taxol Delivery. *Angew. Chem., Int. Ed.* **2009**, *48,* 9493-9497.

50. Carrico, Z.M., Romanini, D.W., Mehl, R.A., Francis, M.B. Oxidative coupling of peptides to a virus capsid containing unnatural amino acids. *Chem. Commun*. **2008**, *10*, 1205-1207.

51. Romanini, D.W. Methods for T-shaped proteins and virus-based targeted imaging agents. Ph.D. dissertation, University of California, Berkeley, Berkeley, CA, 2008.

52. Behrens, C.R., Hooker, J.M., Obermeyer, A.C., Romanini, D.W., Katz, E.M., Francis, M.B. Rapid Chemoselective Bioconjugation Through the Oxidative Coupling of Anilines and Aminophenols. *J. Am. Chem. Soc.* **2011**, *133*, 16398-401.

Chapter 2: A Palladium Catalyzed Tyrosine Allylation for MS2 Interior Modification

2.1 Taxol bioconjugation to the interior surface of MS2.

Many pharmaceutical compounds have poor water solubility, and in the case of taxol, necessitate the use of toxic carrier vehicles when injected.[1] The use of an MS2 viral capsid delivery system could theoretically attenuate the water-insoluble nature of drug molecules via selective bioconjugation to the interior of the water-soluble protein. This would also serve as the first step in constructing an MS2-based targeted drug delivery system. Previous work in our group had attempted to use a diazonium reagent based tyrosine modification reaction to attach the drug molecules to the interior of MS2 by targeting Y85.[2] However, the low solubility of taxol and other similar drugs proved to be a difficult factor in achieving effective bioconjugation.

The tyrosine-selective $Pd(OAc)_2$-catalyzed bioconjugation reaction developed by S. David Tilley offers several potential advantages over the previously used diazonium reaction for the attachment of drug molecules to MS2 capsids.[3] Most notably, the $Pd(OAc)_2$-based catalyst system displaces a leaving group on the allylic substrate (Figure 2-1a). The use of a water solubilizing unit at this leaving group site allows the bioconjugation of previously water insoluble compounds to tyrosine side chains. This reaction was previously used to modify the protein chymotrypsinogen A with long chain alkane substrates bearing a sulfonate-based leaving group. This resulted in the formation of proteinacious small unilamellar vesicles. Upon bioconjugation of a drug mol-

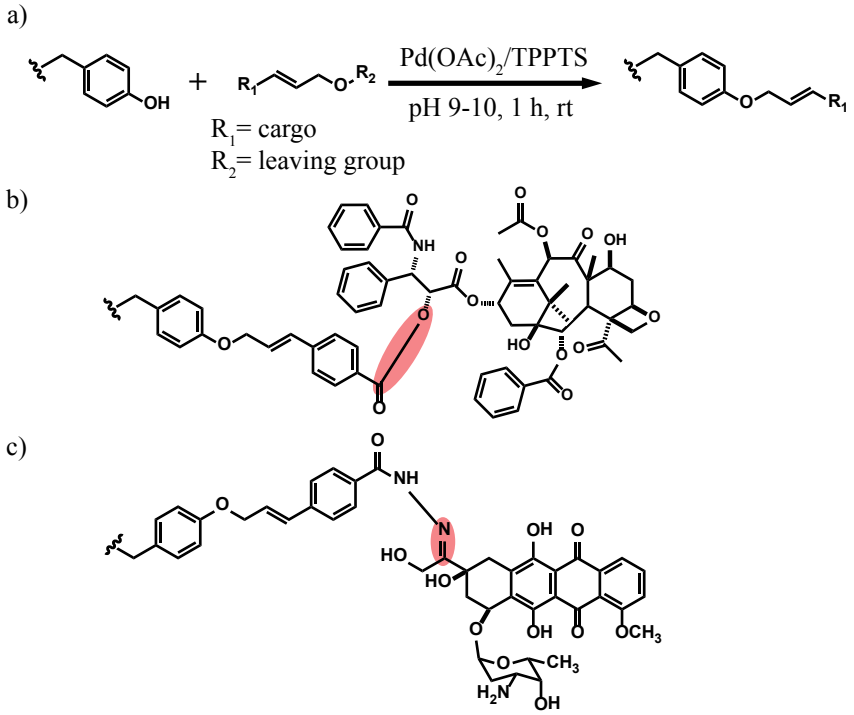

Figure 2-1. a) Scheme for tyrosine modification using a Pd-catalyzed allylation reaction. b) Proposed taxol-tyrosine conjugate, with a hydrolyzable ester bond highlighted in red. c) Proposed doxorubicin-tyrosine conjugate, with an acid-sensitive, hydrolyzable hydrazone bond highlighted in red.

ecule, the appropriate drug release could then be achieved by the use of linkers that are sensitive to conditions within a cell or associated with cellular uptake. Examples include the use of ester or amide bonds (Figure 2-1b), which can be hydrolyzed by esterases within the cell,[4] or the use of acid-sensitive hydrazone linkages that can hydrolyze in the low pH endosomal or lysosomal environment encountered after cellular uptake (Figure 2-1c).[5]

The attachment of these hydrophobic groups to the interior Y residues of MS2 has been difficult to achieve in previous experiments. In addition, little is known about the compatibility of genome-free MS2 capsids with this reaction. To explore this possibility, the research described herein details the synthesis of allylic acetates bearing functional groups suitable for drug cargo attachment, as well as tyrosine-specific bioconjugation studies with these molecules using $Pd(OAc)_2$-catalyzed alkylation.

Of the various elements of constructing a drug-delivery vehicle from MS2, we presently focus on the attachment of drug molecules to the interior surface of the viral capsid. This process can be divided into several parts. First is the production of MS2, removal of the RNA, and purification of the viral capsids. Next is the synthesis of a linker that can undergo tyrosine bioconjugation using the $Pd(OAc)_2$-catalyzed reaction, and provide an additional site for cargo attachment. Last is the testing and optimization of the bioconjugation reaction with the new drug-linker substrate and MS2 capsids. In this chapter, we use native MS2 that was grown infectiously in *E. coli* and emptied of the RNA genome using successive high pH hydrolysis and PEG precipitation steps, as described previously.[2]

2.2 Allylic linker synthesis.

The basic design of the linker features a functional group for drug molecule attachment, and a water-soluble disposable group (Figure 2-2a). The core of the linker was a 1,4-subsituted aromatic ring that provided a rigid spacer and facilitated compound characterization during synthesis. On one side of the ring was the allylic alcohol necessary for the tyrosine-specific $Pd(OAc)_2$-catalyzed bioconjugation. Attached to this allylic alcohol was a disposable group of choice that

a)

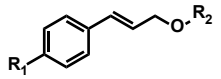

R_1= functionality for drug molecule attachment
R_2= leaving group

b)

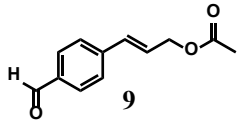

9

c)

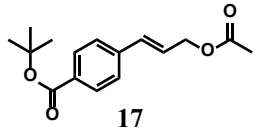

17

Figure 2-2. a) General linker design for tyrosine alklyation reaction. b) An aldehyde containing linker. c) A linker containing a protected carboxylic acid.

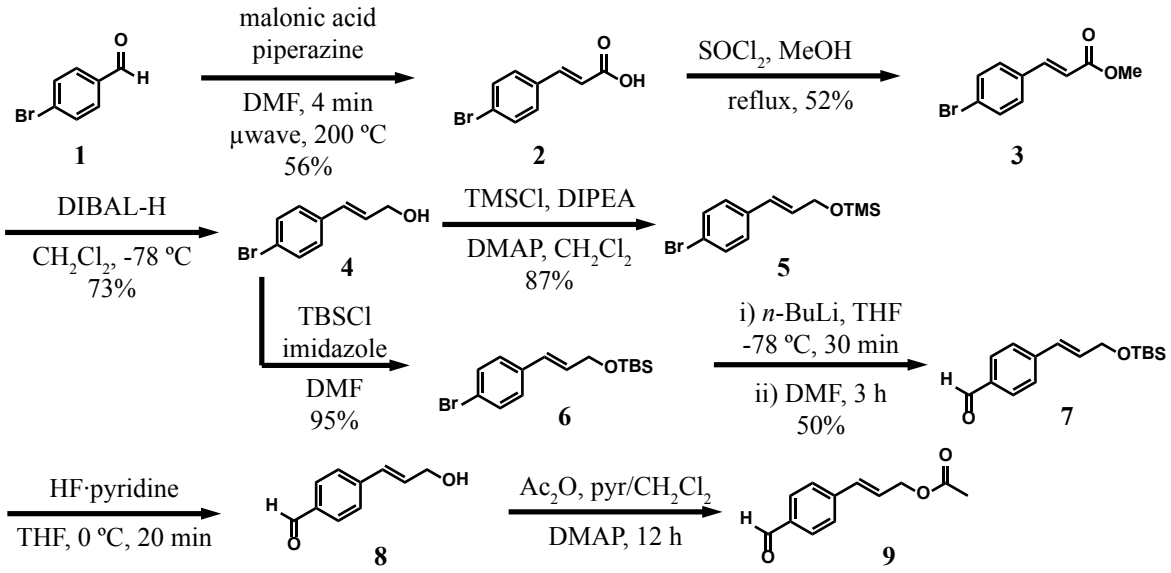

Figure 2-3. Synthetic scheme for the synthesis of aldehyde-allylic acetate linker **9**.

could serve to solubilize hydrophobic drug molecules. For our initial bioconjugation studies, we chose to use a simple acetate group as the leaving group to simplify the synthesis. Two synthetic routes were ultimately developed to arrive at aldehyde or carboxylic acid functionalized linker for future derivatization (Figures 2-2b-c). We used these preliminary linkers first to assess the compatibility of the Pd-catalyzed tyrosine alkylation on MS2.

The first substrate tested was aldehyde **9** (Figure 2-2b), which could be reacted with alkoxy-amine-functionalized small molecules to produce stable oxime linkage bioconjugates. Starting with 4-bromo-benzaldyde (**1**), we planned to install the aldehyde in a later step to avoid the precautions necessary (Figure 2-3). A microwave protocol was used to effect the Knoevenagel reaction on **1** and subsequent decarboxylation in only four minutes. Compound **3** was synthesized from the acid chloride by heating in methanol and thionyl chloride and then reduced to allylic alcohol **4** with DIBAL-H. This alcohol was initially protected with a TMS group which unfortunately proved to be too labile for column chromatography upon scale up. Protection as TBS ether **6**, followed by lithium-halogen exchange and addition to DMF gave aldehyde **7.** TBAF deprotection conditions proved too harsh for our compound and several alternative deprotection schemes were tested, including the use of a THP protecting group as an alternative. Ultimately, HF·pyridine proved to be effective in the removal of the TBS group to furnish allylic alcohol **8**.

We also planned to synthesize compound **17**, bearing a protected carboxylic acid (Figure 2-4), to facilitate the coupling of hydroxyl groups and amines to the bioconjugation reagent. The synthesis of **17** began with commercially available 4-carboxybenzaldehyde (**10**) and started with the protection of the carboxylic acid as the *t*-butyl ester. Traditional DCC coupling to *t*-butanol, acid-catalyzed esterification with isobutylene, and conversion to the acid chloride with subsequent displacement by *t*-butanol were unsuccessful in producing the desired product in any appreciable yield. Eventually, the use of a commercially available DMF di-*t*-butyl acetal reagent gave *t*-butyl ester **11** in 70% yield**.** We first attempted to extend **11** to cinnamic derivative **12** using a Knoevenagel condensation, followed by subsequent decarboxylation. The Knoevenagel condensation

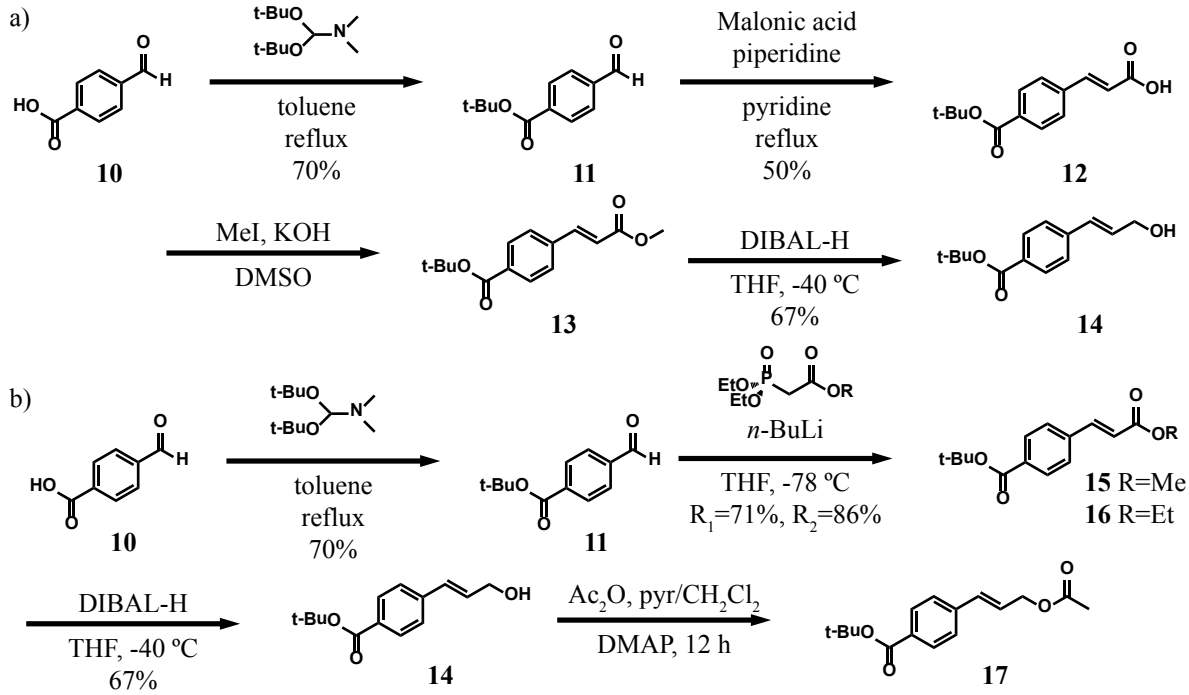

Figure 2-4. Two synthetic pathways to allylic alcohol **14** bearing a protected carboxylic acid.

indeed proceeded in high yield to give **12**, but the formation of the methyl ester proved to be difficult. In contrast to the above bromo-substituted molecule, the presence of the *t*-butyl ester on this molecule precluded the use of reactions that required acid, such as Fischer esterification or conversion to the acid chloride. Instead, reaction with methyl iodide in highly polar solvent under basic conditions eventually gave **13** in low yield. Selective DIBAL-H reduction of the methyl ester was tested at several temperatures, DIBAL-H equivalents, and reaction times, yielding optimal conditions of two hours, -40 °C, and three equivalents of DIBALH to produce **14**.

The above pathway to **14** provided a few inconveniences, such as long reaction times for the Knoevenagel condensation and a difficult purification of the methyl ester from DMF. A Horner-Wadsworth-Emmons reaction to give esters **15** and **16** (Figure 2-4b) using an available ethyl phosphonate ester, and later reactions performed with a commercially available methyl phosphonate ester gave improved yields. The HWE reaction and subsequent DIBALH reduction also provided high selectivity for the *trans* isomer of **14**.

Reaction of **8** and **14** with acetic anhydride and pyridine provided allylic acetate **9** and **17**, which were needed to begin testing the compatibility of the bioconjugation reaction with MS2. However, the synthesis of a water-soluble disposable group was necessary for drug delivery purposes. Our group's previous method achieved this through the attachment of a taurine carbamate through a nitrophenyl carbamate intermediate. Nitrophenyl carbonate **18** was successfully synthesized and the displacement of nitrophenol by taurine was attempted (Figure 2-5a). However, dealing with the reaction conditions and purification of **22** was rather difficult and substrate dependent, so several alternative leaving groups were investigated. The simplest functionality to add was an acetate group, which was easily appended using acetic anhydride. In addition, cyclic anhydrides such as succinic, glutaric, and diglycolic anhydride were easily ring-opened to give

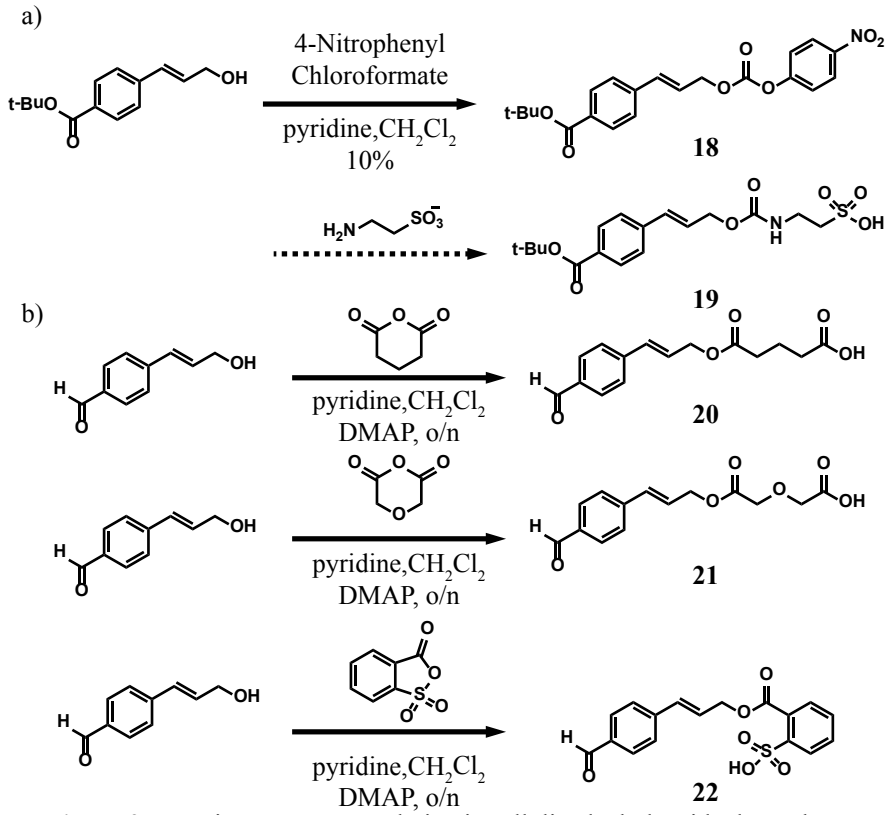

Figure 2-5. Various attempts to derivatize allylic alcohols with charged leaving groups.

charged functionalities that could increase water solubility (Figure 2-5b).

2.3 Pd-catalyzed protein modification using allylic linkers.

Initial protein modification reactions were carried out with genome free MS2 viral capsids (monomer mass = 13,732 Da), and substrates **9** and **17** (Figure 2-2) to test the effectiveness of the $Pd(OAc)_2$-catalyzed bioconjugation on MS2 and with the new class of substrate. Chymotrypsinogen A (mass = 25,656 Da) was used as a positive control protein since it had previously been shown to undergo bioconjugation using the $Pd(OAc)_2$ catalyst.[3] Several methods of protein purification were tested. The use of NAP-5 size exclusion columns, followed by spin concentration, removed most of the small molecules, but occasionally protein was lost in the column. Alternatively, the use of Microspin columns filled with G-25 resin also removed substantial amounts of small molecules, and could often negate the need for a subsequent spin concentration. The use of repeated spin concentration was also shown to purify the protein from small molecules.

Our initial experiments focused on synthesized linker **17**. As this compound itself does not possess a site for further modification, analysis of the conjugation reaction was done solely using LC/MS. Initial reactions showed substantial single and double modification of chymotrypsinogen, which is consistent with the reaction of this protein with other pi-allyl substrates.[3] Modification of chymotrypsinogen was similar at catalyst concentrations of 400 μM and 1 mM. Similar conditions for MS2 modification however yielded negligible additions of compound **17**. Unfortunately, MS2 modification was too low to compare modification dependence on catalyst concen-

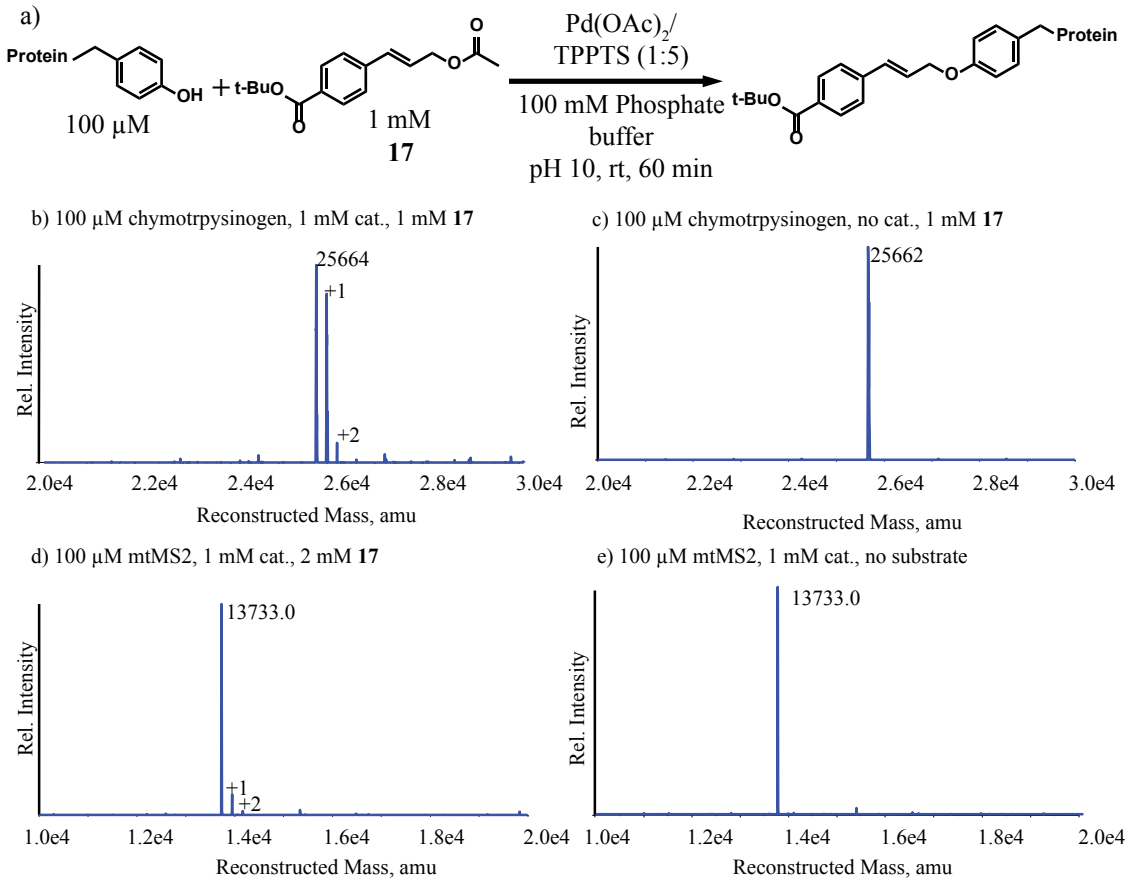

Figure 2-6. (a) A typical protein reaction with compound **17** and MS2/chymotrypsinogen, followed by LC/MS analysis. (b) Single and double modification of chymotrypsinogen. (c) Control sample of chymotrypsinogen shows no modification. (d) Low levels of single and double modification of mtMS2. (e) Control sample of mtMS2 shows no modification.

tration. Possible reasons include poor catalyst accessibility to the interior surface, poor catalyst accessibility to Y85, and poor substrate solubility. However, these initial experiments showed the possibility of attaching the desired substrate to MS2.

In order to screen conditions for MS2 modification more quickly, we next turned to compound **9** due to the aldehyde functionality that could be reacted with further probes to assay for protein modification. We could then use SDS-PAGE to characterize the bioconjugation products, both through oxime formation with an Alexa Fluor alkoxyamine dye, and by detecting a gel shift after oxime formation with PEG-2000 alkoxyamine. In contrast to LC/MS analysis, the use of gel analysis required fewer purification steps and allowed more samples to be run and assayed concurrently via appearance of fluorescent protein or gel shift.

2.4 Screening conditions for MS2 modification.

Using aldehyde functionalized linker **9** and the assay described above, we then proceeded to test various conditions such as substrate and catalyst concentrations, temperature, and conditions for the secondary bioconjugation with PEG-ONH_2. Initial experiments with the gel-based assay focused on the effects of temperature using standard reaction conditions (Figure 2-7a). As

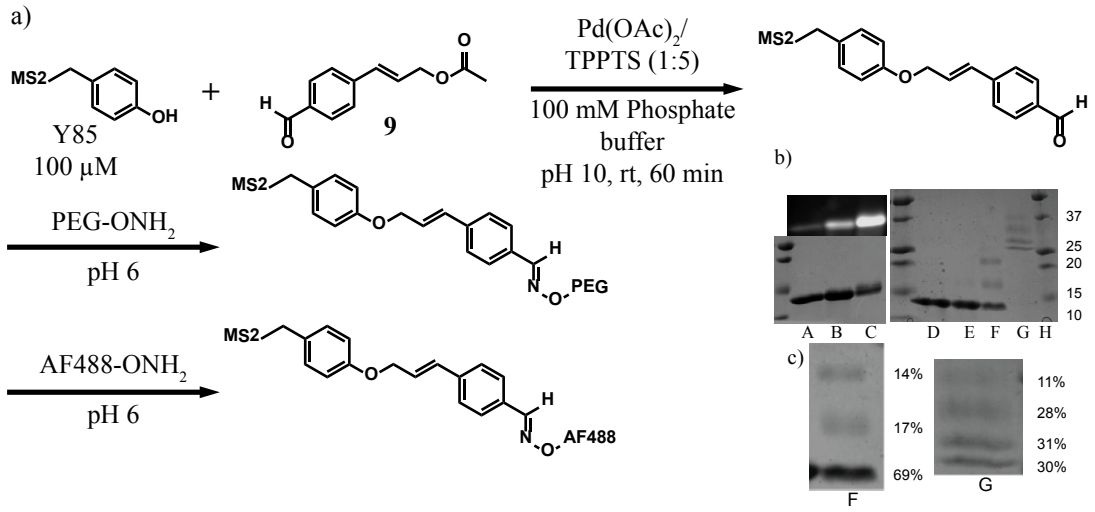

Figure 2-7. Modification of MS2 with compound **9** as analyzed by SDS-PAGE. a) Reaction scheme for MS2 modification followed by secondary bioconjugation with aminooxy PEG and fluorescent dye. b) Analysis of the resulting bioconjugates via SDS-PAGE, fluorescent imaging and Commassie staining. Lanes A-C show the reaction of MS2 at temperatures 25/37/50 °C with AF488-ONH_2, and both a fluorescent image and Coomassie stained gel are shown. Lanes D-F show reaction with PEG-ONH_2 at the same temepratures as A-C. Lane G is a chymotrypsinogen positive control that had also been reacted with **9** at 25 °C, followed by PEG-ONH_2. Lane H contains a protein ladder. c) Lanes F and G have been enlarged to show the PEG additions more clearly. The accompanying percentages are densitometric measurements of the modification levels (unmodified, +1, +2, +3).

expected, at room temperature, MS2 showed no modification by PEG shift and barely detectable levels of modification upon reaction with a fluorescent alkoxyamine (Figure 2-7b). In contrast, chymotrypsinogen exhibited high levels of multiple modifications even at room temperature. For the MS2 samples however, raising the temperature up to 50 °C seemed to increase the modifica-

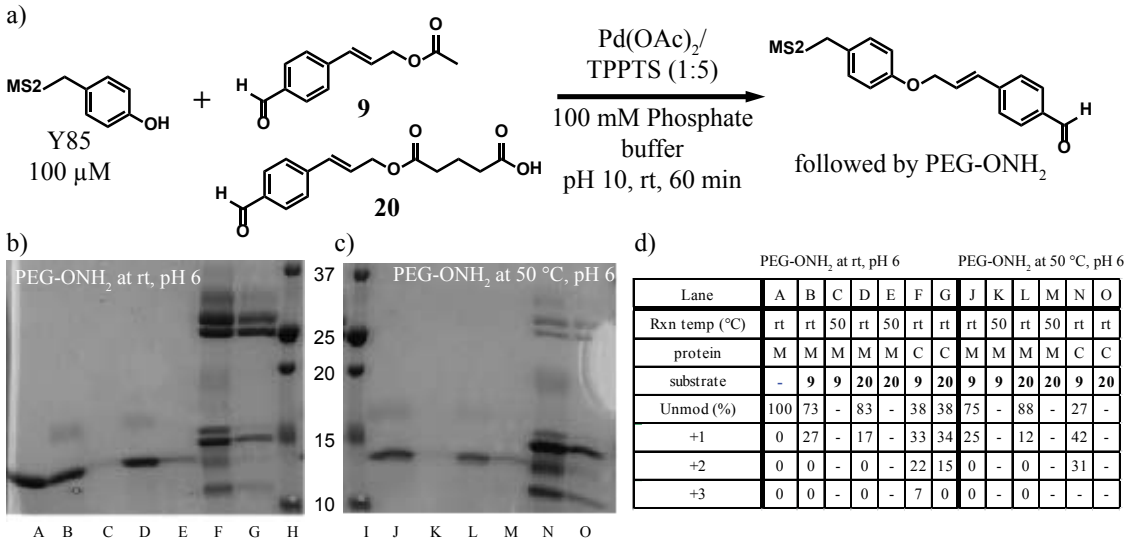

d)

	PEG-ONH_2 at rt, pH 6							PEG-ONH_2 at 50 °C, pH 6					
Lane	A	B	C	D	E	F	G	J	K	L	M	N	O
Rxn temp (°C)	rt	rt	50	rt	50	rt	rt	rt	50	rt	50	rt	rt
protein	M	M	M	M	M	C	C	M	M	M	M	C	C
substrate	-	**9**	**9**	**20**	**20**	**9**	**20**	**9**	**9**	**20**	**20**	**9**	**20**
Unmod (%)	100	73	-	83	-	38	38	75	-	88	-	27	-
+1	0	27	-	17	-	33	34	25	-	12	-	42	-
+2	0	0	-	0	-	22	15	0	-	0	-	31	-
+3	0	0	-	0	-	7	0	0	-	0	-	-	-

Figure 2-8. Attempts to raise MS2 modification level. a) General scheme for mtMS2 modification using **9** and **20.** After Pd catalyzed modification, the samples were exposed to PEG2K-ONH_2 at either rt or 50 °C. b) SDS-PAGE of samples exposed to PEG-ONH_2 at rt. c) SDS-PAGE of samples exposed to PEG-ONH_2 at 50 °C. d) Tabulated modification levels for both gels. Proteins labelled M correspond to MS2, while those labelled C are chymotrypsinogen positive controls.

tion levels, detectable both by fluorescence and PEG shift assays, as well as the number of modifications. At 50 °C, the MS2 capsid is still fairly stable; however, the appearance of the second modification, clearly seen on the PEG shift assay shows that a second reaction site (besides Y85) may be participating. Additionally, even at this elevated temperature, 69% of MS2 monomers remained unmodified (Figure 2-7c).

The next set of experiments attempt to raise the single modification levels of MS2 capsid, using both molecules **9** and **20** solubilized in DMSO. Chymotrypsinogen was again used as a positive control protein and we measured protein modification by secondary bioconjugation with PEG2K-ONH_2. The first experiment in Figure 2-8 showed degradation of MS2 at 50 °C (Lanes C, E, K, and M, unlike what had previously been observed. Compound **9** showed higher levels of modi-

a)

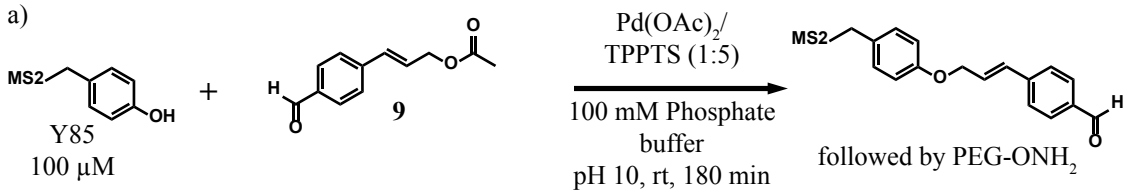

b)

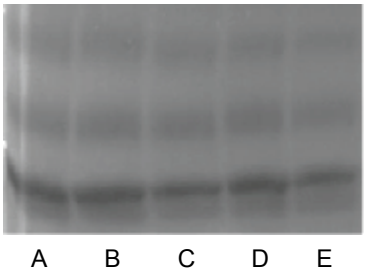

c)

Lane	A	B	C	D	E
Cat conc (µM)	100	200	400	800	1600
Substrate conc (µM)	250	500	1000	2000	4000
% unmod	59	58.4	58.9	62	65
+1	23.5	25.4	25.3	24.9	23
+2	17.3	16.2	15.8	13	12

Figure 2-9. Reaction time is extended to three hours and catalyst/substrate concentration varied. a) Reaction scheme for MS2 modification followed by PEG-ONH_2 addition. b) SDS-PAGE analysis of modified MS2. c) Tabulated modification levels of MS2.

a)

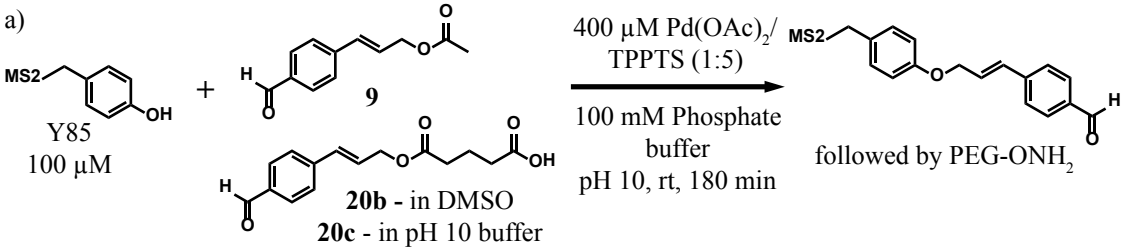

b)

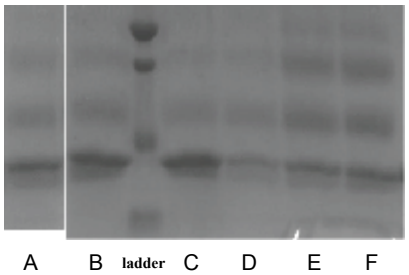

c)

Lane	A	B	C	D	E	F
substrate	9	20b	20c	9	20b	20c
Temp (°C)	rt	rt	rt	37	37	37
unmod	58.9	59.6	68	49.8	38.9	37.7
1	25.3	27	23	35.5	32.4	32
2	15.8	13.4	8	14.7	23.9	25.2
3	0	0	0	0	4.8	5

Figure 2-10. Temperature and substrate effects. a) Reaction scheme for MS2 modification followed by PEG-ONH_2 addition. b) SDS-PAGE analysis of modified MS2. c) Tabulated modification levels of MS2.

fication than **20** on MS2 (comparing lanes B and D), indicating that water solubility of the small molecule was not a large factor for this compound. Chymotrypsinogen on the other hand exhibited similar levels of modification between substrates **9** and **20**. In Figure 2-8c, the same samples as in Figure 2-8a were reacted with PEG2K-ONH_2, but rather than doing the actual alkylation at 50 °C, only the oxime formation step was done at an elevated temperature. In this case though, MS2 loss was still observed at 50 °C, and compound **9** still fared better than **20**.

In the next experiment, we extended the reaction time to 3 h and varied the catalyst and substrate concentrations (Figure 2-9). The ratio of catalyst to substrate was held at 2:5 and catalyst concentration examined from 100 µM to 1.6 mM. Overall, double modification was observed at all concentrations of catalyst. The interesting observation was that above 400 µM catalyst, modification levels decreased, and in fact, the lowest concentrations tested (100 µM catalyst) exhibited comparable modification levels to higher catalyst concentrations. In the end we chose to use 400 µM catalyst and 1 mM substrate and 3 h reaction times for future experiments. Using these new conditions, we again examined temperature and substrate effects (Figure 2-10). Since MS2 stability at 50 °C had been observed to be unpredictable, we examined modification gains at 37 °C instead, and indeed we see that modification was raised ~5-10% compared to that at rt. We observed that **20b** was as effective as **9** under these conditions. In addition we began to see trace levels of a third modification occurring.

a)

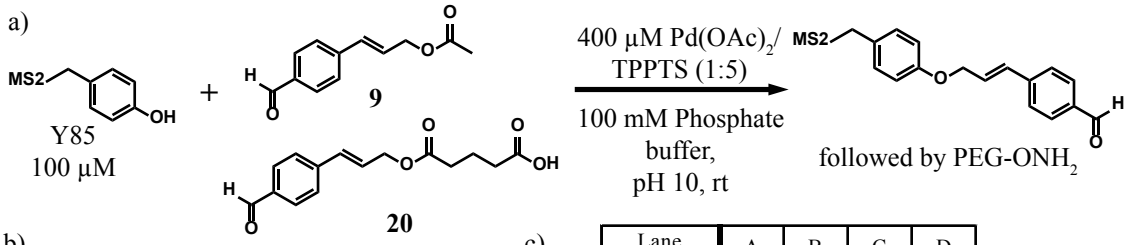

b)

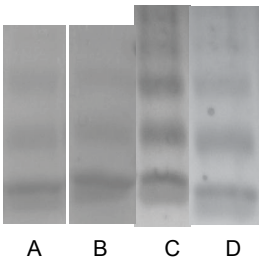

c)

Lane	A	B	C	D
substrate	**9**	**20**	**9**	**20**
Time (h)	3	3	24	24
unmod	58.9	59.6	48.3	53.3
1	25.3	27	30.4	34
2	13.8	13.4	17.5	12.7
3	0	0	3.7	0

Figure 2-11. Extended reaction time effects. a) Reaction scheme for MS2 modification followed by PEG-ONH_2 addition. b) SDS-PAGE analysis of modified MS2. c) Tabulated modification levels of MS2.

Lastly, we also tested the reaction at longer reaction times. Figure 2-11 compares the modifications observed after 3 h and 24 h. Densitometry measurements indicated another ~5-10% gain in modification with longer reaction times, as well as the appearance of third modifications. The above experiments indicated that it was difficult to raise modification levels without concurrently raising the number of modifications. While for drug delivery purposes, the more drug molecules loaded the better, the high variability in modification number and site selectivity potentially makes the release of the drug non-uniform.

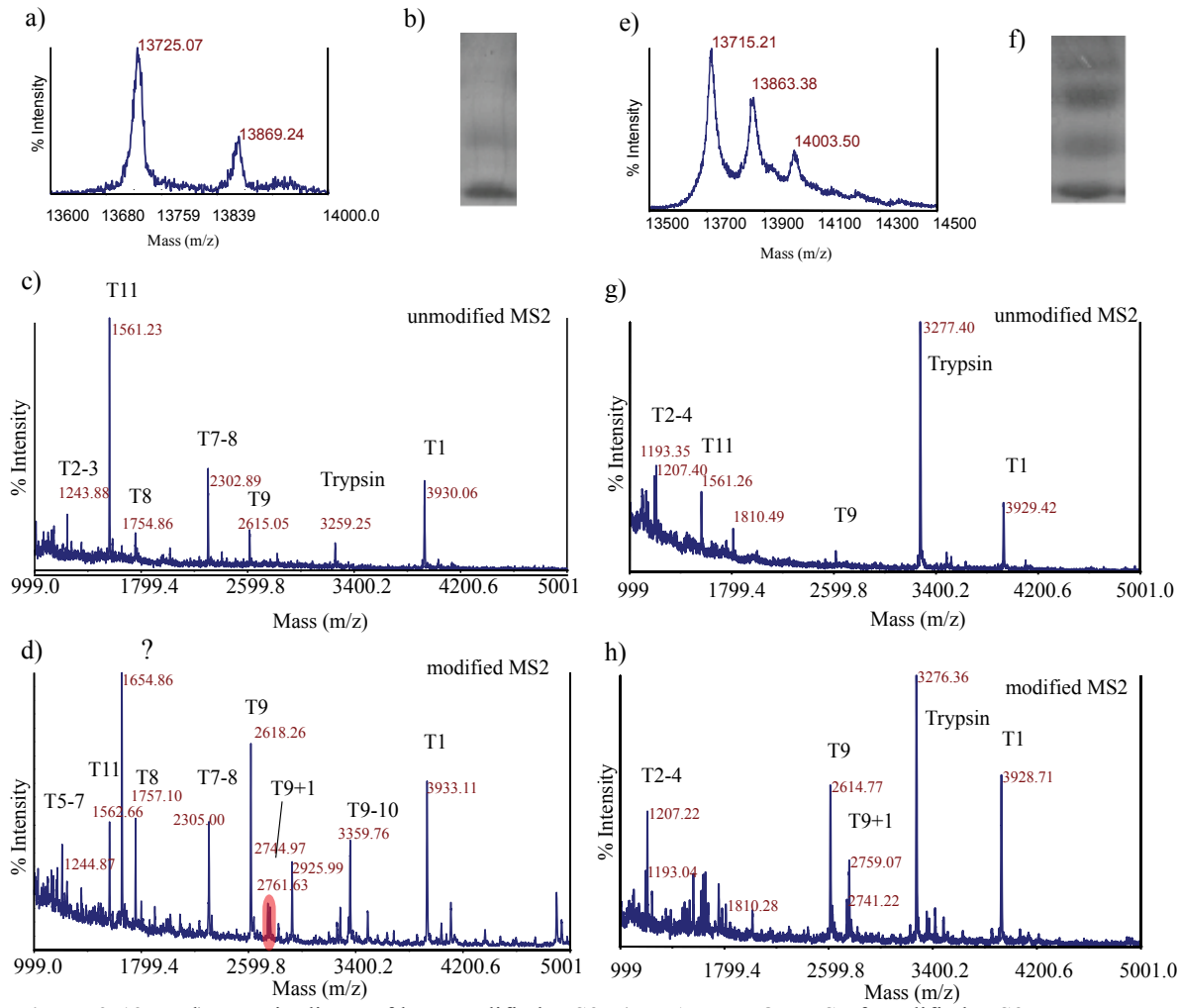

Figure 2-12. a-d) Trypsin digest of low-modified MS2 a) MALDI-TOF MS of modified MS2. Unmodified MS2 expected mass = 13732 amu, modified MS2 expected mass = 13877 amu b) SDS-PAGE analysis of modified MS2. c) MALDI-TOF MS analysis of trypsin digest of unmodified MS2. d) MALDI-TOF MS analysis of trypsin digest of modified MS2 with expected +145 amu mass gain in T9. e-h) Trypsin digest of highly-modified MS2 e) MALDI-TOF MS of modified MS2. Unmodified MS2 expected mass = 13732 amu, MS2 +1 addition expected mass = 13877 amu, MS2 +2 addition expected mass = 14022 amu f) SDS-PAGE analysis of modified MS2. g) MALDI-TOF MS analysis of trypsin digest of unmodified MS2. h) MALDI-TOF MS analysis of trypsin digest of modified MS2 with expected +145 amu mass gain in T9.

To investigate the site selectivity of these multiple modifications, we performed a tryptic digest on modified MS2 to assess where the mass additions were occurring. The first sample tested was MS2 with a low modification level, to assess whether the first modification is actually happening at Y85. Upon tryptic digest, we observed a mass adduct corresponding to the correct digest fragment plus the expected mass (T9 + 1), indicating that the initial modifications most likely are at Y85. Next we examined a sample that had up to three modifications. In this case, again, the T9 + 1 mass adducts were observed, but further T9 adducts were not seen. This indicated that the other modifications did not take place at Y85. This ruled out the possibility of the multiple modifications all occurring on Y85 through C-alkylation or Claisen Rearrangements (revealing the phenolic oxygen for further O-alkylation).

As a last measure, we also synthesized the taxol-containing version of compound **17**. This molecule was easily synthesized through EDC coupling at the 2'-OH of taxol with the BOC-de-protected version of **17** (Figure 2-13). Compound **24** could be dissolved in DMSO up to 1 mM. However, upon addition to a buffered MS2 solution, **24** immediately precipitated out of solution. This was indicated by the immediate appearance of a white solid that could be then centrifuged, leaving only unmodified MS2 in solution. Even raising the DMSO cosolvent ratio to 10% did not improve solubility.

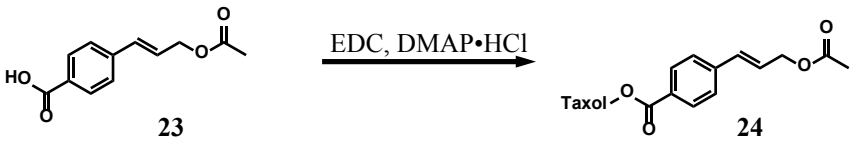

Figure 2-13. Synthesis of a taxol derivatized allylic acetate linker.

In conclusion, a new route has been developed to access allylic carbonates for $Pd(OAc)_2$-catalyzed bioconjugation reactions. These substrates were shown to be compatible with the reaction using chymotrypsinogen as a substrate. Genome-free native MS2 viral capsids have been produced and have been modified site selectively at Y85. However, these capsids have not yet been extensively modified using this reaction despite efforts at optimization for MS2 modification by screening temperature, buffer composition and pH, catalyst concentrations, and substrate concentrations. At elevated temperatures, increased modification is observed, coupled with off-site modifications as observed by SDS-PAGE and tryptic digest. Due to the desire for high modification levels for higher drug loading, and the observed heterogeneity of the MS2 capsid at the conditions required for high modification, we eventually decided to pursue alternative strategies for taxol solubilization and bioconjugation to MS2.

2.5 Material and Methods.

General Procedures and Materials

Unless otherwise noted, all chemicals were obtained from commercial sources and used without further purification. Analytical thin layer chromatography (TLC) was performed on EM Reagent 0.25 mm silica gel 60-F_{254} plates with visualization by ultraviolet (UV) irradiation at 254 nm and/or staining with potassium permanganate and/or staining with vanillin. Purifications by flash chromatography were performed using EM silica gel 60 (230-400 mesh). The eluting system for each purification was determined by TLC analysis. Chromatography solvents were used without distillation. All reactions were carried out under an argon atmosphere in flame dried glassware unless otherwise noted. All organic solvents were removed under reduced pressure using a rotary evaporator. Dichloromethane (CH_2Cl_2), tetrahydrofuran (THF), and pyridine were distilled under a nitrogen atmosphere from calcium hydride. Water (ddH_2O) used in biological procedures or as a reaction solvent was deionized using a NANOpure$_{TM}$ purification system (Barnstead, USA) purchased from Aldrich.

Instrumentation and Sample Analysis Preparations

IR. Infrared spectra were recorded from thin film samples on a sodium chloride plate using a Genesis FTIR™ (ATI Mattson, USA) or a Varian 3100 FT-IR Excalibur Series (Varian, USA).

NMR. ^{1}H and ^{13}C spectra were measured with a Bruker AVQ-400 (400 MHz) spectrometer, Bruker AVB-400 (400 MHz) spectrometer, or a Bruker AV-300 (300 MHz) spectrometer as noted. ^{1}H NMR chemical shifts are reported as δ in units of parts per million (ppm) relative to $CDCl_3$ (δ 7.26, singlet), or dimethyl sulfoxide-d_6 (δ 2.50, pentet). Multiplicities are reported as follows: s (singlet), d (doublet), t (triplet), q (quartet), dd (doublet of doublets), dt (doublet of triplets), or m (multiplet). Coupling constants are reported as a J value in Hertz (Hz). The number of protons (n) for a given resonance is indicated as nH, and is based on spectral integration values. ^{13}C NMR chemical shifts are reported as δ in units of parts per million (ppm) relative to $CDCl_3$ (δ 77.2, triplet), or dimethyl sulfoxide-d_6 (δ 39.5, septet).

Mass Spectrometry. Fast Atom Bombardment (FAB) and Electron Impact (EI) mass spectra were obtained at the UC Berkeley Mass Spectrometry Facility. Electrospray LC/MS analysis was performed using an API 150EX system (Applied Biosystems, USA) equipped with a Turbospray source and an Agilent 1100 series LC pump. Protein chromatography was performed using a Phenomenex Jupiter$_{TM}$ 300 5μ C5 300 Å reversed-phase column (2.0 mm x 150 mm) with a MeCN:ddH_2O gradient mobile phase containing 0.1% formic acid (250 μL/min). Protein mass reconstruction was performed on the charge ladder with Analyst software (version 1.3.1, Applied Biosystems). MALDI-TOF analysis was performed on a Voyager-DE instrument (Applied Biosystems), and all spectra were analyzed using Data Explorer software. The matrix solution was a 10 mg/mL solution of sinapic acid in in 50% acetonitrile, 50% water, 0.1 % TFA.

High Perfomance Liquid Chromatography. HPLC was performed on an Agilent 1100 Series HPLC System (Agilent Technologies, USA). Size exclusion chromatography was accomplished on an Agilent Zorbax$_{®}$ GF-250 with isocratic (0.5 mL/min) flow using an aqueous mobile phase (100 mM Na_2HPO_4 with 0.005% NaN_3, pH 7.2). Sample analysis for all HPLC experiments was achieved with an inline diode array detector (DAD) and an inline fluorescence detector (FLD).

Fast Performance Liquid Chromatography. Size exclusion chromatography (SEC) was performed on a BioRad$_{®}$ BioLogic$_{TM}$ DuoFlow FPLC System equipped with a HiPrep$_{TM}$ 16/60 Sephacryl$_{TM}$ S-200 High Resolution Column (Amersham Biosciences, USA) using an aqueous buffer as the mobile phase.

SDS-PAGE Analysis. For protein analysis, sodium dodecyl sulfate-polyacrylamide gel electrophoresis (SDS-PAGE) was accomplished on a Mini-Protean apparatus (Bio-Rad, USA), following the general protocol of Laemmli.[6] Commercially available markers (Bio-Rad, USA) were applied to one lane of the gel for calculation of apparent molecular weights. Visualization of protein bands was accomplished by staining with Coomassie® Brilliant Blue R-250 (Bio-Rad, USA). Gel imaging was performed on an EpiChem3 Darkroom system (UVP, USA).

Microwave reactions were conducted in 2 mL microwave vials (Biotage No. 352016) and heated in a Biotage InitiatorTM Eight microwave synthesizer. UV-Vis spectroscopic measurements were conducted on a Tidas-II benchtop spectrophotometer (J&M, Germany). Centrifugations were conducted with the following: 1) Allegra 64R Tabletop Centrifuge (Beckman Coulter, Inc.,

USA); 2) Sorvall RC5C refrigerated high-speed centrifuge (Sorvall, USA); or 3) Microfuge® 18 centrifuge (Beckman Coulter, Inc., USA). General desalting and removal of other small molecules of biological samples were achieved using Microspin G-25 spin columns (Amersham Biosciences), or NAP-5 gel filtration columns (Amersham Biosciences). Protein samples were concentrated by way of centrifugal ultrafiltration using Amicon Ultra-4 or Ultra-15 100 kD molecular weight cut off (MWCO) centrifugal filter units (Millipore), or Amicon Microcon 10 kD, 30 kD, and 100 kD MWCO (Millipore) centrifugal filter units.

***Tert*-butyl 4-formylbenzoate (11).** This compound was previously synthesized by Pritchard and co-workers, and the reported procedure was followed.[7] The desired product was isolated after flash chromatography (EtOAc:Hex) (64%). ^{1}H NMR (300 MHz, $CDCl_3$): δ, 1.61 (s, 9H) 7.92 (d, 2H, J = 5.8 Hz), 8.13 (d, 2H, J = 5.8 Hz), 10.09 (s, 1H). The obtained spectral data matched the previous report.

***Tert*-butyl 4-((*E*)-2-(methoxycarbonyl)vinyl)benzoate (15).** This compound was previously synthesized by Miwa and co-workers.[8] To a solution of methyl diethylphosphonoacetate (0.367 mL, 2.00 mmol) in 10 mL of THF at -78 °C was added dropwise 0.91 mL of a 2.2 M solution of *n*-BuLi in hexanes (2.00 mmol). After cooling for 20 min, a solution of 0.400 g of **11** (1.94 mmol) in 3 mL of THF was added to the reaction. The reaction mixture was stirred for 1 h at rt, after which 20 mL of sat. $NaHSO_4$ solution was added. The aqueous solution was extracted with two 20 mL portions of diethyl ether, and the combined organic layers were washed with brine and dried over Na_2SO_4. The resulting extract was concentrated under reduced pressure and purified by flash chromatography (EtOAc:Hex) to give 0.410 g of the product as a clear oil (86%). ^{1}H NMR (300 MHz, $CDCl_3$): δ, 1.50 (s, 9H), 3.70 (s, 1H, J = 15.9 Hz), 6.40 (d, 1H, J = 16.1 Hz), 7.45 (d, 2H, J = 8.3 Hz), 7.59 (d, 1H, J = 16.1 Hz), 7.89 (d, 2H, J = 8.3 Hz). The obtained spectral data matched the previous report.

***Tert*-butyl 4-((*E*)-2-(ethoxycarbonyl)vinyl)benzoate (16).** To a solution of triethylphosphonoacetate (1 mL, 5 mmol) in 10 mL of THF at -78 °C was added dropwise 2.28 mL of a 2.2 M solution of *n*-BuLi in hexanes (5.02 mmol). After cooling for 20 min, 1.00 g of **11** (4.85 mmol) in 3 mL of THF was added to the solution. The reaction mixture was stirred for 1 h at rt after which 20 mL of sat. $NaHSO_4$ solution was added. The aqueous solution was extracted with two 30 mL portions of diethyl ether, and the combined organic layers were washed with brine and dried over Na_2SO_4. The resulting extract was concentrated under reduced pressure and purified by flash chromatography (EtOAc:Hex) to give 0.980 g of the product as a clear oil (71%). IR (thin film): 3065, 2980, 2935, 1714, 1640, 1608, 1570 cm^{-1}, ^{1}H NMR (400 MHz, $CDCl_3$): δ, 1.34 (t, 3H, J = 7.1 Hz), 1.59 (s, 9H), 4.28 (q, 2H, J = 7.1 Hz), 6.50 (d, 1H, J = 15.9 Hz), 7.55 (d, 2H, J = 8.4 Hz), 7.69 (d, 1H, J = 16.2 Hz), 7.99 (d, 2H, J = 8.4 Hz), ^{13}C NMR (100 MHz, $CDCl_3$): δ, 14.3, 28.1, 60.7, 81.4, 120.3, 127.7, 129.9, 133.2, 138.1, 143.3, 165.1, 166.6. HRMS (EI+) calculated for $C_{16}H_{20}O_4$ ($[M]^+$) 276.13616, found 276.13984.

***Tert*-butyl 4-((*E*)-3-hydroxyprop-1-enyl)benzoate (14).** To a solution of **15** (0.500 g, 1.81 mmol) dissolved in 25 mL of CH_2Cl_2 and cooled to -40 °C was slowly added a 1 M solution of DIBALH in hexanes (3.99 ml, 1.81 mmol). After 4 h of stirring at -40 °C, the reaction was quenched with 10 mL of 1 M HCl and allowed to warm to rt. The solution was diluted with 50 mL of CH_2Cl_2, filtered through Celite, and extracted with two 50 mL portions of EtOAc. The

combined organic layers were washed with brine and dried over Na_2SO_4. Flash chromatography (EtOAc:Hex) afforded 0.280 g of product **14** as a clear oil (67%). IR (thin film): 3442, 2979, 2932, 1708, 1606 cm^{-1}, ^1H NMR (300 MHz, $CDCl_3$): δ, 1.59 (s, 9H), 4.36 (dd, 2H, J = 1.5 Hz, 5.4 Hz), 6.45 (dt, 1H, J = 5.4 Hz, 16.0 Hz), 6.65 (d, 1H, J = 16.0 Hz), 7.40 (d, 2H, J = 8.3 Hz), 7.93 (d, 2H, J = 8.4 Hz), ^{13}C NMR (75 MHz, $CDCl_3$): δ, 28.5, 63.7, 81.3, 126.4, 130.1, 130.2, 131.2, 131.2, 141.0, HRMS (EI+) calculated for $C_{14}H_{18}O_3$ ($[M]^+$) 234.12559, found 234.12539.

***Tert*-butyl 4-((*E*)-3-acetoxyprop-1-enyl)benzoate (17).** A modified procedure of S. David Tilley was followed.[3] To a solution of **14** (0.050 g, 0.21 mmol) in 10 mL of CH_2Cl_2 was added Ac_2O (0.02 mL, 0.22 mmol), pyridine (0.017 mL, 0.22 mmol), and DMAP (0.005 g, 0.04 mmol). After 30 min, the reaction mixture was diluted with 40 mL of CH_2Cl_2 and washed with three 50 mL portions of 0.1 M HCl, two 50 mL portions of sat. $NaHSO_4$ solution, and two 50 mL portions of brine. The combined organic layers were dried over Na_2SO_4, concentrated, and purified by flash chromatography (EtOAc:Hex), yielding 0.020 g of **17** as a clear oil (33%). IR (thin film): 3065, 2979, 2934, 1743, 1712, 1608, 1569 cm^{-1},^1H NMR (300 MHz, $CDCl_3$): δ, 1.59 (s, 9H), 2.11 (s, 3H), 4.74 (d, 2H, J = 6.1 Hz), 6.37 (dt, 1H, J = 6.2 Hz, 15.9 Hz), 6.67 (d, 1H, 16.0 Hz), 7.41 (d, 2H, J = 8.3 Hz), 7.93 (d, 2H, J = 8.3 Hz), ^{13}C NMR (100 MHz, $CDCl_3$): δ, 21.0, 28.2, 64.8, 81.1, 125.6, 126.3, 129.3, 131.4, 133.0, 140.1, 165.5, 170.8. LRMS (FAB+) calculated for $C_{16}H_{20}O_4$ ($[M]^+$) 276, found 276.

4-(*Tert*-butoxycarbonyl)cinnamyl 4-nitrophenyl carbonate (18). A modified procedure of S. David Tilley was followed.[3] A solution of **14** (0.116 g**,** 0.500 mmol) and pyridine (0.08 mL, 1 mmol) in 10 mL of CH_2Cl_2 was slowly added a solution of nitrophenyl chloroformate (0.300 g, 1.49 mmol) dissolved in 10 mL of CH_2Cl_2. The reaction mixture was stirred for 1 h until complete conversion was observed by TLC. The reaction mixture was washed with three 30 mL portions of 0.1 M HCl, five 30 mL portions of sat. $NaHSO_4$ solution, two 50 mL portions of H_2O, and one 30 mL portion of brine. The crude product was dried over Na_2SO_4, concentrated, and purified by flash chromatography (EtOAc:Hex), giving 0.020 g of **18** as a white solid (10%). IR (thin film): 3120, 3088, 2979, 2934, 1768, 1709, 1608, 1595, 1570, 1527, 1493 cm^{-1}, ^1H NMR (400 MHz, $CDCl_3$): δ, 1.60 (s, 9H), 4.96 (dd, 2H, J = 1.2 Hz, 6.5 Hz), 6.44 (dt, 1H, J = 6.5 Hz, 15.9 Hz), 6.80 (d, 1H, J = 15.8 Hz), 7.41 (d, 2H, J = 9.2 Hz), 7.45 (d, 2H, J = 8.3 Hz), 7.96 (d, 2H, J = 8.4 Hz), 8.29 (d, 2H, J = 9.2 Hz), ^{13}C NMR (100 MHz, $CDCl_3$): δ, 28.2, 69.4, 81.2, 121.8, 123.5, 125.4, 126.6, 129.9, 131.9, 134.0, 139.6, 145.5, 152.4, 155.5, 165.4, HRMS (EI+) calculated for $C_{21}H_{21}NO_7$ ($[M]^+$) 399.13180, found 399.13141.

(*E*)-3-(4-bromophenyl)acrylic acid (2). This compound was previously synthesized by Mikroyannidis and co-workers.[9] A previously reported procedure of Khosropour was modified for the synthesis of **2**.[10] Bromobenzaldehyde (0.370 g, 2.00 mmol), malonic acid (0.208 g, 2.00 mmol), and piperazine (0.172 g, 2.00 mmol) were added to 2 mL of DMF in a microwave vial, and microwaved for 4 min at 200 °C. The resulting clear orange solution was added dropwise to 100 mL of 0.1 M HCl, and the pale orange precipitate was collected and dried by filtration (1.28 g, 56%). ^1H NMR (300 MHz, DMSO): δ, 6.54 (d, 1H, J = 15.9 Hz), 7.54 (d, 1H, J = 16.5 Hz), 7.58 (d, 2H, J = 9.0 Hz), 7.64 (d, 2H, J = 8.7 Hz), 12.54 (s, 1H). The obtained spectral data matched the previous report.

(*E*)-methyl 3-(4-bromophenyl)acrylate (3). A modified procedure of Stone was followed.[11] To

a suspension of **2** (2.400 g, 10.48 mmol) in 200 mL of MeOH was added 1.1 mL of $SOCl_2$ (15 mmol) and the reaction mixture heated to reflux. Approximately 5 mL of additional $SOCl_2$ was added until the solid was completely dissolved. The dark orange solution was heated at reflux for 3 h and the solvent removed under reduced pressure, leaving crude product as orange crystals. After purification by flash chromatography (EtOAc:Hex), 1.3 g of product was isolated as a pale yellow solid (52%). ^{1}H NMR (300 MHz, $CDCl_3$): δ, 3.81 (s, 3H), 6.43 (d, 1H, J = 15.9 Hz), 7.39 (d, 2H, J = 8.2 Hz), 7.52 (d, 2H, J = 7.4 Hz), 7.63 (d, 1H, J = 15.9 Hz). The obtained spectral data matched the previous report.

(*E*)-3-(4-bromophenyl)prop-2-en-1-ol (4). This compound was previously synthesized by Avery and co-workers.[12] To a solution of **3** (0.100 g, 0.415 mmol) in 2 mL of CH_2Cl_2 and cooled to -78 °C was slowly added 1.3 mL of a 1 M solution of DIBALH in hexanes. After 5 min, 3 mL of 0.1 M HCl was added and the mixture was warmed to rt. After filtering through Celite, the organic layer was dried over Na_2SO_4 and concentrated under reduced pressure to yield 0.062 g of **4** as a yellow solid (73%). ^{1}H NMR (300 MHz, $CDCl_3$): δ, 4.31 (d, 2H, J = 5.1 Hz), 6.35 (dt, 1H, J = 5.5 Hz, 15.9 Hz), 6.56 (d, 1H, J = 15.9 Hz), 7.24 (d, 2H, J = 8.0 Hz), 7.43 (d, 2H, J = 8.5 Hz).

(4-Bromocinnamyloxy)trimethylsilane (5). A round-bottom flask was charged with **4** (0.062 g, 0.24 mmol), TMSCl (0.034 mL, 0.26 mmol), DIPEA (0.046 mL, 0.26 mmol), DMAP (0.003 g, 0.02 mmol), and 6 mL of CH_2Cl_2 and the resulting mixture stirred for 12 h. The resulting mixture was purified directly by flash chromatography (EtOAc:Hex) yielding 0.060 g of product as a pale yellow solid (87%). ^{1}H NMR (300 MHz, $CDCl_3$): δ, 0.17 (s, 9H), 4.48 (dd, 2H, J = 1.6 Hz, 5.2 Hz), 6.28 (dt, 1H, J = 5.2 Hz, 15.8 Hz), 6.52 (d, 1H, J = 15.8 Hz), 7.24 (d, 2H, J = 8.5 Hz), 7.42 (d, 2H, J = 8.5 Hz).

(4-Bromocinnamyloxy)(*tert*-butyl)dimethylsilane (6). This compound was previously synthesized by Couladorous and co-workers, and the reported procedure was followed.[13] A round-bottom flask was charged with **4** (0.400 g, 1.88 mmol), TBSCl (0.317 g, 2.07 mmol), imidazole (0.320 g, 4.70 mmol), and 2 mL of DMF and the resulting mixture stirred for 1 h. The solution was diluted with 50 mL of EtOAc, and washed with four 50 mL portions of H_2O, one 50 mL portion of 0.1 M HCl, one 50 mL portion of brine and dried over Na_2SO_4. Flash chromatography (EtOAc:Hex) afforded 0.586 g of product **6** as a white solid (95%). ^{1}H NMR (400 MHz, $CDCl_3$): δ, 0.11 (s, 6H), 0.94 (s, 9H), 4.33 (dd, 2H, J = 1.8 Hz, 4.9 Hz), 6.27 (dt, 1H, J = 4.9 Hz, 15.8 Hz), 6.53 (d, 1H, J = 15.8 Hz), 7.23 (d, 2H, J = 8.4 Hz), 7.42 (d, 2H, J = 8.5 Hz). The obtained spectral data matched the previous report.

(4-Formylcinnamyloxy)(*tert*-butyl)dimethylsilane (7). This compound was previously synthesized by Berthiol and co-workers.[14] To a solution of **6** (0.300 g, 0.917 mmol) in 10 mL of THF and cooled to -78 °C was slowly added 1.14 mL of a 1.77 M solution of *n*-BuLi in hexanes (2.02 mmol). After stirring for 30 min, DMF was dripped into the reaction mixture. After stirring for one hour, the solution was warmed to rt and stirred for another hour. The solution was diluted with 50 mL of EtOAc, and washed with two 50 mL portions of H_2O, one 50 mL portion of brine and dried over Na_2SO_4. The solvent was removed under reduced pressure and flash chromatography (EtOAc:Hex) afforded 0.125 g of product **7** as a white solid (50%). ^{1}H NMR (300 MHz, $CDCl_3$): δ, 0.12 (s, 9H), 0.95 (s, 9H), 4.39 (dd, 2H, J = 1.8 Hz, 4.5 Hz), 6.46 (dt, 1H, J = 4.5 Hz, 15.8 Hz), 6.68 (d, 1H, J = 15.9 Hz), 7.52 (d, 2H, J = 8.2 Hz), 7.82 (d, 2H, J = 8.3 Hz). The obtai-

ned spectral data matched the previous report.

(*E*)-4-(3-hydroxyprop-1-en-1-yl)benzaldehyde (8). A 15 mL Falcon tube was charged with a solution of **7** (50 mg, 0.181 mmol) in 1.81 mL THF and cooled to 0 °C. To the solution was added dropwise 0.543 mL HF·pyridine (3 eq, 0.543 mmol). After stirring for 10 min, no starting material was observed by TLC, and the reaction was quenched with 20 mL saturated $NaHCO_3$. After extraction with three 50 mL portions of ethyl acetate, the organic layers were combined and washed with three portions of 0.1 M HCl, one portion of brine, and dried over Na_2SO_4. The solvent was removed under reduced pressure and flash chromatography (1:1 EtOAc:Hex) afforded 21.5 mg of product **8** as a white solid (73%). ^{1}H NMR (300 MHz, $CDCl_3$): δ, 4.39 (t, 2H, J = 5.5 Hz), 6.53 (dt, 1H, J = 16.0, 5.2 Hz), 6.70 (d, 1H, J = 16.0 Hz), 7.53 (d, 2H, J = 8.1 Hz), 7.83 (d, 2H, J = 8.2 Hz), 9.98 (s, 1H).

(*E*)-3-(4-formylphenyl)allyl acetate (9). To a solution of **8** (15 mg, 0.093 mmol) in 2 mL CH_2Cl_2 and 2 mL pyridine was added acetic anhydride (0.127 mmol, 0.012 mL) and 0.01 g DMAP. After 12 h, the reaction was diluted with ethyl acetate, washed with three portions of 0.1 M HCl, two portions of saturated $NaHCO_3$, one portion of brine, and dried over Na_2SO_4. The solvent was removed under reduced pressure and flash chromatography (1:3 EtOAc:Hex) afforded product **9** as a white solid. ^{1}H NMR (400 MHz, $CDCl_3$): δ, 2.12 (s, 3H), 4.76 (d, 2H, J = 6.1Hz), 6.44 (dt, 1H, J = 6.1, 15.9 Hz), 6.70 (d, 1H, J = 15.9 Hz), 7.54 (d, 2H, J = 8.0 Hz), 7.84 (d, 2H, J= 8.0 Hz), 9.99 (s, 1H).

(*E*)-5-((3-(4-formylphenyl)allyl)oxy)-5-oxopentanoic acid (20). To a solution of **8** (15 mg, 0.093 mmol) in 2 mL CH_2Cl_2 and 0.015 mL pyridine was added glycolic anhydride (2 eq, 0.185 mmol, 21.1 mg) and one flake of DMAP. After 12 h, the reaction was diluted with ethyl acetate, washed with three portions of 0.1 M HCl, one portion of brine, and dried over Na_2SO_4. The solvent was removed under reduced pressure, and flash chromatography (1:1 EtOAc:Hex) afforded product **20** as a white solid (42%). ^{1}H NMR (300 MHz, $CDCl_3$): 2.00 (p, 2H, J = 7.3 Hz), 2.47 (td, 4H, J = 7.3, 3.3 Hz), 4.78 (d, 2H, J = 5.9 Hz), 6.43 (dt, 1H, J = 15.9, 6.1 Hz), 6.70 (d, 1H, J = 16.0 Hz), 7.54 (d, 2H, J = 8.0 Hz), 7.84 (d, 2H, J = 8.2 Hz), 9.99 (s, 1H).

Experimental – Protein Experiments

Bacteriophage MS2. Routine propagation of MS2 was carried out in a one-liter batch process using a modified procedure of Strauss and Sinsheimer[15] developed by Ernest Kovacs.[2] The growth medium for the host bacteria, *E. coli*, was prepared by the addition of 10 g of TryptoPeptone, 5 g of Bacto$_{TM}$ Yeast Extract, and 8 g of NaCl to 1 L of ddH_2O. After autoclave sterilization of the resulting broth, 10 mL of sterile 10% glucose solution, 2 mL of sterile 1 M $CaCl_2$ solution, and 1 mL of a sterile solution of 10 mg/mL thiamine hydrochloride solution were added. Culture media were infected with revived Hfr+ *E. coli* that had been grown from a single colony originally isolated from a freeze-dried pellet (American Type Culture Collection, ATCC, No. 15669; Rockville, MD). The infected culture was incubated at 37 °C under aerobic conditions until an optical density (OD) of 0.2 at 600 nm was reached, signifying exponential growth of the host bacteria. Inoculation of the bacteria was accomplished by the addition of a small aliquot of MS2 suspension (stored at 4 °C) that had previously been propagated from purchased stock (ATCC No.15597-B1) by a similar procedure. Propagation of the virus was carried out at 37 °C

for at least 4 h, but typically overnight to ensure complete lysis of the bacterial culture. Isolation of the MS2 phage was performed by separation of lysed bacterial debris by centrifugation at 4500 rcf for 30 min at 4 °C, followed by selective precipitation by the addition of 10% (w/v) poly(ethylene glycol)-6000 and NaCl to a final concentration of 0.5 M. The precipitated MS2 was then separated from the supernatant by centrifugation at 13,000 rcf for 1 h at 4 °C. The resulting pellet was resuspended in 50 mL of aqueous buffer (0.5 M Na_2PO_4, 0.1 M NaCl, pH 7.2) and passed through a 0.22 μm sterile filter (Millipore Corp., USA) under vacuum to afford MS2 phage as the only protein in solution, as determined by SDS-PAGE. Further purification of MS2 by FPLC was performed to remove residual polymer from the precipitation step.

Empty MS2 Capsids from phage (large scale preparation) (mtMS2). To a 40 mL solution of MS2 virions (typically 1 mg/mL in 10 mM NaH_2PO_4, pH 7.2 buffer) was added 10 mL of a high concentration buffer (500 mM Na_2HPO_4, pH 11.8). The resulting solution was incubated at rt for 1 h and then treated with 10% (w/v) poly(ethylene glycol)-6000 and NaCl to a final concentration of 0.5 M. The precipitate was separated via centrifugation and then dissolved in 40 mL of an aqueous buffer (10 mM Na_2HPO_4, pH 7.2) by gentle inversion. The process (pH adjustment and precipitation) was repeated two additional times. The final precipitate mixture was centrifuged at 10,000 rcf for 30 min at 4 °C and the pellet was dissolved in a minimal volume (typically 5-10 mL) of aqueous buffer (10 mM Na_2HPO_4, pH 7.2). Any insoluble material was removed by centrifugation and the clarified solution was passed through a gel filtration column via FPLC-SEC (as outlined above). The overall process afforded empty capsids in 80-90% yield of the initial phage as determined by UV measurements at 260 nm ($OD_{260}/8.03 \approx$ concentration of capsids in mg/mL).

Preparation of catalyst/ligand solution for protein modification reactions.[3] To a mixture of $Pd(OAc)_2$ (6.9 mg) and Strem TPPTS (110.4 mg) (1:5 Pd/unoxidized ligand, taking into account previously determined amounts of phosphine oxide and DMSO contaminants) was added 3.74 mL of distilled water. After sparging with nitrogen for 1 min, the mixture was sonicated until the $Pd(OAc)_2$ was dissolved. The solution was again sparged with nitrogen for an additional 30 min to yield a homogeneous bright yellow solution. This solution was stored in sealed ampules under argon.

Typical protein reaction with allylic substrate 9. A solution of mtMS2 (4 μL, 240 μM, final concentration = 100 μM, 1 equiv.) was diluted by adding 12.5 μL of phosphate buffer (100 mM, pH 10.0). To this solution was then added **9** (1 μL, 20 mM in DMSO, final concentration = 1 mM, 10 equiv, 5% DMSO) and catalyst mixture (1 μL, 8 mM $Pd(OAc)_2$, 2 mM TPPTS, final concentration = 400 μM $Pd(OAc)_2$, 4 equiv; 2 mM TPPTS, 20 equiv). The reaction mixture was incubated at rt for 1 h.

Typical conjugation of aldehyde-modified protein and alkoxyamine for gel analysis. After 1 h of reaction as described above, 10 μL of the reaction mixture was exchanged into pH 7 phosphate buffer. An aliquot of the protein solution (2 μL, 100 μM) was mixed with PEG-2K alkoxyamine (1 μL, 50 mM), or Alexafluor 488 alkoxyamine (0.5 μL, 5 mM). After 12 h, loading buffer was added to bring the total volume to 10 μL, followed by gel analysis.

Preparation of modified protein for LC/MS analysis: NAP-5 purification. A typical protein

reaction was carried out as described above. To a pre-equilibrated NAP-5 column was added the reaction mixture (diluted to a total volume of 200 μL in phosphate buffer). After the solution had settled into the gel bed, additional phosphate buffer (300 μL) was added to account for the void volume of the column. The protein solution was then eluted with phosphate buffer (1.5 mL). The partially purified reaction mixture was then concentrated by centrifugation against 10 kDa MWCO spin concentrators to a final volume of 20 μL.

Preparation of modified protein for LC/MS analysis: Spin Column purification. A typical protein reaction was carried out as described above. The reaction mixture was applied to a spin column previously equilibrated with phosphate buffer. After centrifugation, the partially purified reaction mixture was then, if necessary, concentrated by centrifugation against 10 kDa MWCO spin concentrators to a final volume of 20 μL.

Procedure for trypsin digest. An aliquot of a NAP5-purified (into 10 mM pH 7 phosphate buffer) typical MS2 bioconjugation reaction (75 μL) wass mixed with sequencing grade trypsin (1.27 uL, in 50 mM AcOH), and MeCN (8.4 μL). The mixture was allowed to incubate at 37 °C for 4-12 h in a warm water bath. The reaction mixture was desalted using C18 Zip-tips and spotted on a MALDI plate for analysis by MALDI-TOF.

2.6 References.

1. (a) Singla, A., Garg, A., Aggarwal, D. Paclitaxel and its formulations. *Int. J. Pharm.* **2002**, *235*, 179-192; (b) Tije, A. J., Verweij, J., Loos, W. J., Sparreboom, A. Pharmacological effects of formulation vehicles: implications for cancer chemotherapy. *Clin. Pharmacokinet.* **2003**, *42*, 665-685.
2. Hooker, J.M., Kovacs, E.W., Francis, M.B. Interior surface modification of bacteriophage MS2. *J. Am. Chem. Soc*. **2004**, *126,* 3718-3719.
3. Tilley, S. D., Francis, M. B. Tyrosine-selective protein alkylation using pi-allylpalladium complexes. *J. Am. Chem. Soc.* **2006**, *128*, 1080-1081.
4. (a) Wang, B., Zhang, H., Zheng, A., Wang, W. Coumarin-Based Prodrugs. Part 3: Structural Effects on the Release Kinetics of Esterase-sensitive Prodrugs of Amines. *Bioorg. Med. Chem.* **1998**, *6*, 417-426; (b) Menger, F. M., Ladika, M. Remote enzyme-coupled amine release. *J. Org. Chem.* **1990**, *55*, 3006-3007.
5. (a) Trail, P. A., Willner, D., Lasch, S. J., Henderson, A. J., Hofstead, S., Casazza, A. M., Firestone, R. A., Hellstrom, I., Hellstrom, K. E. Cure of xenografted human carcinomas by BR96-doxorubicin immunoconjugates. *Science* **1993**, *261*, 212-215; (b) Willner, D., Trail, P. A., Hofstead, S. J., King, H. D., Lasch, S. J., Braslawsky, G. R., Greenfield, R. S., Kaneko, T., Firestone, R. A. (6-Maleimidocaproyl)hydrazone of doxorubicin. A new derivative for the preparation of immunoconjugates of doxorubicin. *Bioconjug. Chem.* **1993**, *4*, 521-527.
6. Laemmli, U. K. Cleavage of structural proteins during the assembly of the head of bacteriophage T4. *Nature* **1970**, *227*, 680.
7. Adlington, R. M., Baldwin, J. E., Becker, G. W., Chen, B., Cheng, L., Cooper, S. L., Hermann, R. B., Howe, T. J., McCoull, W., McNulty, A. M., Neubauer, B. L., Pritchard, G. J.

Design, Synthesis, and Proposed Active Site Binding Analysis of Monocyclic 2-Azetidinone Inhibitors of Prostate Specific Antigen. *J. Med. Chem.* **2001**, *44*, 1491-1508.

8. Miwa, T., Hitaka, T., Akimoto, H. A. Novel Synthetic Approach to Pyrrolo[2,3-d]pyrimidine Antifolates. *J. Org. Chem.* **1993**, *58*, 1696-1701.
9. Mikroyannidis, J., Spiliopoulos, I. K., Kasimis, T. S. Kulkarni, A.P., Jenekhe, S.A. Synthesis, Photophysics, and Electroluminescence of Conjugated Poly(p-phenylenevinylene) Derivatives with 1,3,4-Oxadiazoles in the Backbone. *Macromolecules* **2003**, *36*, 9295-9302.
10. Khosropour, A. R., Khodaei, M. M., Moghanian, H. Synthesis of trans-cinnamic acids from aryl aldehydes and aryl aldehyde bisulfite adducts with malonic acid using piperazine. *J. Chem. Res.* **2005**, *6*, 364-365.
11. Stone, M. J., Van Dyk, M. S., Booth, P.M., Williams, D. H. An approach to a synthetic carboxylate-binding pocket based on β-avoparcin. *J. Chem. Soc. Perkin Trans. 1* **1991**, *7*, 1629-1635.
12. Avery, T. D., Caiazza, D., Culbert, J. A., Taylor, D. K., Tiekink, E. R. T. 1,2-Dioxines Containing Tethered Hydroxyl Functionality as Convenient Precursors for Pyran Syntheses. *J. Org. Chem.* **2005**, *70*, 8344-8351.
13. Couladouros, E. A., Soufli, I. C., Moutsos, V. I., Chadha, R. K. Total Synthesis of Combretastatins D. *Chem. Eur. J.* **1998**, *4*, 33-43.
14. Berthiol, F., Doucet, H., Santelli, M. Heck Reaction of Protected Allyl Alcohols with Aryl Bromides Catalyzed by a Tetraphosphanepalladium Complex. *Eur. J. Org. Chem.* **2005**, 1367-1377.
15. (a) Strauss, J., Sinsheimer, R. Purification and properties of bacteriophage MS2 and of its ribonucleic acid. *J. Mol. Biol.* **1963**, *7*, 43-54; (b) Cargile, B.J., McLuckey, S.A., Stephenson, J.L., Jr. Identification of Bacteriophage MS2 Coat Protein from E. coli Lysates via Ion Trap Collisional Activation of Intact Protein Ions. *Anal. Chem.* **2001**, *73*, 1277-1285.

Chapter 3: A tri-functional linker for interior modification of N87C MS2 with taxol

3.1 Introduction.

Due to the difficulties in adapting our group's tyrosine modification strategy for the installation of drug cargo selectively to the interior of the MS2 capsid, we turned to thiol alkylation chemistry and an MS2 mutant containing a uniquely reactive cysteine on the interior surface of the capsid. The wild-type MS2 coat protein contains 2 cysteine residues near the exterior surface of the capsid; however, these have previously been observed to exhibit diminished reactivity due to their poor solvent accessibility.[1] Therefore, an amino acid on the interior of the capsid was mutated to a cysteine (N87C) to provide a sulfhydryl group for the attachment of cargo (Figure 3-1). The assembled mutant MS2 capsids can be accessed by recombinant expression of the coat protein,[2] yielding non-infectious genome-free particles with adjustable amino acid composition.

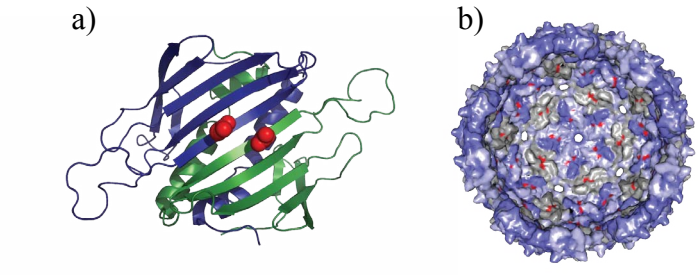

Figure 3-1. Crystal structure representation of the N87C mutant of MS2. a) Interior dimer perspective,with the position 87 highlighted in red. b) An assembled capsid hemisphere viewing the interior surface, with position 87 highlighted in red.

The drug we chose to attach to the MS2 capsid was taxol, a potent chemotherapeutic used in current treatment of breast, lung, and ovarian cancers.[3] However, as discussed previously, taxol suffers from prohibitively low water solubility and therefore must be administered over long periods of time as an infusion containing a toxic detergent.[4] Although the attachment of taxol to a water soluble protein carrier would increase the solubility of the drug during delivery, it was necessary to first solubilize the drug molecule in water to allow protein bioconjugation. Portions of the work described in this chapter have been reported in a separate publication.[5]

3.2 Linker synthesis.

The first attempt to build a water-soluble taxol molecule with cysteine modification functionality was simply to use a commercially available bifunctional PEG molecule. PEG functionalization has been shown to increase the solubility of various drugs, as well as other improvements to biodistribution. The molecule we used was a discrete PEG that contains an NHS-ester on one end and maleimide on the other. The NHS-ester would be used to attach taxol through creation of the 2'-OH ester, while the maleimide could then be used for cysteine modification. A variety

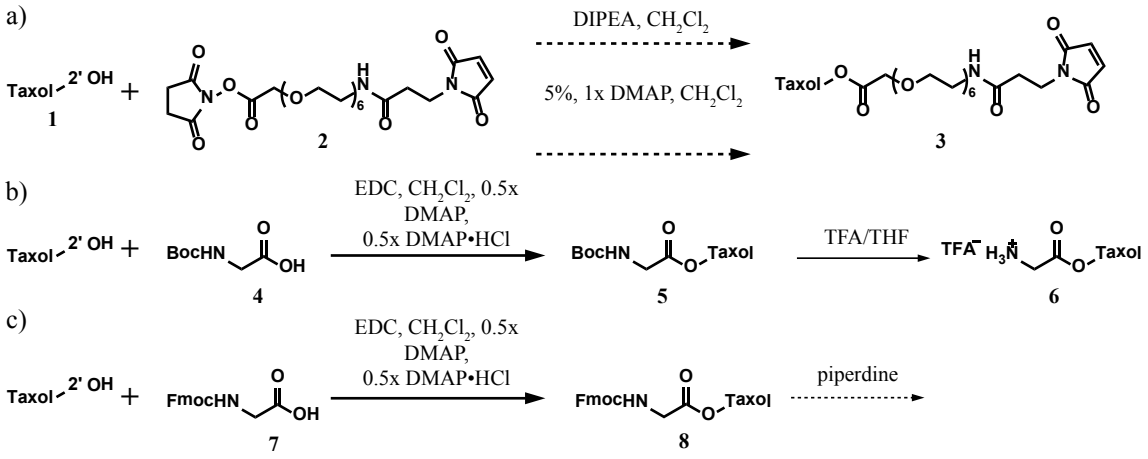

Figure 3-2. Efforts to derivatize Taxol at the 2' OH group. a) Using commercially available $SM(PEG)_6$. b) Ester formation with Boc protected glycine. c) Ester formation with Fmoc protected Glycine.

of bases were used to attempt to effect the ester formation. However, no reaction was observed in any of the tested conditions (Figure 3-2a).

Since one limitation for the ester formation step was the sensitivity of the maleimide functionality, we next attempted to derivatize taxol using a glycine linker. Both Fmoc and Boc protected glycines were successfully attached to taxol at its 2'-OH hydroxyl group (Figure 3-2b-c).[6] However, the respective deprotection steps proved to be difficult, leading to poor recovery of stable products. A literature search showed similar observations by others attempting to derivatize taxol at the 2'-OH group.[7] While several custom amine protecting groups proved possibly effective, we decided to pursue an alternative strategy to taxol modification.

A promising strategy found in the literature was the modification of taxol's 2'-OH using succinic anhydride, revealing a carboxylic acid for further modification, while creating an ester bond that slowly hydrolyzes to release taxol (Figure 3-3).[8] Since this carboxylic acid would not directly react with the PEG molecule as planned above, we sought to design a linker of our own that would incorporate cysteine modification functionality while also increasing water solubility. To do this, we turned to two readily available tri-functional molecules – the amino acids cysteine and lysine. Using cysteine, we envisioned utilizing the thiol functionality for disulfide exchange, and for the lysine molecule, we planned to derivatize the side chain ε-amine as either the maleimide or the iodoacetamide for MS2 modification by cysteine nucleophilic addition.

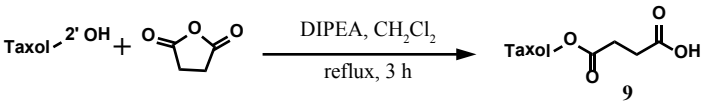

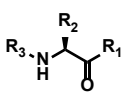

R_1, R_2, R_3 = 1) Taxol, 2) water-solublizing group, and 3) cysteine modifying group, in some order.

Figure 3-3. a) Elaboration of Taxol at the 2' OH using succinic anhydride. b) Amino-acid based trifunctional linker for imparting water solubility and bioconjugation functionality to Taxol.

To construct the cysteine based linker (Figure 3-4) we started off with the Boc protection of the cysteine amine under standard basic conditions with Boc_2O. Disfulide exchange with 2,2'-dithiodipyridine afforded the oxidized thiol as the pyridyl disulfide. The carboxylic acid was then activated as the NHS-ester through a standard DCC reaction, and the activated ester was where we attempted to impart water solubility via reaction with taurine, a molecule containing both an amine for reaction with the NHS-ester and sulfonate to increase charge and water solubility. However, this final step proved difficult due to solubility issues and the sensitivity of the disulfide bond to various reaction conditions.

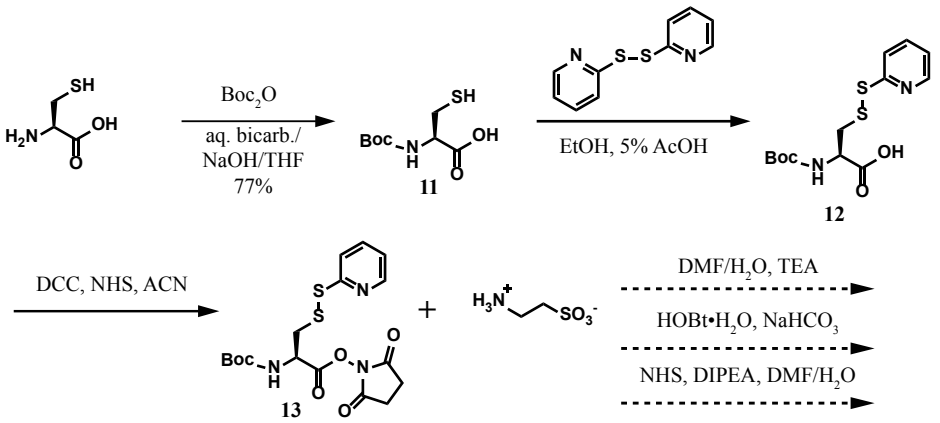

Figure 3-4. Synthetic route to form a trifunctional cysteine disulfide based linker. Various conditions were attempted to attach the charged sulfonate for increased water solubility.

In parallel we also sought to synthesize the analogous lysine based molecule. Early efforts of maleimide synthesis using *N*-(methoxycarbonyl) maleimide (Figure 3-5a) proved ineffective on both amines of lysine, as well as several linear amines. We ultimately discovered in the literature an extremely effective maleimide synthesis procedure of amino acids based on the one-pot ring opening and ring closing of maleic anhydride by primary amines and the concurrent activation of the acid as the NHS-ester (Figure 3-5b).[9] This reaction ran to completion on the simple

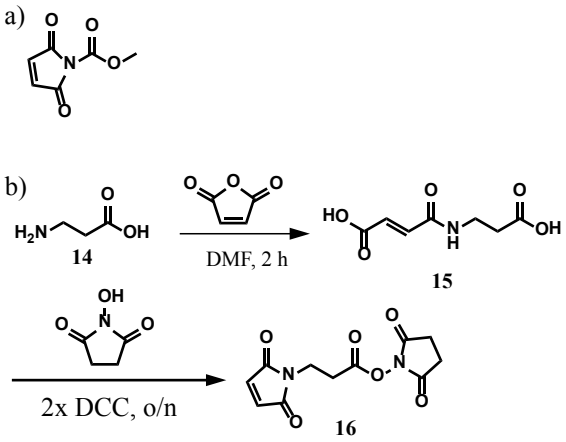

Figure 3-5. a) *N*-(methoxycarbonyl) maleimide. b) Procedure for NHS-maleimide synthesis from amino acid precursors.

amino acids, such as beta-alanine, and we attempted to effect the same reaction using a mono-BOC protected lysine molecule, proving most effective in the situation where the maleimide was formed at the side chain amine (Figure 3-6). Taurine was dissolved in water and reacted with the activated acid in a final solvent ratio of 4:1 DMF/water with 2 equivalents of amine base to install the sulfonate group as a water-solubilizing agent. This was followed by TFA deprotection to liberate the lysine α-amino group for attachment to taxol. To install a suitable attachment group, the 2′-OH of taxol was reacted with succinic anhydride to transform the hydroxyl group into a carboxylic acid functionality (according to a previous literature procedure[6]), which was then attached to **9** under HATU-mediated amide bond forming conditions. After solid phase extraction with an anion exchange resin, crude **21** was purified by reversed phase HPLC and used as a 20 mM solution in DMF. This molecule was also soluble in water and buffer at concentrations up to 2 mM.

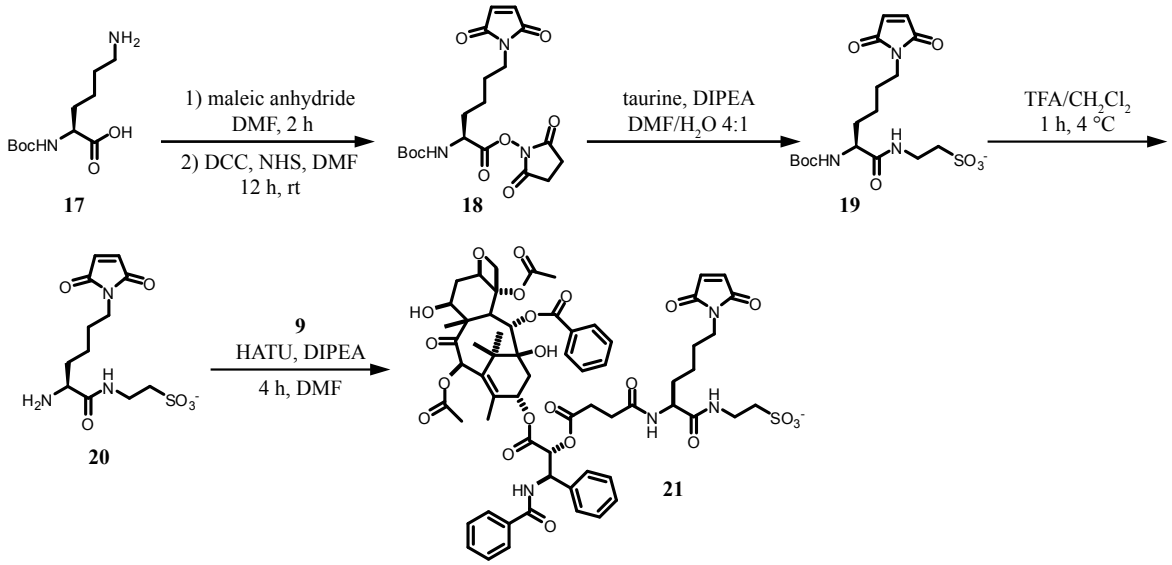

Figure 3-6. Synthetic route to water soluble, maleimide functionalized Taxol.

3.3 MS2 modification with a water-soluble taxol-maleimide.

Reaction of the maleimide group of **21** with the sulfhydryl group of N87C MS2 was achieved at room temperature in 10 mM phosphate buffer at pH 7 (Figure 3-7a). Five equivalents of **21** were added to N87C MS2 and the reaction allowed to proceed for 1 h. The use of higher pH buffers resulted in detectable degradation of the taxol component. The modified capsids were purified from small molecules via size exclusion chromatography. ESI-MS analysis (Figure 3-7b) of the capsid monomers showed significant levels of single modification, while wild type MS2 showed no modification under the same reaction conditions. Thus, the modification is most likely entirely confined to the cysteine residue introduced on the capsid interior. For analysis purposes, reversed phase HPLC (Figure 3-7c) was used to separate modified and unmodified MS2 monomers, allowing the level of conjugation to be quantified. Integration of the tryptophan fluorescence peaks showed up to 65% modification of the MS2 monomer proteins, which translated to ~110 molecules of taxol per capsid, or approximately 2% loading by weight.

3.4 Modified MS2 characterization.

The attachment of so many hydrophobic molecules to the capsid could potentially disturb the stability of the protein assembly. It was therefore necessary to ensure that modified MS2 protein still retained the capsid form. Size exclusion chromatography (Figure 3-7d) indicated that the protein remained as intact capsids. TEM imaging (Figure 3-7g) confirmed the presence of assembled capsids, while dynamic light scattering (DLS) measurements (Figure 3-7e) showed that the modified MS2 capsids were of comparable diameter to wild-type MS2. Thermal denaturation experiments (also followed by DLS) indicated that the capsids were stable up to 64 °C (Figure 3-7f). The modified capsids remained soluble in phosphate buffer at 200 µM (based on MS2 monomer). Higher concentrations of the MS2 conjugates were not examined.

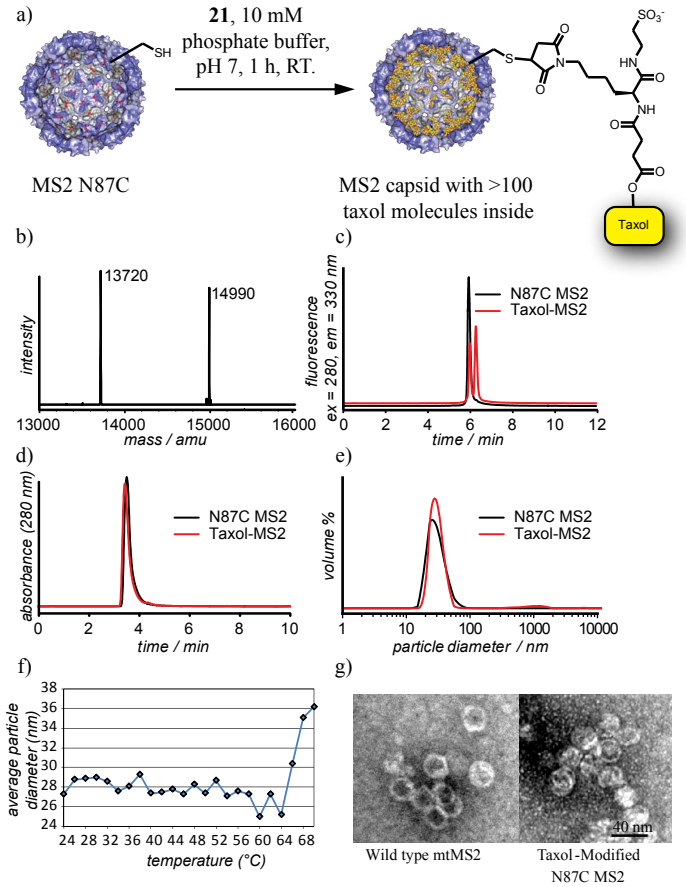

Figure 3-7. a) Synthesis of taxol-MS2 conjugates. b) ESI-MS reconstruction of N87C MS2 and the taxol-MS2 conjugate. Expected mass of N87C MS2 *m/z* [M + H$^+$] = 13719 amu. Expected mass of taxol-MS2 *m/z* [M + H$^+$] =14987 amu. c) Reversed-phase HPLC was used to quantify the modification level based on the increased retention caused by the hydrophobic taxol group. d) Size exclusion chromatography and e) dynamic light scattering analysis of N87C MS2 and Taxol-MS2 confirmed that the capsids remained assembled after modification. f) Thermal stability of MS2-taxol conjugates, as measured using DLS. Capsid instability (which results in aggregation) occurs at temperatures above 64 °C. g) TEM images of modified MS2.

Antibody binding experiments were performed to confirm the presence of taxol on the interior of N87C MS2 capsids. Western blot analysis (Figure 3-8a) showed the presence of taxol only

on the N87C MS2 mutants. Wild-type capsids that had been exposed to maleimide **21** gave no signal, providing further evidence that the native cysteines in the MS2 coat protein were unreactive. The internal location of the taxol molecules was confirmed by performing an immuno dot blot (Figure 3-8b) on intact versus GnHCl-denatured MS2 capsids. α-MS2 antibodies were used to assay for the presence of MS2 protein with similar results, while α-taxol antibodies showed significantly different signal intensities for intact and denatured capsids. Presumably, the taxol molecules on the interior of the capsid are blocked from interacting with the antibodies, which are not able to fit through the capsid pores to access the interior surface. These molecules are only able to interact with the antibodies upon protein denaturation and capsid disassembly.

To determine capsid stability under physiological conditions, samples of MS2 internally labelled with Oregon Green 488 maleimide (to facilitate detection) were incubated for 6 d at 37 ºC in PBS, 10% FBS, and cell culture media. In each case, SEC analysis revealed that >80% of the initial protein sample remained as assembled capsids (Figure 3-9a). Thus, little disassembly is to be expected in the absence of cellular targets.

3.5 Taxol release and cytotoxicity measurements.

A taxol release profile was also determined at pH 7.4. Samples of MS2-taxol conjugates were incubated in 10% FBS for 5 d. At 24 h intervals, samples were taken and the remaining capsids were isolated via selective PEG precipitation

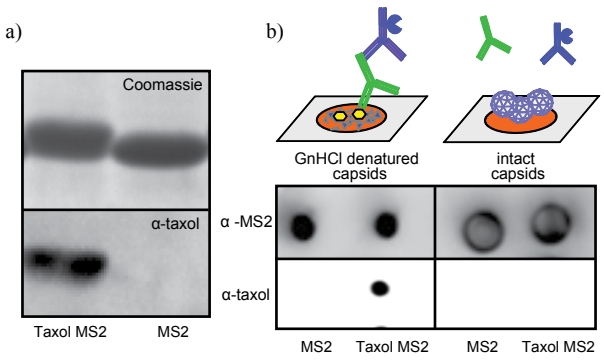

Figure 3-8. Antibody analysis of taxol-MS2 conjugates a) Western blot analysis indicated the presence of taxol on MS2 capsid monomers. b) Immuno dot blot analysis showed different responses to taxol molecules attached to denatured monomers (left) and inside assembled capsids (right).

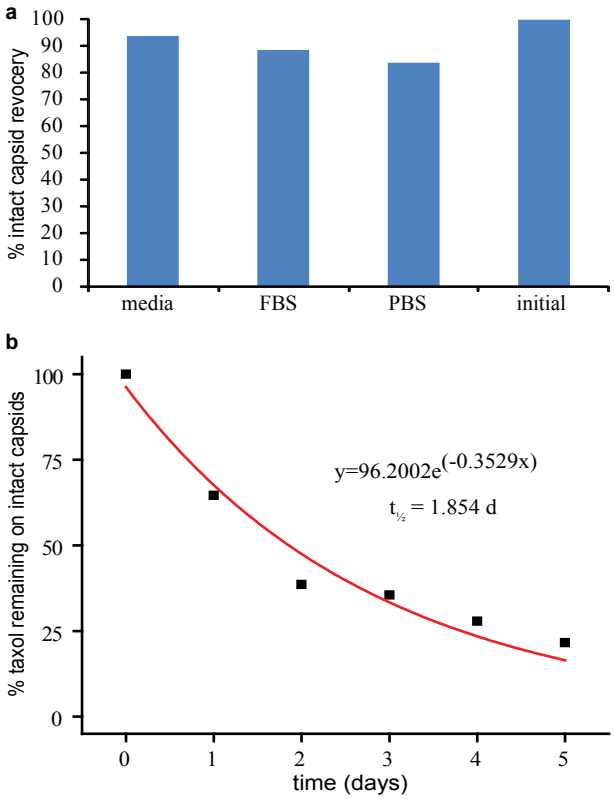

Figure 3-9. Stability of MS2 conjugates under cell culture conditions. a) Samples of MS2 capsids labeled with Oregon Green maleimide at C87 were incubated at 37 °C for six days in the indicated solutions. Following this, the samples were analyzed using SEC. The amounts of the intact capsids remaining were quantified using the UV absorption at 488 nm. All samples were initially 10 μM, based on MS2 capsid monomer. b) A drug release profile was determined for MS2 capsids containing taxol conjugate 6 at 37 °C. The initial capsid concentration was 10 μM in 10% FBS/PBS, pH 7.4. At the indicated time, the remaining intact capsids were isolated via ammonium sulfate precipitation and SEC. Subsequent RP-HPLC analysis of the capsid samples allowed separation of the protein with and without bound taxol (see trace in Figure 3-7c as an example). The taxol remaining in the capsid fraction was quantified using the tryptophan fluorescence (λ_{ex}=280 nm, λ_{em}=330 nm) of the associated protein.

and SEC. RP-HPLC analysis of the resulting material allowed quantification of the amount of taxol that had been released (Figure 3-9b).[10] These experiments indicated a 2 d half-life for the linker under these conditions.

A cell viability assay was used to test the effect of MS2 and taxol-MS2 on cancer cells *in vitro* (Figure 3-10). The release of taxol was expected to occur via hydrolysis of the ester bond at the 2′-OH position.[11] MCF-7 breast cancer cells were assayed using Alamar Blue dye, a fluorescent indicator of cellular metabolic processes[12] that proved to be the most effective out of several cytotoxicity assays (MTT, XTT). Unmodified N87C MS2 was found to have no noticeable effect on MCF-7 viability. However, taxol-containing MS2 caused a significant lowering of cell viability, which was virtually identical to that occurring through the administration of equivalent amounts of taxol solubilized with small amounts of DMSO. Virtually identical results were obtained after 3 d and 5 d incubation times. While it is not known how efficiently the untargeted capsids are uptaken via pinocytosis, the drug release experiments suggest that a reduced amount of taxol would be available through hydrolysis alone over the 3 d time period. However, the equivalent toxicity to that of free taxol suggests that the cells may be playing an active role in the cleavage process. Whether or not this is the case, the addition of targeting groups that bind the drug conjugates to specific cell types would be expected to focus this activity only on the relevant cancer tissue.

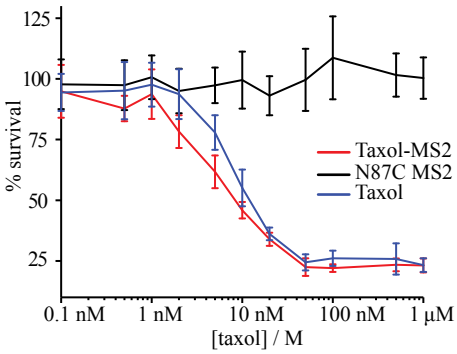

Figure 3-10. Cell viability assay using an MCF-7 cell line. Five days after the initial treatment, the cell survival was calculated relative to an untreated control by measuring the fluorescence resulting from treatment with Alamar Blue. Taxol-MS2 conjugates were delivered as a solution in 10 mM phosphate buffer, and free taxol was applied as a <1% solution of dimethyl sulfoxide in phosphate buffer. Error bars represent the standard deviation resulting from six replicate experiments.

In conclusion, a water-soluble derivative of the chemotherapeutic drug taxol containing bioconjugation functionality was synthesized and attached to MS2 viral capsids. The modified capsids remained in their capsid form and released taxol when incubated with MCF-7 cells, resulting in cell viability levels similar to that of free taxol in solution. We are presently investigating the use of linkers that undergo cell-specific cleavage between cargo and capsid, as well as the generation of MS2 capsids with both drug cargo and active targeting groups. Equally valuable is the new water soluble taxol derivative itself, which can be attached to a variety of drug delivery carriers in addition to the viral capsids described herein.

3.6 Materials and methods.

General Procedures and Materials

Unless otherwise noted, all chemicals were obtained from commercial sources and used without further purification. Analytical thin layer chromatography (TLC) was performed on EM Reagent 0.25 mm silica gel 60-F_{254} plates with visualization by ultraviolet (UV) irradiation at 254 nm and/or staining with potassium permanganate. Purifications by flash chromatography were performed using EM silica gel 60 (230-400 mesh). The eluting system for each purification was determined by TLC analysis. Chromatography solvents were used without distillation. All

organic solvents were removed under reduced pressure using a rotary evaporator. Water (ddH_2O) used in biological procedures or as a reaction solvent was deionized using a NANOpure™ purification system (Barnstead, USA) purchased from Aldrich. Solid phase extraction (SPE) columns were purchased from Phenomenex, Inc. (www.phenomenex.com) and used as specified, unless otherwise noted. Monoclonal goat Anti-mouse−Peroxidase (sc-205) and Mouse Anti-taxol IgG antibodies (sc-69899) were obtained from Santa Cruz Biotechnology (Santa Cruz, CA) and used without further purification. Polyclonal goat anti-rabbit antibodies (ab6721) were obtained from Abcam Inc. (Cambridge, MA) and used without further purification. Polyclonal rabbit anti-MS2 antibodies were obtained from a previously reported procedure.[13] All cell culture reagents were obtained from Gibco/Invitrogen Corp (Carlsbad, CA) unless otherwise noted.

Instrumentation and Sample Analysis Preparations

NMR. ^1H and ^{13}C spectra were measured with a Bruker AV-500 (500 MHz), or a Bruker DRX-500 (500 MHz) spectrometer, as noted. ^1H NMR chemical shifts are reported as δ in units of parts per million (ppm) relative to $CDCl_3$ (δ 7.26, singlet), or methanol-d_4 (δ 3.31, pentet). Multiplicities are reported as follows: s (singlet), d (doublet), t (triplet), or m (multiplet). Coupling constants are reported as a *J* value in Hertz (Hz). The number of protons (n) for a given resonance is indicated as nH, and is based on spectral integration values. ^{13}C NMR chemical shifts are reported as δ in units of parts per million (ppm) relative to $CDCl_3$ (δ 77.2, triplet), or methanol-d_4 (δ 49.00, septet).

Mass Spectrometry. High resolution Electrospray (ESI) and Fast Atom Bombardment (FAB^+) mass spectra were obtained at the UC Berkeley Mass Spectrometry Facility. Electrospray LC/MS analysis was performed using an API 150EX system (Applied Biosystems, USA) equipped with a Turbospray source and an Agilent 1100 series LC pump. Protein chromatography was performed using a Phenomenex Jupiter™ 300 5μ C5 300 Å reversed-phase column (2.0 mm x 150 mm) with a MeCN:ddH_2O gradient mobile phase containing 0.1% formic acid (250 μL/min). Protein mass reconstruction was performed on the charge ladder with Analyst software (version 1.3.1, Applied Biosystems).

High Perfomance Liquid Chromatography. HPLC was performed on an Agilent 1100 Series HPLC System (Agilent Technologies, USA). Size exclusion chromatography was accomplished on an Agilent Zorbax® GF-250 with isocratic (0.5 mL/min) flow or a Phenomenex PolySep-GFC-P 5000 (PS5K) column (300 x 7.8 mm, flow rate 1.0 mL/min) using an aqueous mobile phase (10 mM Na_2HPO_4, pH 7.2) . Reversed-phase liquid chromatography on protein samples was accomplished on a Agilent Poroshell 300 SB-C18 column (2.1 x 75 mm) using a MeCN:ddH_2O gradient mobile phase containing 0.1% trifluoroacetic acid. Semi-preparatory scale purification was performed using a Agilent Zorbax 300 SB-C18 column (9.4 mm x 25 cm). Sample analysis for all HPLC experiments was achieved with an inline diode array detector (DAD) and an inline fluorescence detector (FLD).

Gel Analyses. Sodium dodecyl sulfate-poly(acrylamide) gel electrophoresis (SDS-PAGE) was accomplished on a Mini-Protean apparatus from Bio-Rad (Hercules, CA) with 10-20% gradient

polyacrylamide gels (BioRad, CA), following the protocol of Laemmli.[14] All electrophoresis protein samples were mixed with SDS loading buffer in the presence of dithiothreitol (DTT) and heated to 100 °C for 10 min to ensure reduction of disulfide bonds and complete denaturation unless otherwise noted. Commercially available molecular mass markers (Bio-Rad) were applied to at least one lane of each gel for calculation of the apparent molecular masses. Gel imaging was performed on an EpiChem3 Darkroom system (UVP, USA).

Immunoblot Analyses. Western blot and dot blot analyses was performed using nitrocellulose membranes (GE Osmonics, Minnetonka, MN). Membrane blocking was achieved using a solution of 2% bovine serum albumin (BSA) in phosphate-buffered saline. Chemiluminescent signal was generated from horseradish peroxidase conjugates after a 1 min incubation with Western Lighting Chemiluminescence Reagent Plus (Perkin Elmer, USA) and captured with a Molecular Imager ChemiDoc XRS+ System (BioRad, USA).

Centrifugations were conducted with an Allegra 64R Tabletop Centrifuge (Beckman Coulter, Inc., USA). General desalting and removal of other small molecules of biological samples were achieved using NAP-5 gel filtration columns (GE Healthcare). Protein samples were concentrated by way of centrifugal ultrafiltration using Amicon Ultra-4 or Ultra-15 100 kDa molecular weight cut off (MWCO) centrifugal filter units (Millipore), or Amicon Microcon 10 kDa, 30 kDa, and 100 kDa MWCO (Millipore) centrifugal filter units.

Dynamic Light Scattering. DLS measurements were performed on a Zetasizer Nano ZS (Malvern Instruments, UK). Samples were taken in 10 mM phosphate buffer pH 7.2 at 24 ºC. Data points are calculated from an average of three measurements, each of which consists of 10 runs of 45 seconds each.

Transmission Electron Microscopy (TEM). TEM images were obtained at the UC-Berkeley Electron Microscope Lab (www.em-lab.berkeley.edu) using a FEI Tecnai 12 transmission electron microscope with 100 kV accelerating voltage.

Experimental Procedures

N87C MS2 production.

The pBAD-MS2 plasmid and protein expression has been previously reported.[2] The pBAD-MS2-N87C mutant was made by site-directed mutagenesis of the pBAD-MS2 plasmid. Position 87 was converted to a cysteine using the following forward and reverse primers:

Forward: 5'–AGCCGCATGGCGTTCGTACTTATGTATGGAACTAACCATTC–3'

Reverse: 5'–GAATGGTTAGTTCCATACATAAGTACGAACGCCATGCGGCT–3'

Growth and purification of MS2-N87C was identical to that of wtMS2. Yields are slightly less than the 100 mg/L reported for wtMS2.

(*S*)-2,5-dioxopyrrolidin-1-yl-2-(*tert*-butoxycarbonylamino)-6-(2,5-dioxo-2,5-dihydro-1*H*-pyrrol-1-yl)hexanoate (18). A solution of Boc-lysine (**17**, 492 mg, 2 mmol) and maleic anhydride (215.6 mg, 2.2 mmol) in 1 mL of DMF was stirred for 2 h at RT. The reaction was then cooled to 0 ºC for 10 min, followed by the addition of DCC (906 mg, 4.4 mmol) and NHS (288 mg, 2.5 mmol). The reaction was warmed to RT and stirred overnight, resulting in a pale orange slurry. The solid was isolated via filtration and washed with approximately 100 mL of CH_2Cl_2. The combined organic filtrates were washed with three 100 mL portions of dilute aqueous $NaHCO_3$ and one portion of brine, and then dried over Na_2SO_4. The resulting solution was filtered and the solvent was removed under reduced pressure. After purification by flash chromatography (1:1 to 8:2 EtOAc:Hexanes), 380 mg of product was isolated as a white filmy solid (45%). ^{1}H NMR (500 MHz, $CDCl_3$): δ, 1.39 (m, 11H), 1.59 (m, 2H), 1.78 (m, 1H), 1.91 (m, 1H), 2.78 (s, 4H), 3.48 (t, 2H, *J* = 7.0 Hz), 4.57 (m, 1H), 5.18(d, 2H, *J* = 8.5 Hz), 6.64 (s, 2H). ^{13}C NMR (125 MHz, $CDCl_3$): δ, 22.1, 25.6, 28.0, 28.3, 32.1, 37.3, 51.8, 80.4, 134.1, 154.9, 168.4, 168.8, 170.9. HRMS (FAB$^+$) calculated for $C_{19}H_{25}N_3O_8$ ([M+ Li]$^+$) 430.1802, found 430.1802.

(*S*)-2-(2-(*tert*-butoxycarbonylamino)-6-(2,5-dioxo-2,5-dihydro-1*H*-pyrrol-1-yl)hexanamido) ethanesulfonate (19). To a solution of **18** (190 mg, 0.45 mmol) in 5 mL of DMF was added DIPEA (0.9 mmol, 161 uL) and taurine (0.45 mmol) as a 0.5 M aqueous solution. The reaction solution was stirred for 6 h. The solvent was removed under reduced pressure and the resulting yellow oil was dissolved in MeOH. Purification was achieved using a Phenomenex Strata X-AW SPE column (loaded with MeOH, washed with MeOH and water, and eluted with 2% NH_4OH in MeOH) leaving a yellow solid (111 mg, 54%). ^{1}H NMR (500 MHz, MeOD): δ, 1.28-1.40 (m, 2H), 1.44 (s, 9H), 1.59 (m, 3H), 1.76 (m, 1H), 2.95 (t, 2H, *J* = 6.6 Hz), 3.49 (6, 2H, *J* = 7 Hz), 3.58 (t, 2H, *J* = 6.8 Hz), 3.93 (m, 1H), 6.80 (s, 4H). ^{13}C NMR (125 MHz, MeOD): δ, 24.2, 28.7, 29.2, 32.8, 36.6, 38.3, 51.4, 56.2, 80.7, 135.4, 157.9, 169.9, 172.6, 175.0. HRMS (ESI) calculated for $C_{17}H_{26}N_3O_8S^-$ ([M]$^-$) 432.1446, found 432.1453.

(*S*)-2-(2-amino-6-(2,5-dioxo-2,5-dihydro-1H-pyrrol-1-yl)hexanamido)ethanesulfonate (20). To a solution of **19** (10 mg, 23.2 μmol) in 1 ml of CH_2Cl_2 cooled to 0 ºC was added 1 mL of TFA. The resulting solution was stirred for 15 min. The resulting solution was concentrated under reduced pressure, and the product was precipitated by triturating with three 1 mL portions of EtOAc. The product was obtained as a white solid (6.7 mg, 90%). HRMS (ESI) calculated for $C_{12}H_{18}N_3O_6S^-$ ([M]$^-$) 332.0922, found 332.0924.

Taxol maleimide conjugate 21. To a solution of taxol-succinate (10 mg, 0.011 mmol),[6] **20** (4.18 mg, 0.0126 mmol), and DIPEA (7.18 μL, 0.42 mmol) in 1 mL of DMF was added HATU (6 mg, 0.0158 mmol). The resulting solution was stirred for 4 h. After the solvent was removed under reduced pressure, the reaction mixture was first purified on a Phenomenex Strata X-AW SPE column (loaded with MeOH, washed with MeOH and water, and eluted with 2% NH_4OH in MeOH). The yellow solid was then purified by reversed phase HPLC on a C-18 semi-preparative column, using an isocratic 34% ACN/66% H_2O/ 0.1% TFA mobile phase. ^{1}H NMR (500 MHz, MeOD): δ, 1.13 (m, 6H), 1.23-1.35 (m, 15H), 1.54-1.66 (m, 6H), 1.70-1.84 (m, 3H), 1.91 (s, 3H), 2.10-2.20 (m, 4H), 2.39 (s, 3H), 2.44-2.68 (m, 3H), 2.78 (t, 2H, *J* = 6.6 Hz), 2.94 (m, 2H), 3.48 (t, 2H, *J* = 6.9 Hz), 3.52-3.66 (m, 2H), 3.80 (d, 1H, *J* = 7.2), 4.15-4.22 (m, 3H), 4.34 (m, 1H), 5.01 (m, 1H), 5.50 (d, 1H, *J* = 6.8 Hz), 5.62 (d, 1H, *J* = 7.2 Hz), 5.77 (t, 1H, *J* = 7.8

Hz), 6.04 (t, 1H, *J* = 9.1 Hz), 6.45 (s, 1H), 6.79 (s, 2H), 7.25 (t, 1H, *J* = 7.5 Hz), 7.41-7.56 (m, 6H), 7.61 (t, 2H, *J* = 7.7 Hz), 7.69 (t, 1H, *J* = 7 Hz), 7.85 (d, 2H, *J* = 7.3 Hz), 8.11 (d, 2H, *J* = 7.4 Hz). HRMS (ESI) calculated for $C_{63}H_{71}N_4O_{22}S^-$ ($[M]^-$) 1267.4286, found 1267.4304.

(*R*)-2-((*tert*-butoxycarbonyl)amino)-3-(pyridin-2-yldisulfanyl)propanoic acid (12). A solution of **11** (100 mg) and 2,2'-dithiodipyridine (5 eq, 500 mg) in 5 mL of EtOH/5% AcoH was stirred for 4 h, after which the solvent was removed under vacuum. The crude product was purified by flash chromatography two times, (solvent system 1 – 1:1:0.5% Ethyl acetate:Hexanes:AcOH, solvent system 2 – 15:85:0.5% Ethyl acetate:Hexanes:AcOH). The clear fractions of the second column were pooled and solvent removed under reduced pressure to yield the mixed disulfide. The desired product can also be recrystallized using ethyl acetate/hexanes. In addition, the product can be precipitated out from the crude reaction by addition of CH_2Cl_2. ^{1}H NMR(400 MHz, $CDCl_3$): δ = 1.42 (s, 9H), 2.84 (dd, 1H, J = 14.3, 10.5 Hz), 3.44 (dd, 1H, J = 14.3, 4.1 Hz), 4.38 (m, 1H), 6.08 (d, 1H, J = 6.8 Hz), 7.26 (s, 3H), 7.43 (d, 1H, J = 8.2 Hz), 7.69 (t, 1H, J = 7.8 Hz), 8.47 (d, 1H, J = 5.0 Hz).

(*R*)-2,5-dioxopyrrolidin-1-yl 2-((*tert*-butoxycarbonyl)amino)-3-(pyridin-2-yldisulfanyl) propanoate (13). A solution of **12** (50 mg, 0.152 mmol), DCC (1.1 eq., 0.167 mmol, 34.33 mg), and NHS (1.1 eq., 0.167 mmol, 19.2 mg) in acetonitrile (25 mL) was stirred for 3 h. A white solid precipitate formed. After 3 h, the reaction was cooled to 0 °C for 1 h. The solvent was then removed under vacuum and the residue dissolved in ethyl acetate. The solution was wash with two portions of water and one portion of brine and dried over Na_2SO_4. After two purifications by flash chromatography (50:50:0.5% Ethyl acete:Hexanes:AcOH), 45 mg of the product was isolated (69%). ^{1}H NMR(400 MHz, $CDCl_3$): δ , 1.47 (s, 9H), 2.83 (d, 4H, J=8.5 Hz), 3.46 (m, 2H), 4.88 (td, 1H, J=7.1, 4.3 Hz), 7.16 (q, 1H, J=6.4, 5.9 Hz), 7.38 (d, 1H, J=7.5 Hz), 7.46 (d, 1H, J=7.9 Hz), 7.62 (td, 1H, J=7.7, 1.9 Hz), 8.61 (d, 1H, J=4.8 Hz).

2,5-dioxopyrrolidin-1-yl 3-(2,5-dioxo-2,5-dihydro-1*H*-pyrrol-1-yl)propanoate (16). This compound was previously synthesized by Ede and co-workers, and the reported procedure was followed.[9] A solution of beta-alanine (0.91 g,10.2 mmol) and maleic anhydride (1 g, 10.3 mmol) was stirred in DMF (10 mL). After 2 h, the solution was cooled to 0 °C for 2 min and NHS (1.44 g, 12.5 mmol) and DCC (4.12 g, 20 mmol) were added. A white solid immediately precipitated, and after 1 h it became difficult to stir the reaction. Another 15 mL of DMF was added and the ice was removed after 5 min of reaction. The reaction was allowed to stir for 16 h and the white solid DCU was filtered off. The filtrate was diluted in ~250 mL CH_2Cl_2 and washed with 3x5% $NaHCO_3$, brine, and dried over Na_2SO_4. The organic solvent was removed under reduced pressure yielding the desired product (95%). It was also possible to precipitate the product by adding Et_2O. ^{1}H NMR(400 MHz, $CDCl_3$): δ, 2.82 (s, 4H), 3.02 (t, 2H, J=7.0 Hz), 3.93 (t, 2H, J=7.0 Hz), 6.74 (s, 2H).

Typical MS2 modification with taxol maleimide 21. To a solution of N87C MS2 (5 nmol, 33 μL, 300 μM in phosphate buffer) was added **21** (25 nmol, 25 μL, 2 mM in pH 7.2 10 mM phosphate buffer). The reaction mixture was incubated at RT for 1 h, followed by purification by size exclusion chromatography (NAP-5). Longer reaction times and/or higher buffer pH led to detectable degradation of both the starting maleimide and the taxol-MS2 conjugates. The use of higher concentrations of protein, as well as more equivalents (20x) of **21**, were able to increase

the yield to almost 75%. However, this was typically avoided to maintain a workable volume of protein solution, and to conserve **21**. A control reaction was also run with wild type MS2, which lacked the N87C mutation, to test the reactivity of the native cysteine residues in the presence of **21**. No appreciable amounts of reaction product were observed using the conditions described above demonstrating the low reactivity of the native cysteine residues.

Transmission Electron Microscopy. TEM grids were prepared by charging carbon-coated, Formvar-supported copper mesh grids with argon plasma (40 mA at 0.1 mbar for 30 s) in a Cressington 108 Auto Sputter Coater. Protein samples were prepared for TEM analysis by pipetting 5 μL samples onto these grids and allowing them to equilibrate for 3 minutes. The samples were then wicked with filter paper and rinsed with ddH_2O. The grids were then exposed to 5 μL of a 1% (w/v) aqueous solution of uranyl acetate for 90 s as a negative stain. After excess stain was removed, the grid was allowed to dry in air.

General Procedure for Analysis of taxol-MS2 by Dot Blot. Taxol-MS2 was prepared using the procedure described above. MS2 samples were denatured by making 1:1 solutions of 5 M aqueous GnHCl and MS2 in 10 mM phosphate buffer. To small rectangles of dry nitrocellulose membrane were applied 2 μl of 50 uM solutions of either wtMS2 or taxol-MS2. The membranes were air-dried for approximately 30 min before being blocked overnight with 2% BSA in phosphate buffered saline (PBS). After the removal of the blocking buffer, the nitrocellulose membranes were incubated with mouse anti-taxol IgG or rabbit anti-MS2 antibody (1:5000 dilution) for 30 min in PBS/0.1% Tween containing 2% BSA. The membranes were then washed four times (30 min each) with PBS/0.1% Tween. The membranes were then incubated with anti-mouse or anti-rabbit-HRP antibodies (1:5000 -1:20,000 dilution) for 30 min in PBS/0.1% Tween containing 2% BSA. The membranes were washed four times (30 min each) with PBS/0.1% Tween before imaging.

Evaluation of Cytotoxicity. Cell culture was conducted using standard sterile technique. MCF-7 cells were grown in Dulbecco's Modified Eagle Media supplemented with 10% (v/v) fetal bovine serum (FBS, HyClone), 1% non-essential amino acids, and 1% penicillin/streptomycin (P/S, Sigma). Antiproliferative activities of N87C MS2, taxol-MS2, and unconjugated taxol were determined using the Alamar Blue cytotoxicity assay.[12] Samples of 2.5×10^3 cells were added to individual wells of a 96-well microtiter plate and incubated at 37 °C for 24 h in 160 μL of media. Following this, 40 μL of sterile-filtered MS2-taxol (in PBS) was added to the cells. Concentrations ranged from 1×10^{-10} to 1×10^{-6} M, measured in terms of taxol (or in the equivalent concentration of unmodified MS2 monomer for the N87C control sample). The stock solutions were prepared in equal volumes of PBS, and in the case of pure taxol, with <1% DMSO as co-solvent. After 72 or 120 h of incubation in media at 37 °C, the media was removed via aspiration, and a 5% Alamar Blue solution in 10% FBS in PBS was added. The plates were then incubated for 4 h, and the inhibition of cell proliferation was quantified by determining the fluorescence at 530ex/590em with a microplate reader (Molecular Devices, San Diego, CA). For each sample, cell survival was calculated compared to untreated cells. Average cell survival values and standard deviations were calculated from six simultaneous replicate samples.

Determination of Capsid Thermal Stability After taxol Incorporation. A 2 μM sample of MS2 capsids that were 60% labeled with taxol-maleimide **21** was prepared in 10 mM phosphate

buffer, pH 7.4. The particle volume distributions were determined using Dynamic Light Scattering (DLS) at 2 °C temperature increments, with 2 min sample equilibration at each time point. Capsid instability (which resulted in aggregation) was observed at temperatures above 64 °C.

Determination of Capsid Stability Under Cell Culture Conditions. To verify that intact capsids were the predominant form of MS2 that was present during the cell culture experiments, N87C MS2 was labeled with Oregon Green maleimide dyes (Invitrogen) to allow facile detection in media samples. These samples were incubated for 6 days at 37 ºC in PBS, 10% FBS in PBS, and in media (all samples at pH 7.4). The amount of intact capsid was then measured using SEC (PolySep 5k column, with assembled capsids eluting at 8 min using a 1 mL/min flow rate), with tracking of the Oregon Green absorbance at 488 nm. For all samples, more than 80% of the labeled MS2 capsids were recovered in the assembled state

Determination of taxol Release Kinetics. The quantitative determination of liberated taxol and/or remaining taxol-MS2 conjugates was made difficult by (1) the presence of numerous serum proteins in the FBS culture media and (2) the lack of a distinguishing UV signal for taxol itself. To circumvent these issues, taxol release was measured by first purifying intact capsids from the culture medium, and then by determining the percentage of capsid monomers still bearing taxol groups using RP-HPLC. Taxol-MS2 samples were incubated at 37 ºC for 5 days in 10% FBS and aliquots were removed and analyzed every 24 h. Each sample was mixed with an equal volume of saturated ammonium sulfate. This served to isolate the capsids from most other serum proteins via precipitation of the capsids. The resulting suspension was centrifuged and the isolated pellet was resuspended in PBS (10 mM, pH 7.4). The resulting solution was next subjected to SEC using a PolySep 5k column. Intact capsids eluted at approximately 8 minutes using a 1 mL/min flow rate. The capsid-containing fractions were subjected to centrifugal ultrafiltration against a 100 kDa cutoff filter to concentrate the samples. Finally, the isolated capsids were analyzed by reversed-phase HPLC to separate MS2 monomers bearing and lacking taxol groups. The percentages of protein monomers still bearing taxol were calculated from the chromatograms, based on tryptophan fluorescence at 330 nm (280 nm excitation).

3.7 References.

1. Kovacs, E.W. The Covalent Modification of MS2 Viral Capsids for the Development of Drug Delivery Vehicles. Ph.D. dissertation, University of California, Berkeley, Berkeley, CA, 2006.
2. Carrico, Z.M., Romanini, D.W., Mehl, R.A., Francis, M.B. Oxidative coupling of peptides to a virus capsid containing unnatural amino acids. *Chem. Commun*. **2008**, *10*, 1205-1207.
3. a) Khayat, D., Antoine, E.-C., Coeffic, D. Taxol in the Management of Cancers of the Breast and the Ovary. *Cancer Invest.* **2000**, *18*, 242-260; b) Saijo, N. Recent trends in the treatment of advanced lung cancer. *Cancer Sci.* **2006**, *97*, 448-452.
4. a) Sparreboom, A., Van Tellingen, O., Nooijen, W.J., Beijnen, J.H. Nonlinear pharmacokinetics of paclitaxel in mice results from the pharmaceutical vehicle Cremophor EL. *Cancer Res.* **1996**, *56*, 2112-2115; b) Singla, A., Garg, A., Aggarwal, D. Paclitaxel and its formulations. *Int. J. Pharm.* **2002**, *235*, 179-192.

5. Wu, W., Hsiao, S.C., Carrico, Z.M., Francis, M.B. Genome-Free Viral Capsids as Multivalent Carriers for Taxol Delivery. *Angew. Chem., Int. Ed.* **2009**, *48,* 9493-9497.

6. Deutsch, H.M., Glinkso, J.A., Hernandez, M., Haugwitz, R.D., Narayanan, V.L., Suffness, M., Zalkow, L.H. Synthesis of congeners and prodrugs. 3. Water-soluble prodrugs of taxol with potent antitumor activity. *J. Med.Chem.* **1989**, *32*, 788-792.

7. Greenwald, R.B., Zhao, H., Reddy, P. Synthesis, isolation, and characterization of 2'-Paclitaxel glycinate: An application of the Bsmoc protecting group. *J. Org. Chem.* **2003**, *68*, 4894-4896.

8. Liu, D.Z., Sinchaikul, S., Reddy, S.V.G., Chang, M.Y., Chen, S.T. Synthesis of 2'-paclitaxel methyl 2-glucopyranosyl succinate for specific targeted delivery to cancer cells. *Bioorg. Med. Chem. Lett.* **2007**, *17*, 617-620.

9. Ede, N.J., Tregear, G.W., Haralambidis, J. Routine preparation of thiol oligonucleotides: Application to the synthesis of oligeonucleotide-peptide hybrids. *Bioconjug. Chem.* **1994**, *5*, 373-378.

10. Direct detection of the released taxol using RP-HPLC yielded data that were consistent with these findings. However, the lack of a distinct chromophore and the large number of small molecules in FBS limited the accuracy of this method.

11. a) Mathew, A.E., Mejillano, M.R., Nath, J.P., Himes, R.H., Stella, V.J. Synthesis and evaluation of some water-soluble prodrugs and derivatives of taxol with antitumor activity. *J. Med. Chem.* **1992**, *35*, 145-151; b) Chen, X., Plasencia, C., Hou, Y., Neamati, N. Synthesis and Biological Evaluation of Dimeric RGD Peptide−Paclitaxel Conjugate as a Model for Integrin-Targeted Drug Delivery. *J. Med. Chem.* **2005**, *48*, 1098-1106; c) Lavis, L.D. Ester Bonds in Prodrugs. *ACS Chem. Biol.* **2008**, *3*, 203-206.

12. Nakayama, G. R., Caton, M. C., Nova, M. P., Parandoosh, Z. Assessment of Cell Proliferation with Resazurin-Based Fluorescent Dye. *J. Immunol. Methods* **1997**, *204*, 205-208.

13. Kovacs, E. W., Hooker, J. M., Romanini, D. W., Holder, P. G., Berry, K. E., Francis, M. B. Dual-Surface-Modified Bacteriophage MS2 as an Ideal Scaffold for a Viral Capsid-Based Drug Delivery System. *Bioconjug. Chem.* **2007**, *18*, 1140-1147.

14. Laemmli, U. K. Cleavage of structural proteins during the assembly of the head of bacteriophage T4. *Nature* **1970**, *227*, 680.

Chapter 4: Active Targeting of MS2 capsids via exterior modification using an oxidative coupling bioconjugation reaction.

4.1 An oxidative coupling reaction for MS2 exterior modification.

Previous work in the Francis group had successfully attached short targeting peptides to the exterior surface of MS2 using a sodium periodate mediated oxidative coupling reaction between phenylene diamines and anilines (Figure 4-1a). This reaction had been developed for protein bioconjugation purposes previously in our group by Jacob Hooker and demonstrated on a variety of proteins, including GFP and lysozyme.[1] In these cases, anilines were chemically introduced to the proteins of interest via lysine modification using NHS esters and isatoic anhydride, or via native chemical ligation. Zac Carrico extended the use of this reaction to the exterior surface of MS2 and applied the Schultz *in vitro* amber stop codon suppression technique to incorporate aniline containing amino acids at position 19 of the MS2 capsid.[2] Using these T19pAF mutants, Zac was able to attach several short peptides to the exterior of the MS2 capsid (Figure 4-1b). These peptides had been selected for their putative targeting capabilities to a variety of cancer markers. We therefore sought to integrate the drug delivery capabilities described in chapter three with the targeting capabilities of peptide modified MS2 capsids.

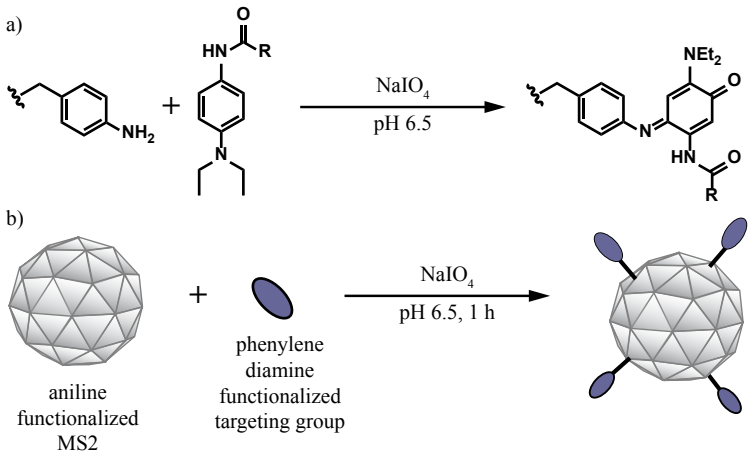

Figure 4-1. An oxidative coupling reaction. a) Reaction scheme for the periodate-mediated aniline-phenylene diamine oxidative coupling. b) Application of the oxidative coupling reaction to MS2 exterior surface modification.

4.2 Chemical modification of N87C MS2 capsids for aniline incorporation.

The capsid substrate necessary for dual modification requires the N87C mutation for internal modification, as well as a pAF mutation to provide the aniline for exterior oxidative coupling modification. While this double mutant (N87C pAF19 MS2) plasmid had been constructed,[3] the combination of both mutations proved to decrease MS2 expression levels greatly and thus limit subsequent capsid recovery. In order to circumvent this limitation, we chose to incorporate the external modification handle (an aniline) chemically, using various lysine modification techniques. As noted in Chapter 1, the MS2 capsid contains several lysine residues, including some on the interior surface, which would not be amenable to exterior modification by targeting

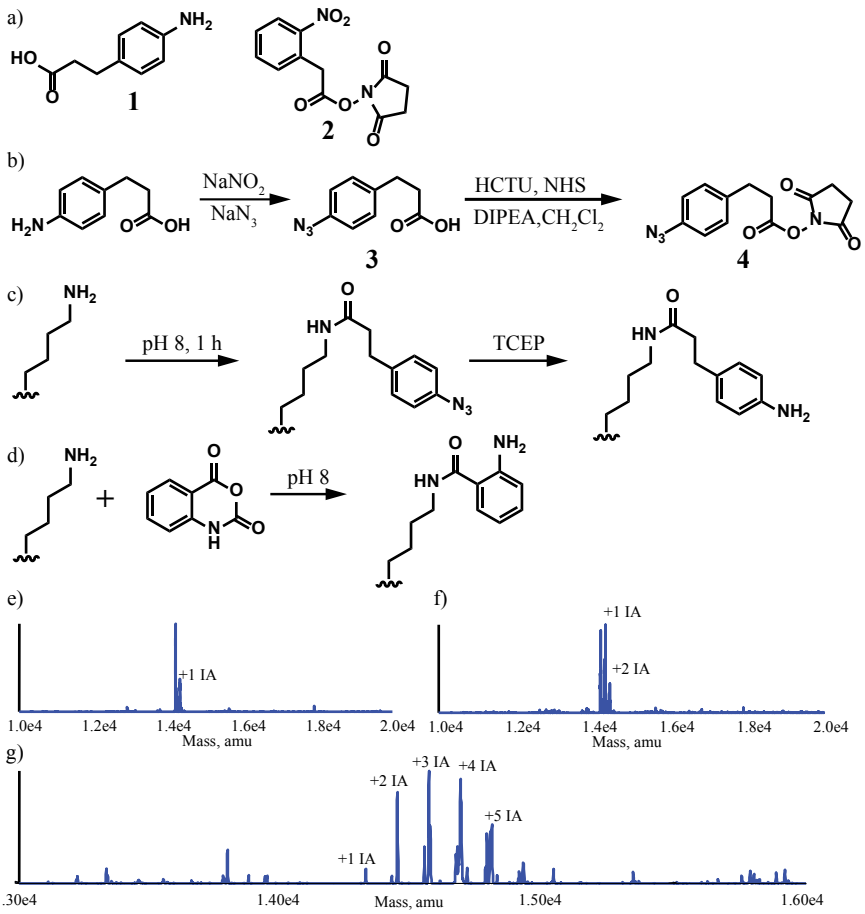

Figure 4-2. Chemical incorporation of anilines to MS2 capsids. a) Compounds **1** and **2** for attempted chemical incoporation of anilines into MS2. b) Synthesis of an azide-protected aniline-NHS ester. c) Modification of lysine residues using the NHS ester of an aryl azide and subsequent TCEP reduction. d) Modification of lysine residues using isatoic anhydride. e-g) LCMS analysis of aniline bearing MS2 monomers via isatoic acid incorporation. The samples in e-g were reacted for 1 h, 1 d, and 4 d, respectively.

groups. However, we relied on the fact that since our targeting molecule (a peptide) was fairly large (>1700 g/mol), it would not be able to access the interior surface of the capsid.

We first tested several conventional methods for lysine modification in order to install the aniline functionality on MS2 capsids. We first tried to modify the lysine resides using compound **1** (Figure 4-2a) and forming an NHS ester *in situ*. Even at high equivalents of **1**, low levels of modification were observed, up to 30%. Next we tried to synthesize and isolate the aniline-containing NHS-ester using DCC, and in organic solvent. However, the isolated product proved insoluble in a variety of solvents. We next attempted to form the NHS-ester of the protected aniline, in the form of a nitro group, in hopes of later performing a dithionite mediated reduction to access the required aniline functionality. However, this product (**2**) also was found to be insoluble in DMF or DMSO.

We ultimately were successful in isolating the NHS-ester of the aryl-azide protected aniline **4**, which we were able to dissolve in DMSO (Figure 4-2b). We were able to tune the conditions so

that this molecule was able to modify MS2 to the +1 and +2 states. This reaction was followed by subsequent reduction with TCEP. In parallel, we also were able to use commercially available isatoic anhydride to incorporate ortho substituted anilines, a technique previously utilized by Jacob Hooker[1] for the chemical incorporation of anilines for the oxidative coupling reaction (Figure 4-2d). This reaction proved to be much more convenient and reliable than the NHS-ester reaction, incorporating up to 5 anilines per MS2 monomer, as shown by LCMS (Figure 4-2e-g). In general, both of these techniques are used in this chapter for the introduction of anilines on N87C MS2 capsids.

4.3 p160 – A peptide for breast cancer cell targeting.

The targeting peptide that we chose to attach to MS2 capsids had been previously discovered by the Schwab group at the University of Heidelberg using random peptide phage display and shown to selectively bind to several breast cancer and neuroblastoma tumor cells.[4] The original peptide of interest, named p160, is a 12-mer of the following sequence –VPWMEPAYQRFL - to which we added a glycine residue at the C-terminus to maximize resin loading for SPPS (Figure 4-3). Previous work in the Francis group had attached this peptide along with 2 others to the exterior of MS2 using an oxidative coupling reaction. We chose to test the p160 peptide further because it was the only sequence without a disulfide bond present, as well as the only one targeted to a breast cancer cell line. We followed our group's previously reported procedure for the solid-phase synthesis of the desired p160 peptide, as well as appending the required phenylene-diamine functionality at the N-terminus.

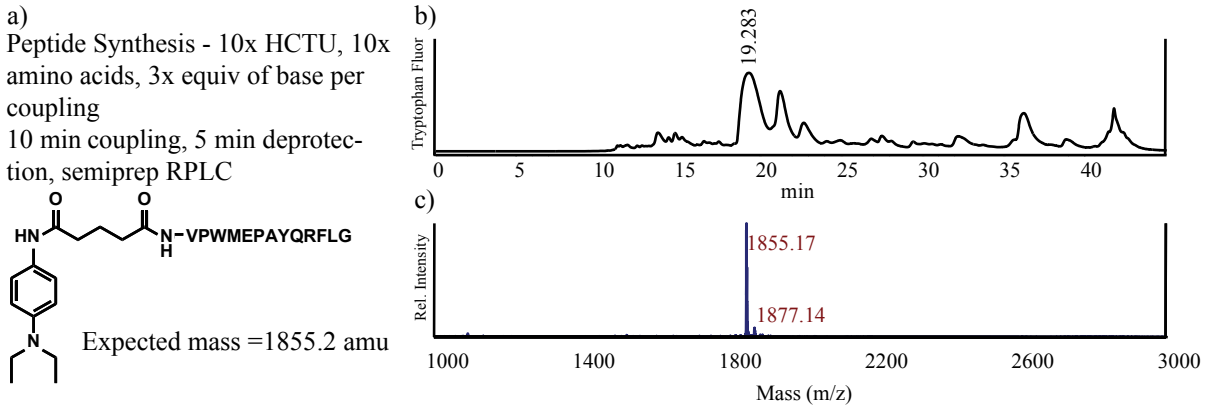

Figure 4-3. a) p160 peptide is synthesized using conventional Fmoc solid-phase peptide synthesis techniques with the necessary phenylene diamine linker appended at the N-terminus. b) The peptide is purified using RPLC. c) The large peak at 19 min was analyzed using MALDI-TOF MS, indicating the desired mass for the p160 peptide.

In order to test the feasibility of constructing dual-modified capsids, we were able to obtain a small amount of N87CpAF19 MS2 for initial modification and binding studies. The general procedure for dual modification involved initial interior modification by an Oregon Green maleimide and subsequent oxidative coupling with the phenylene-diamine modified peptides (Figure 4-4a). The coupling product could then be analysed using SDS-PAGE to look for a gel shift from the mass addition of the peptide. As shown in Figure 4-4b, lane A, in the presence of

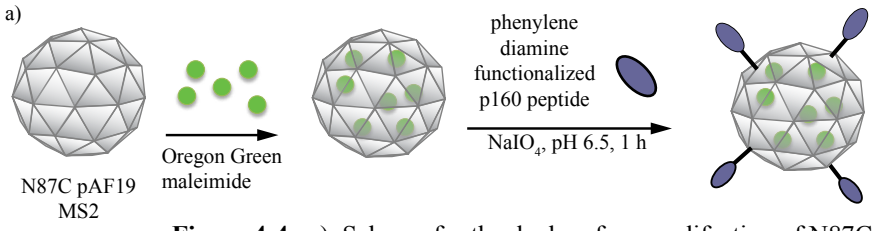

Figure 4-4. a) Scheme for the dual surface modifaction of N87C pAF19 MS2 capsids. The interior is modified first with Oregon Green maleimide, followed by exterior modification of the pAF residue with p160 targeting peptides. b) The resulting dual conjugates were analyzed by SDS-PAGE. Lane A clearly showed a gel shift corresponding to the addition of the peptide to approximately 40% of the MS2 monomers. In addition, the attached Oregon Green dye can be visualized via fluorescent imaging of the gel. Lane B has Oregon Green present, but has no $NaIO_4$ present in the reaction, and therefore no peptide addition.

$NaIO_4$, two bands were visible. The lower band corresponded to unmodified MS2 and the higher band corresponded to MS2 monomer/peptide conjugates. Without periodate, no peptide mass addition was observed, and a trace amount of MS2 dimerization was observable only in the fluorescence channel. In addition, exposing N87C MS2 without the exterior pAF mutation resulted in no observable modification.

Due to the difficulty in purifying appreciable amounts of the N87CpAF19 MS2 capsids however, we also sought to perform the same dual modification (Oregon Green interior/p160 peptide exterior) using N87C MS2 and chemically incorporated anilines (Figure 4-5a). For this process, we again first modified N87C MS2 using Oregon Green maleimide. After this cargo loading step, we then exposed the OG-MS2 to isatoic anhydride overnight and purified the modified capsids. These aniline bearing capsids were then reacted with p160-phenylene diamine and $NaIO_4$. To our surprise, our initial experiments showed only the presence of the MS2 dimer (Figure 4-5b lane A). Upon further investigation, it was suggested that trace glycerine present in the purification steps (NAP5 and spin concentration) could quench the periodate oxidant. Experiments with

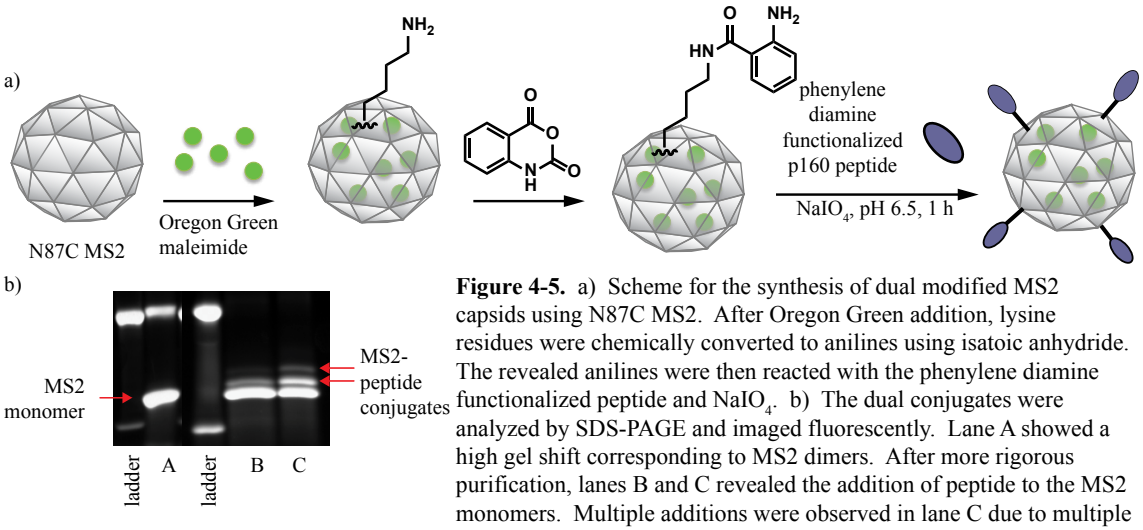

Figure 4-5. a) Scheme for the synthesis of dual modified MS2 capsids using N87C MS2. After Oregon Green addition, lysine residues were chemically converted to anilines using isatoic anhydride. The revealed anilines were then reacted with the phenylene diamine functionalized peptide and $NaIO_4$. b) The dual conjugates were analyzed by SDS-PAGE and imaged fluorescently. Lane A showed a high gel shift corresponding to MS2 dimers. After more rigorous purification, lanes B and C revealed the addition of peptide to the MS2 monomers. Multiple additions were observed in lane C due to multiple isatoic anhydride additions.

both unpurified OG-isatoic anhydride MS2 and purification using pre-rinsed spin concentrators successfully resulted in peptide addition to the MS2 capsids. In addition, due to the heterogeneous nature of isatoic anhydride mediated aniline incorporation, multiple additions of peptide were observed per MS2 monomer via SDS-PAGE, with higher levels of modification when OG-IA-MS2 had been purified and concentrated using pre-rinsed spin concentrators (Figure 4-5b lane C).

We next used fluorescence microscopy to assess the targeting capabilities of p160-decorated capsids to breast cancer cells. However, binding experiments on both MCF-7 and MDA-MB-435 breast cancer cell lines showed little binding and no uptake of the modified capsids. In fact, in the case of MCF-7 cells, the results were in sharp contrast to those of untargeted MS2 capsids which exhibited moderate levels of nonspecific binding and internalization to this cell line. In trying to decipher the behaviour of this peptide, we found that there was little literature characterization of the peptide's mechanism of association to cancer cells, although it was speculated that there is a tumor receptor interaction involved. The cell line also proved difficult to culture and recent research has also indicated that the MDA-MB-435 cell line may actually not be a breast cancer cell line, and in fact is contaminated with a M14 melanoma line.[5] In combination with our observations of the lack of binding to the cell line in question, these factors led us to pursue alternative targeting moieties.

4.4 DNA Aptamer targeting of MS2.

Concurrent work in the Francis group had focused on the attachment of DNA aptamers to the exterior of MS2 capsids using the same aniline/phenylene diamine. DNA aptamers are short DNA sequences that have been selected and commonly evolved to bind certain desired targets with selectively and with high affinity, including overexpressed receptors on cancer cells. Gary Tong was able to use a DNA aptamer developed by the Tan group against certain T-cells and functionalize an amine-derivatized version with the phenylene diamine functionality required

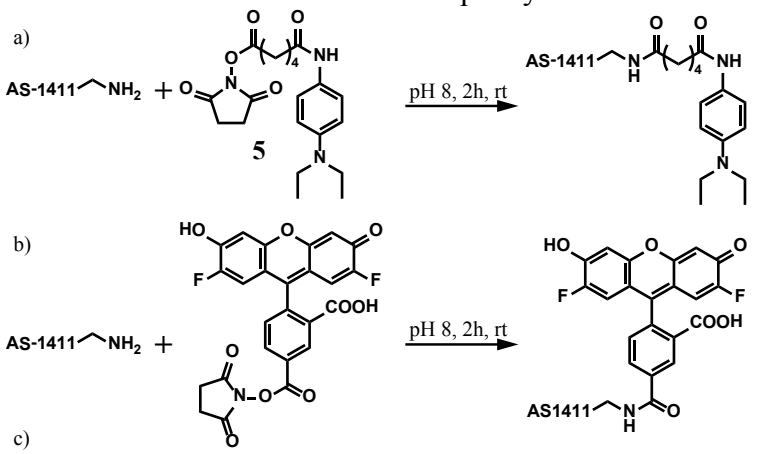

AS1411-NH_2: H_2N-3'-TTTTTTTTTGGTGGTGGTGGTTGTGGTGGTGGTGG-5'
Scramble-NH_2: H_2N-3'-TTTTTTTTTGGTGGGTTGGGTTTGGGGTTGGGGTG-5'
Random-NH_2: H_2N-3'-TTTTTTTTTACATAGTCGTAGACTACGATGTCGCC-5'

Figure 4-6. Scheme for AS1411 aptamer modification. a) Amine-DNA was functionalized at the 3' end using a phenlyene diamine NHS-ester for further oxidative coupling. b) Fluorescent aptamer was synthesized similarly using Oregon Green NHS-ester.

for the oxidative coupling reaction[6]. He was then able to attach up to 100 copies of the 20-mer aptamer to the exterior of MS2 capsids. These targeted capsids showed selective binding to the expected cell lines and were observed to internalize via LDL-associated endocytosis pathways. In subsequent work, aptamer-targeted capsids that had been loaded with light-reactive porphyrins were able to produce singlet oxygen and selectively effect cytotoxicity on the targeted immune cell line.[3]

Because of these promising targeting capabilities by aptamer functionalized MS2 capsids, we sought to attach an aptamer that would target solid tumors such as breast cancer. The first aptamer we tested is called AS1411, a G-rich oligeonucleotide that was at the time in preliminary phase II clinical trials for the treatment of acute myeloid leukemia.[7] AS1411 had been initially discoevered during a screen of G-rich oligonucleotides. These GROs exhibit several beneficial qualities for biomedical purposes, including the tendency to form stable G-quadraplex structures that may increase binding affinity and specifity, as well as protect the aptamer from nuclease degradation. Other studies had shown elevated binding of AS1411 to MCF-7 breast cancer cell lines and low binding to a negative control (MCF-10A) breast cell line. Notably, this aptamer was shown to bind nucleolin, a nucleolar protein known to bind bcl-2 mRNA that is implicated in cancer apoptotic pathways, and not to cause hybridization based effects. It was suggested that aptamer binding to nucleolin would thus decrease bcl-2 mRNA stability, resulting in an apoptotic cascade resulting in cell death.[8]

Using the same oxidative coupling strategy as with the above p160 peptide, we sought to attach the AS1411 targeting aptamer to the exterior of MS2 capsids. The apatamer was purchased as the 3'terminal amine along with a 10 nucleic acid thymidine spacer. Amine-DNA was de-

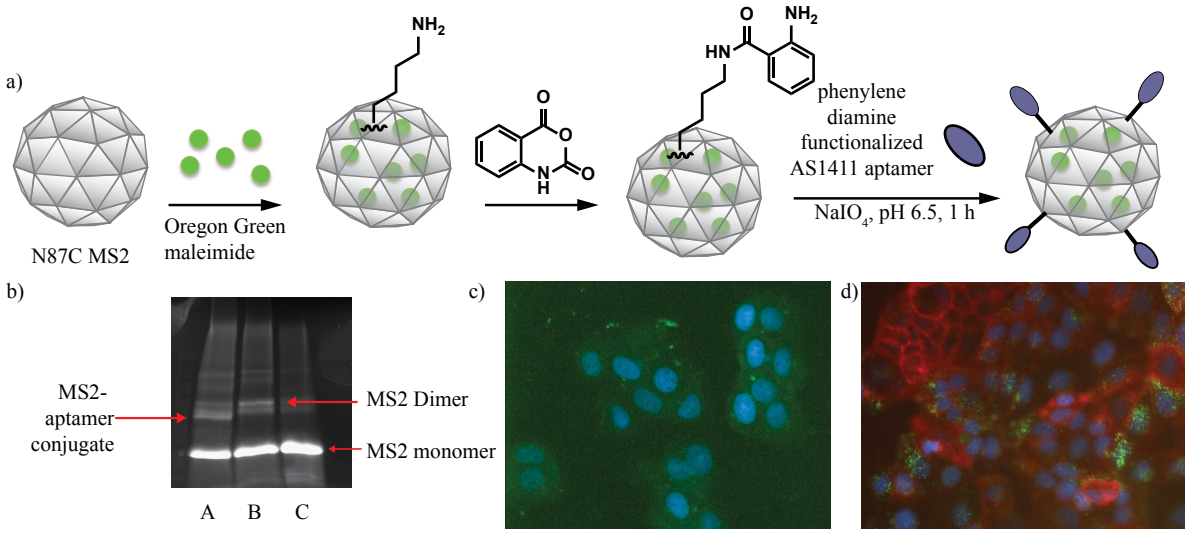

Figure 4-7. a) Aptamer functionalized fluorescent MS2 capsids were synthesized from N87C MS2 in an analagous fashion to peptide-functionalized capsids. b) MS2-aptamer conjugates were analyzed using SDS-PAGE. Lane A shows fluorescent aptamer-DNA conjugates, lane B shows isatoic anhydride functionalized MS2 after exposure to periodate, and lane C shows only isatoic anhydride functionalized MS2. c) Binding of Oregon Green modified AS1411 aptamers (green) to MCF7 cells was observed using fluorescence microscopy. Cell nuclei were stained with DAPI (blue). d) AS1411-MS2 conjugates (green) and Alexa Fluor 647 labelled transferrin (red) were incubated with MCF7 cells and observed by fluorescence microscopy.

rivatized as previously demonstrated, a 2 h incubation with the phenylene diamine NHS-ester **5** (Figure 4-6a). In addition to the AS1411 sequence, a scrambled and random sequence were also tested (Figure 4-6c). To examine the binding of the aptamer alone, we also labelled the free amine with an Oregon Green NHS-ester (Figure 4-6b).

Next, we again prepared Oregon Green labelled MS2 capsids with isatoic anhydride incorporated anilines on the exterior surface for dual modification with phenylene diamine AS1411 (Figure 4-7a). The functionalized aptamer and capsids were incubated with 10 mM $NaIO_4$ for 1 h at neutral pH to allow the oxidative coupling reaction to occur. Reactions were analyzed by SDS-PAGE, looking for the corresponding gel shift (Figure 4-7b). However, the MS2 dimer band (lane B) that appears in capsids with IA-incorporated anilines that have been exposed to $NaIO_4$ proved to be problematic due to a similar gel shift to the putative aptamer-MS2 conjugates. One notable difference was the appearance of a possible second addition band above the +1 modification shift. In addition, a large gain in 260 absorbance observed in the aptamer-modified capsids indicated that the DNA strand was indeed attached.

We first attempted to assess aptamer binding using fluorescence microscopy. Studies on MCF7 cells and OG labeled aptamer alone showed slight possible uptake after 1 h incubation. We next incubated MCF7 cells with the AS1411-MS2 conjugates as well as AF647 labelled Transferrin (Tf) to investigate the uptake pathway of the aptamer. What we observed was cellular association of the aptamer-MS2 conjugates, but no colocalization with Tf. Microscopy studies on the negative cell line were difficult to evaluate quantitatively, so we next turned to flow cytometry to analyze the binding of the aptamer and aptamer-MS2 conjugates to cancer cell lines (Figure 4-8). Both the AS1411 aptamer and the scrambled version on MS2 capsids showed similar levels of elevated binding. The random sequence on MS2 shows intermediate binding, and MS2 with no aptamer showed lower levels of intermediate binding. Interestingly, the aptamer itself (not on MS2) showed this same level of lower binding. In comparison, on the negative cell line (MCF10A), all the MS2 samples showed similar levels of elevated binding, whereas the aptamer alone showed similar, lower levels of binding. Overall, there seemed to be high levels of non-specific binding by the aptamers tested on the MCF7 and MCF10A cell lines. Additionally, there

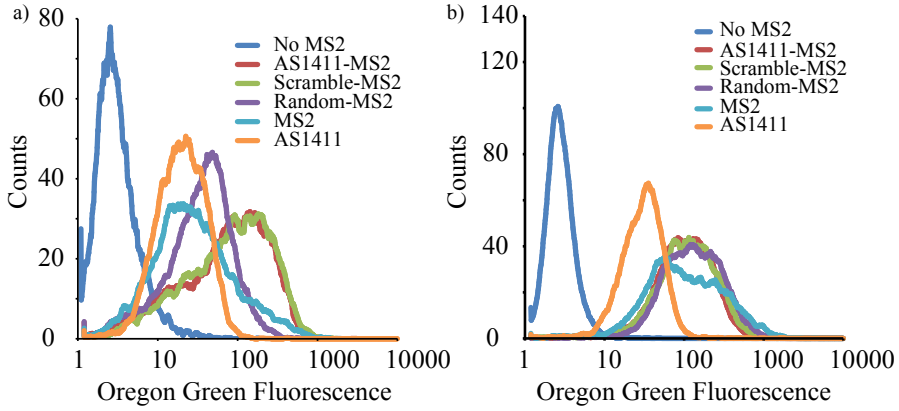

Figure 4-8. a) Various fluorescently labeled MS2 capsids were incubated with MCF7 cell lines and analyzed by flow cytometry. The overlay histogram shows the relative levels of agent binding to the cells. The blue trace corresponds to cell autofluorescence. MS2 capsids were labeled on the interior first with Oregon Green maleimide. The AS1411, scrambled, or random aptamers were then attached to the exterior. The orange trace corresponds to fluorescently labeled apatamer alone (no capsid). b) The same samples were incubated with MCF10A cells, to which the AS1411 aptamer reportedly does not bind.

was little differential binding between the positive and negative cell lines. Lastly, the control cell line MCF10A proved to be particularly difficult to culture due to cell clumping and high non-specific binding. For these above reasons, we decided to pursue an alternative aptamer for targeting.

The second aptamer we tested was targeted against Mucin 1, a cell surface protein that has particularly high glycosylation patterns and has been shown to be overexpressed in several cancers. An aptamer against the MUC1 protein was evolved and identified using the SELEX process in 2006 by Missailidis and coworkers[9] and shown to bind, by flow cytometry, to breast cancer cell lines such as MCF7 and T47D. In addition, the negative cell line utilized were CHO cells. The SELEX process was carried out on the protein core of MUC1 because it has been shown that upon overexpression of MUC1 in cancerous cells, aberrant glycosylation patterns are observed, exposing the protein core. Since all the tested cell lines were readily available and proved to be well-behaved and fairly simple to culture, we chose to attach the MUC1 apatamer to the exterior of MS2 capsids. Utilizing the same process as with the above NCL aptamer, we attached several copies of the MUC1 aptamer to intact MS2 capsids that were loaded with an AlexaFluor 488 dye. The binding of targeted capsids to MCF7, T47D, and CHO cells was measured using flow cytometry. Analysis showed no preferential binding of the targeted capsids in comparison to a randomized DNA aptamer and unmodified MS2, and in fact, the highest binding was observed with unmodified capsids (Figure 4-9). Both the MUC1 and control aptamers also showed low levels of background binding. As we were troubleshooting these issues, we found a recent paper by the Ellington group that corroborated our observations of a lack of selective binding by this specific MUC1 aptamer, which they attributed to significant background binding:[10]

Cells	Sample	MFI
MCF7	No MS2	4.3
	MUC1-MS2	17
	Random-MS2	20.9
	MS2	35.6
CHO	No MS2	2.3
	MUC1-MS2	19.5
	Random-MS2	25.8
	MS2	66.6

Figure 4-9. Tabulated mean fluorescence intensity values (MFI) from flow cytometry analysis of MUC1 aptamer -MS2 conjugate binding to MCF7 and CHO cell lines.

"The significant background binding exhibited by aptamers may also account for the apparent selection of an anti-MUC1 aptamer that does not appear to bind specifically to its target cell line."

With this shared observation, we thus chose to try alternative targeting strategies. Aptamers still hold high potential due to their unique binding capabilities and the power of the SELEX process. In fact, the original scg8c aptamer that our group attached to MS2 not only has shown selective binding to its targeted immune cells, but our own experiements have shown that this aptamer may also selectively bind to certain breast cancer cell lines. However, the binding of aptamers *in vitro* is subject to the binding conditions. Another practical consideration is that while functionalized medium-length aptamers are readily available commercially, the quantity and cost make them not amenable to large scale experimentation.

4.5 Attachment of Affibodies to MS2 capsids.

The next class of targeting groups we investigated were several engineered protein scaffolds that have been in development as next generation antibody therapeutics. Protein-based targeting groups provide the advantage of being able to be expressed in-house and allow for genetic-level manipulation to test various sequences. The main problem with using a protein-based targeting group is the difficulty of protein-protein bioconjugation (since the MS2 capsid is a protein as well). Using traditional bioconjugation reactions, it is typically a challenge to achieve well-defined bioconjugates between two proteins because both proteins share the same side chain functionalities, and any introduced small molecule linker will tend to react with both proteins on both ends of the linker. However, in our case, if we are able to introduce the unique functionalities of aniline and phenylene diamine in the proteins first, we can use our group's oxidative coupling strategy to construct precise bionconjugates.

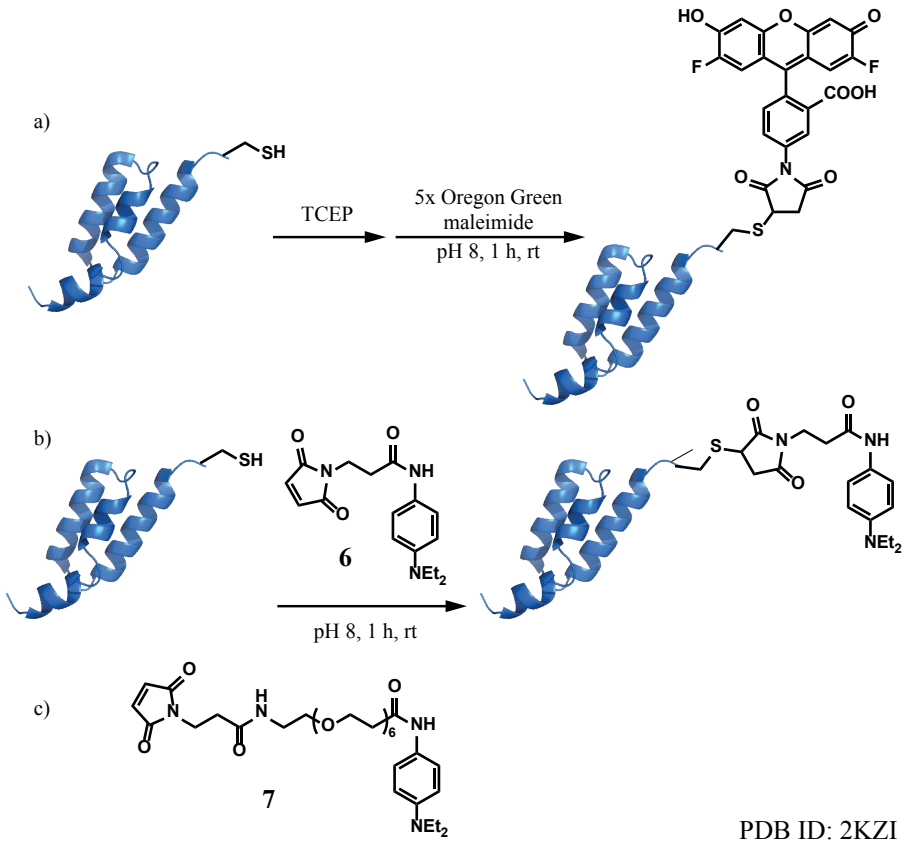

Figure 4-10. C-terminal cysteine modification of an α-HER2 affibody (H2A) with a) Oregon Green maleimide and b) a maleimide functionalized phenylene diamine. c) The affibody was modified with **7** to increase solubility of the protein as well as provide more space.

Of the many possible scaffolds to pursue, we first focused on the smallest class, which are called affibodies.[11] Affibodies are a 58 amino acid protein that is derived from a domain of Protein A, a bacterial binding domain that is best known for binding to the Fc region of human IgG. The specific affibody we chose has been evolved using phage display against the HER2 receptor, and has

a K_d of 22 pM and negligible binding to the related EGF receptor.[12] We chose this class because of their small size (~7-8 kDa) and lack of cysteine residues, which would allow us to engineer in a unique cysteine for elaboration as the phenylene diamine functionality necessary for the oxidative coupling. The lack of cysteines also meant that there were no disulfide bonds that would need to be formed and that in general, the folding of the affibody upon recombinant expression would not be problematic.

We elaborated the original HER2 binding sequence with a C-terminal glycine spacer, His_6 tag for affinity purification, and terminal cysteine residue. We later also appended a glycine residue to the N-terminus upon observation of incomplete Met cleavage with the original valine N-terminus. The affibody was expressed in *E. coli* and purified on Ni-NTA agarose under denaturing conditions, giving unoptimized yields of >50 mg/L. However, upon removal of denaturing urea by NAP desalting columns, the pure protein precipitated in the neutral elution buffer. Acidification to pH 6.5 allowed the protein to remain soluble at ~500 μM at room temperature. Storage for appreciable amounts of time indicated disulfide bond formation as well as various degradation truncations.

We first tested the binding capabilities of the affibody alone. First, the affibody was exposed to TCEP to reduce the slowly forming disulfide dimers, and then exposed to Oregon Green maleimide (Figure 4-10a). The fluorescently labeled affibody showed elevated binding to HER2 positive SKBR3 cells and much lower binding to HER 2 negative PC3 cells by flow cytometry (Figure 4-11). With this binding capability known, we next attempted to attach the affibody to the exterior of MS2 capsids.

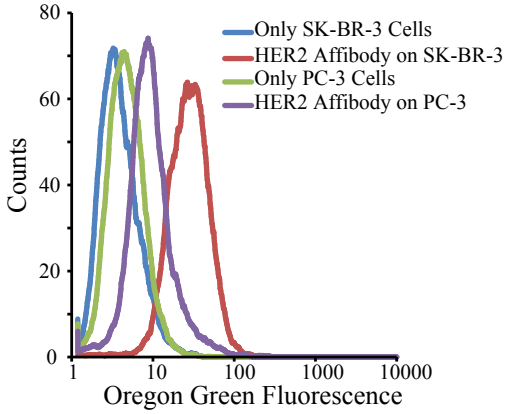

Figure 4-11. Flow cytometry analysis of H2A binding to HER2 (+) (SKBR3) and HER2 (-) (PC3) cell lines.

Since we chose to use cysteine modification to introduce the phenylene diamine functionality onto the affibody, we needed a maleimide functionalized small molecule. Modification of the affibody with **6** followed the protocol for modification with Oregon Green to access phenylene diamine functionalized affibodies (Figure 4-10b). Following the same strategy, we were also able to use PEG-based small molecule linkers (**7-** Figure 4-10c) to increase the space between protein and pheylene diamine reaction site. With this reactive targeting partner in hand, we next carried out the oxidative coupling with pAF19 MS2 using standard reaction conditions and analyzed the

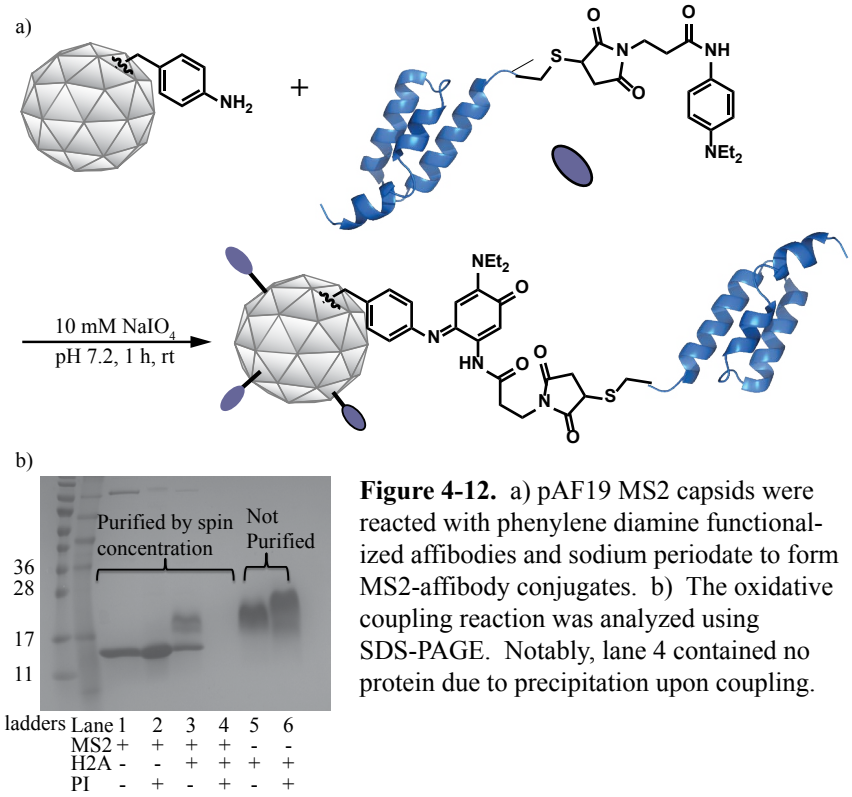

Figure 4-12. a) pAF19 MS2 capsids were reacted with phenylene diamine functionalized affibodies and sodium periodate to form MS2-affibody conjugates. b) The oxidative coupling reaction was analyzed using SDS-PAGE. Notably, lane 4 contained no protein due to precipitation upon coupling.

modification using SDS-PAGE (Figure 4-12b). Unfortunately, despite the low concentration of affibody, the resulting MS2-affibody conjugates were not soluble at neutral pH. While soluble at lower pH, they were not retained by a 100 kDa spin concentrator, indicating capsid disassembly. The inability to spin concentrate these structures also made it difficult to analyze them by SDS-PAGE due to the low reaction concentrations.

To investigate whether the bioconjugation reaction was occurring before precipitate formation, we decided to modify fluorescently labelled MS2 capsids with chemically incorporated exterior

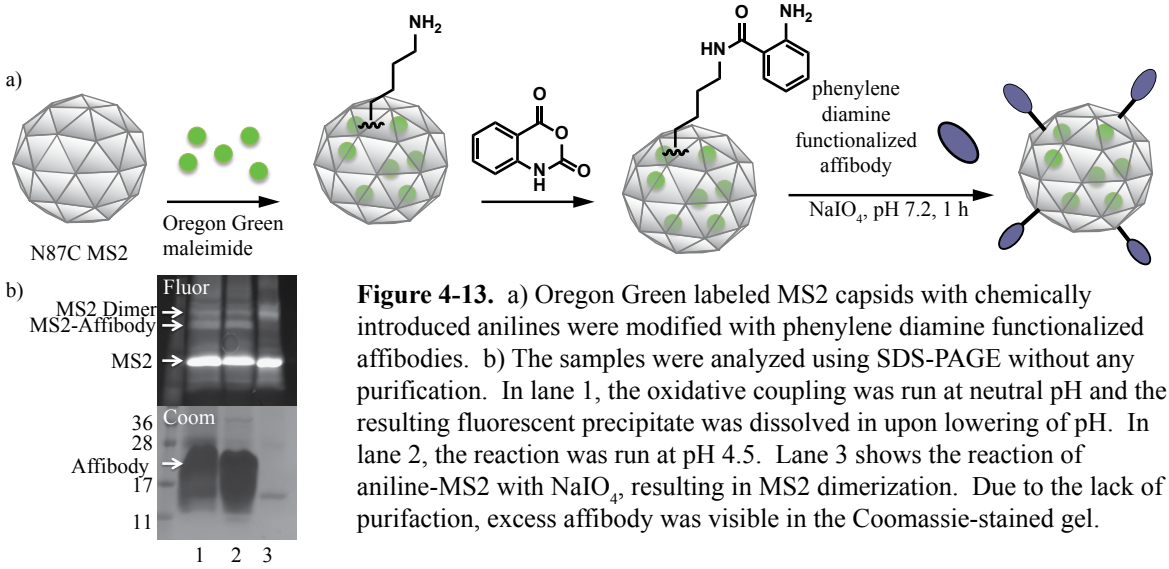

Figure 4-13. a) Oregon Green labeled MS2 capsids with chemically introduced anilines were modified with phenylene diamine functionalized affibodies. b) The samples were analyzed using SDS-PAGE without any purification. In lane 1, the oxidative coupling was run at neutral pH and the resulting fluorescent precipitate was dissolved in upon lowering of pH. In lane 2, the reaction was run at pH 4.5. Lane 3 shows the reaction of aniline-MS2 with $NaIO_4$, resulting in MS2 dimerization. Due to the lack of purifaction, excess affibody was visible in the Coomassie-stained gel.

anilines (Figure 4-13a). Oregon labelled MS2 capsids were reacted with affibodies under oxidative coupling conditions and analysed by SDS-PAGE without purification, using gels with larger loading wells. The reaction at neutral conditions again formed a precipitate upon reaction. The fluorescence in the sample was completely found in the precipitate, indicating that oxidative coupling had indeed occurred since the fluorescent capsids were now precipitating along with the insoluble affibody. To confirm, we acidified the sample and loaded it on an SDS-PAGE gel (Figure 4-13b, lane 1). Due to the fluorescent capsid reporter, we could now observe the MS2-affibody gel shift by fluorescence visualization, as well as the formation of MS2 dimers. Due to the excess affibody in the reaction, the Coomassie stained gel proved less valuable for observing MS2 modification, though it did confirm the presence of protein in the sample. Similar modification levels were observed at pH 4.5 (lane 2), but precipitate again formed upon spin concentration.

Various mutants of the HER2 affibody were made to alleviate the solubility issues. Various amino acid additions and substitutions were tried, as well as the synthesis of a PEG-based maleimide linker, but none of these affibody variants gave soluble conjugates. Notably, the deletion of the His_6 tag rendered the affibody completely insoluble regardless of buffer pH. Due to these solubility problems, we therefore turned our attention to alternative protein targeting groups, which will be detailed in Chapter 5.

4.6 Materials and methods.

General Procedures and Materials

Unless otherwise noted, all chemicals were obtained from commercial sources and used without further purification. Analytical thin layer chromatography (TLC) was performed on EM Reagent 0.25 mm silica gel 60-F_{254} plates with visualization by ultraviolet (UV) irradiation at 254 nm and/or staining with potassium permanganate. Purifications by flash chromatography were performed using EM silica gel 60 (230-400 mesh). The eluting system for each purification was determined by TLC analysis. Chromatography solvents were used without distillation. All organic solvents were removed under reduced pressure using a rotary evaporator. Water (ddH_2O) used in biological procedures or as a reaction solvent was deionized using a NANOpure™ purification system (Barnstead, USA) purchased from Aldrich. Solid phase extraction (SPE) columns were purchased from Phenomenex, Inc. (www.phenomenex.com) and used as specified, unless otherwise noted. All Fmoc-protected amino acids and preloaded Wang resin were obtained from Novabiochem (EMD, Germany). All cell culture reagents were obtained from Gibco/Invitrogen Corp (Carlsbad, CA) unless otherwise noted. Molecular biology reagents and competent cells were purchased from Qiagen, Invitrogen and New England Biolabs. Protein expression reagents were obtained from Invitrogen and protein purification reagents and materials from Biorad and Qiagen.

Instrumentation and Sample Analysis Preparations

NMR. ^{1}H and ^{13}C spectra were measured with a Bruker AV-500 (500 MHz), or a Bruker DRX-500 (500 MHz) spectrometer, as noted. ^{1}H NMR chemical shifts are reported as δ in units of parts per million (ppm) relative to $CDCl_3$ (δ 7.26, singlet), or methanol-d_4 (δ 3.31, pentet).

Multiplicities are reported as follows: s (singlet), d (doublet), t (triplet), or m (multiplet). Coupling constants are reported as a *J* value in Hertz (Hz). The number of protons (n) for a given resonance is indicated as nH, and is based on spectral integration values. ^{13}C NMR chemical shifts are reported as δ in units of parts per million (ppm) relative to $CDCl_3$ (δ 77.2, triplet), or methanol-d_4 (δ 49.00, septet).

Mass Spectrometry. High resolution Electrospray (ESI) and Fast Atom Bombardment (FAB^+) mass spectra were obtained at the UC Berkeley Mass Spectrometry Facility. Electrospray LC/MS analysis was performed using an API 150EX system (Applied Biosystems, USA) equipped with a Turbospray source and an Agilent 1100 series LC pump. Protein chromatography was performed using either a Phenomenex Jupiter™ 300 5μ C5 300 Å reversed-phase column (2.0 mm x 150 mm), Phenomenex Jupiter™ 300 5μ C18 300 Å reversed-phase column (2.0 mm x 150 mm), or Dionex Proswift RP-4H reversed phase column (1mm x 50 mm) with a MeCN:ddH_2O gradient mobile phase containing 0.1% formic acid (250 μL/min). Protein mass reconstruction was performed on the charge ladder with Analyst software (version 1.3.1, Applied Biosystems). MALDI-TOF analysis was performed on a Voyager-DE instrument (Applied Biosystems), and all spectra were analyzed using Data Explorer software. The matrix solution was a 10 mg/mL solution of sinapic acid in in 50% acetonitrile, 50% water, 0.1 % TFA.

High Perfomance Liquid Chromatography. HPLC was performed on an Agilent 1100 Series HPLC System (Agilent Technologies, USA). Size exclusion chromatography was accomplished on an Agilent Zorbax® GF-250 with isocratic (0.5 mL/min) flow or a Phenomenex PolySep-GFC-P 5000 (PS5K) column (300 x 7.8 mm, flow rate 1.0 mL/min) or a Phenomenex BioSEP-4000 (BS4K) column (300 x 7.8 mm, flow rate, 1.0 mL/min) using an aqueous mobile phase (10 mM Na_2HPO_4, pH 7.2) . Reversed-phase liquid chromatography on protein samples was accomplished on a Agilent Poroshell 300 SB-C18 column (2.1 x 75 mm) using a MeCN:ddH_2O gradient mobile phase containing 0.1% trifluoroacetic acid. Semi-preparatory scale purification was performed using a Agilent Zorbax 300 SB-C18 column (9.4 mm x 25 cm). Sample analysis for all HPLC experiments was achieved with an inline diode array detector (DAD) and an inline fluorescence detector (FLD).

Gel Analyses. Sodium dodecyl sulfate-poly(acrylamide) gel electrophoresis (SDS-PAGE) was accomplished on a Mini-Protean apparatus from Bio-Rad (Hercules, CA) with 10-20% gradient polyacrylamide gels (BioRad, CA), following the protocol of Laemmli.[13] All electrophoresis protein samples were mixed with SDS loading buffer in the presence of dithiothreitol (DTT) and heated to 100 °C for 10 min to ensure reduction of disulfide bonds and complete denaturation unless otherwise noted. Commercially available molecular mass markers (Bio-Rad) were applied to at least one lane of each gel for calculation of the apparent molecular masses. Gel imaging was performed on an EpiChem3 Darkroom system (UVP, USA).

Centrifugations were conducted with an Allegra 64R Tabletop Centrifuge (Beckman Coulter, Inc., USA). General desalting and removal of other small molecules of biological samples were achieved using NAP-5 gel filtration columns (GE Healthcare). Protein samples were concentrated by way of centrifugal ultrafiltration using Amicon Ultra-4 or Ultra-15 100 kDa molecular weight cut off (MWCO) centrifugal filter units (Millipore), or Amicon Microcon 10 kDa and 100 kDa MWCO (Millipore) centrifugal filter units.

Experimental Procedures

N87C MS2 production.

The pBAD-MS2 plasmid and protein expression has been previously reported.[2] The pBAD-MS2-N87C mutant was made by site-directed mutagenesis of the pBAD-MS2 plasmid. Position 87 was converted to a cysteine using the following forward and reverse primers:

Forward: 5'–AGCCGCATGGCGTTCGTACTTATGTATGGAACTAACCATTC–3'

Reverse: 5'–GAATGGTTAGTTCCATACATAAGTACGAACGCCATGCGGCT–3'

Growth and purification of MS2-N87C was identical to that of wtMS2. Yields are slightly less than the 100 mg/L reported for wtMS2.

pAF19 MS2 and N87C pAF19 MS2 used in this chapter were expressed and purified by Nick Stephanopolous.

Affibody production. The gene for the HER2 affibody was purchased from Genscript and received in a pUC57 plasmid with ampicillin resistance, flanked by NdeI and BamHI restriction sites as shown below. The restriction sites are highlighted in red.

```
TAA GAA GGA GAT ATA CAT ATG GTG GAT AAT AAA TTC AAT AAA GAA
End Glu Gly Asp Ile His Met Val Asp Asn Lys Phe Asn Lys Glu
ATG CGT AAT GCC TAC TGG GAA ATC GCC CTG CTG CCG AAC CTG AAT
Met Arg Asn Ala Tyr Trp Glu Ile Ala Leu Leu Pro Asn Leu Asn
AAT CAA CAG AAA CGT GCT TTT ATT CGT AGT CTG TAT GAT GAC CCG
Asn Gln Gln Lys Arg Ala Phe Ile Arg Ser Leu Tyr Asp Asp Pro
AGC CAG TCT GCC AAC CTG CTG GCG GAA GCC AAA AAA CTG AAT GAT
Ser Gln Ser Ala Asn Leu Leu Ala Glu Ala Lys Lys Leu Asn Asp
GCA CAA GCT CCG AAA GGC GGC GGC GAA AAT CTG TAC TTC CAG GGT
Ala Gln Ala Pro Lys Gly Gly Gly Glu Asn Leu Tyr Phe Gln Gly
CAC CAC CAT CAT CAT CAC TGT TGA TAA GGA TCC GAA TTC GAG CTC
His His His His His His Cys End End Gly Ser Glu Phe Glu Leu
CGT CGA
```

Arg Arg

The desired gene was PCR amplified using the following primers.

Forward PCR- GGTGGTGGTCATATGGTGGATAATAAATTC-her2 aff forward

Rev PCR- GGTGGTGGTGGATCCTTATCAAC-her2 aff reverse

All cells used for affibody cloning were under ampicillin antibiotic control and grown in sterile LB with 100 mg/L ampicillin or LB-agar-amp plates. The PCR-amplified genes and a pET-20b plasmid were digested using NdeI and BamHI restriction enzymes, the digested plasmid exposed to Antarctic phosphatase, and the desired gene ligated into the digested plasmid using T4 DNA ligase. The ligation mixture was transformed into XL1Blue chemically competent cells and colonies grown. Four colonies were sequenced with a 50% transformation success rate. The mini-prepped DNA was used to transform chemically competent BL21(DE3) cells. The successfully transformed colonies were used to grow 5 mL overnight starter cultures in sterile LB. One starter culture was added to 1 L sterile LB with 100 mg/L solid ampicillin and cultures were grown for 4.5 h and allowed to reach log phase growth (OD_{600}=0.7). Upon reaching log-phase growth, protein expression was induced using 0.6 mM IPTG. The protein was expressed for 3 h and then the cells centrifuged and pelleted. Cell pellets were centrifuged and frozen in 0.5 L aliquots at -80 °C.

Affibody purification. Affibody cell pellets were purified according to the procedure outlined in the following reference for purification under denaturing conditions.[14] Buffer composition is described in the above reference. A cell pellet was thawed and suspended in 20 mL lysis buffer containing 8 M urea. After thawed, the pellet was shaken for 60 min at rt and then the remaining cell debris pelleted. The supernatant was isolated and to it was added 4 mL 50% Ni-NTA agarose (Qiagen). The slurry was allowed to spin on a rotary shaker for 1 h at 4 °C. The agarose with protein bound was washed with 3x 10 mL portions of pH 6.3 wash buffer containing 8 M urea. The purified protein was then eluted using 10 mL elution buffer at pH 4.5 and 8 M urea. The eluent was concentrated using 100 kDa MWCO spin concentrators and urea removed using NAP-25 gel filtration columns.

3-(4-azidophenyl)propanoic acid (3). The synthesis of **3** closely followed the procedure of Carnazzi and coworkers.[15] A solution of 1 M $NaNO_2$ (6.67 mL, 1.1 eq.) was slowly added to a solution of **1** (1 g, 6 mmol, 1 eq.) in 2 M HCl for 15 min at 0 °C. A solution of 1 M NaN_3 (1.05 eq) was added, resulting in vigorous bubbling. After 10 min, ethyl acetate was added and the bubbles dissipated. The reaction was diluted with water and extracted with 3 portions of ethyl acetate. The combined organics were washed with water and brine, dried over Na_2SO_4, and the solvent removed under reduced pressure to yield a solid product that was used without further purification (58%). ^{1}H NMR(500 MHz, $CDCl_3$): δ, 2.66 (t, 2H, J=7.5 Hz), 2.93 (t, 2H, J=7.5 Hz), 6.96 (d, 2H, J=8 Hz), 7.20 (d, 2H, J=8 Hz).

2,5-dioxopyrrolidin-1-yl 3-(4-azidophenyl)propanoate (4). A solution of **3** (100 mg, 0.52

mmol), HCTU (226 mg, 1.05 eq.), NHS (65.8 mg, 1.1 eq.), and DIPEA (181 μL, 2 eq.) in 5.2 mL of CH_2Cl_2 (0.1 M reaction) was stirred for 10 min. The HCTU and DIPEA were the last two reagents added, and portions of the HCTU remained insoluble. The reaction was monitored by TLC and no starting material remained after 10 min. The solvent was removed under reduced pressure and the residue resuspended in ~ 1 mL of CH_2Cl_2. The crude material was purified using flash chromatography (25:72 -1:1 ethyl acetate:hexanes), yielding a pale yellow solid (87 %). ^{1}H NMR(500 MHz, $CDCl_3$): δ, 2.84 (s, 4H), 2.90 (t, 2H, J=7.5 Hz), 3.04 (t, 2H, J=7.5 Hz), 6.98 (d, 2H, J=7.5 Hz), 7.22 (d, 2H, J=7.5 Hz).

Peptide synthesis

Peptides were synthesized using standard Fmoc-based chemistry and adapted from procedures by Zac Carrico, Dante Romanini, and Leah Witus.[16] Side chain protecting groups used were: Asn(Trt), Asp(tBu), Arg(Pbf), Cys(Trt), Gln(Trt), Glu(tBu), His(Trt), Lys(Boc), Ser(tBu), Thr(tBu), Trp(Boc), Tyr(tBu). The resin linkers used was benzyloxybenzyl alcohol (Wang) polystyrene. Synthesis was accomplished manually, using 10 equivalents of amino acid in dimethylformamide with (2-(6-Chloro-1*H*-benzotriazole-1-yl)-1,1,3,3-tetramethylaminium hexafluorophosphate) (HCTU) (10 eq) as the coupling reagent *N*,*N*-diisopropylethylamine (DIPEA) (20 eq) as additives for 10 min. Iterative Fmoc deprotection and amino acid coupling steps were performed to synthesize the desired sequence. After each coupling, the general procedure for rinsing excess reagents away from the resin was performed, which was to drain the solution from the resin, add approximately 10 mL DMF, shake briefly, drain, and repeat for a total of 5 rinses. The general rinsing protocol was performed after each of the deprotection and coupling steps.

The Fmoc deprotection was accomplished by incubation (with rotation on a LabQuake shaker) with 10 mL of Fmoc deprotection solution (20% by volume piperidine in DMF) for 5 minutes followed by replacement of the deprotection solution and a second 2.5 min incubation. If a particular amino acid was used more than once in a peptide sequence, a stock solution was made in DMF and aliquots were added for each coupling.

Addition of phenylene-diamine

Once all of the amino acids had been coupled to the growing peptide on resin, the N-terminal Fmoc group was removed with 20% piperidine in DMF. After washing, the resin was suspended in DMF and one thawed aliquot of NHS-ester **8** (1.66 eq) in DMSO was added. The resin was incubated with gentle shaking for 3 h and washed thoroughly. The peptide was then cleaved from the resin using a cocktail of 94% trifluoroacetic acid, 5% H_2O, and 1% triisopropylsilane. Crude peptides were precipitated in cold *tert*-butylmethylether, purified using preparative reversed-phase HPLC, and lyophilized before use.

Typical MS2 modification with Oregon Green maleimide. To a solution of N87C MS2, or N87C pAF19 MS2 (100 nmol, 200 μL, 500 μM in 100 mM pH 7.2 phosphate buffer) was added Oregon Green maleimide (200 nmol, 10 μL, 20 mM in DMSO). The reaction mixture was incubated at RT for 1 h, followed by purification by size exclusion chromatography (NAP-5) and several spin concentration cycles until the flow-through was colorless. Longer reaction times and/or higher buffer pH led to detectable double modification. Dye-labeled MS2 monomers were

characterized using LC-MS and the expected mass addition was observed.

Typical modification of Oregon Green MS2 with isatoic anhydride. To a solution of Oregon Green modified N87C MS2 (75 nmol) in 100 mM pH 8 phosphate buffer was added isatoic anhydride (100 eq., 75 μL of a 0.1 M solution in DMF) and enough buffer to reach 100 μM MS2. The reaction was allowed to proceed for 3-72 h, after which excess isatoic anhydride waspurified away by NAP-10 gel filtration and successive spin concentration against 100 kDa MWCO spin concentrators.

Typical procedure for the modification of amine-containing aptamers. To a solution of amine-functionalized DNA (150 nmol) in 100 mM pH 8 phospate buffer and 150 mM NaCl was added **5** (15 μmol, 60 μL of a 0.25 M solution in DMSO) and enough buffer to reach 100 μM DNA final concentration. The reaction was allowed to proceed for 2 h and then purified by 3 successive NAP gel filtration columns. The eluted fractions were then lyophilized and resuspended in buffer.

Typical procedure for the modification of an affibody cysteine with maleimide reagents. To a solution of affibody (250 nmol) in 100 mM pH 4.5 acetate buffer was added **6** (5 eqs, 25 μL of 50 mM solution in DMF) and enough buffer to reach 500 μM affibody. After 1 h of reaction, the protein was purified using NAP gel filtration columns and successive spin concentration against 3kDa MWCO spin concentrators. The modification was monitored by MALDI or LC-ESI-MS.

Typical procedure for the modification of aniline-MS2 with phenylene-diamine functionalized targeting group. The following procedure is adapted from a general procedure for DNA conjugation to MS2 developed by Gary Tong.[6] An Eppendorf tube was charged with either *p*AF19 MS2 or N87C *p*AF19 MS2 (20 μM) (with the interior cysteine first modified with maleimide reagents), phenylene diamine-containing targeting group (20-1 mM), and $NaIO_4$ (2-10 mM). The reaction was carried out in 10 mM pH 7.0 phosphate buffer, containing 150 mM NaCl if the targeting group was a DNA aptamer. The reaction was briefly vortexed and allowed to react at rt for 1 h. After an hour, for a 50 μL reaction, the reaction is quenched by the addition of 5 μL of pH 7, 500 mM tris(2-carboxyethyl)phosphine hydrochloride (TCEP). For purification, the sample was first buffer exchanged by gel filtration (NAP) into the desired buffer. The excess targeting group was then removed by successive centrifugal filtration using 100k molecular weight cutoff filters (Millipore).

Cell culture. Immortalized human breast cancer cells were maintained according to ATCC guidelines. MCF-7, SK-BR-3 and PC3 cells were from the Tissue Culture Facility, Department of Molecular & Cell Biology, UC Berkeley, and were grown in DMEM supplemented with 10% FBS. MCF-10A cells were acquired from ATCC and grown in MEBM media supplemented with 100 ng/ml cholera toxin. All cells were grown at 37 °C in 5% CO_2.

Flow cytometry of cells exposed to fluorescent capsids. Flow cytometry analysis was acquired on a FACSCalibur flow cytometer (BD Biosciences, USA) using a standard 488 Ar laser. Data were collected for at least 10,000 live cells for all experiments. Cells ($1x10^6$ cells in 100 μL) were treated with fluorescent capsids in culture media or 1% FBS and incubated either on ice or at 37 ºC for 30-60 min in Eppendorf tubes or multi-well plates. After incubation, the cells were

washed twice with 1% FBS, suspended in 500 μL 1% FBS, and then analyzed on the flow cytometer.

4.7 References.

1. Hooker, J.M., Esser-Kahn, A.P., Francis, M.B. Modification of Aniline Containing Proteins Using an Oxidative Coupling Strategy. *J. Am. Chem. Soc*. **2006**, *128*, 15558-15559.
2. Carrico, Z. M., Romanini, D. W., Mehl, R. A., Francis, M. B. Oxidative coupling of peptides to a virus capsid containing unnatural amino acids. *Chem. Commun.* **2008**, 1205-1207.
3. Stephanopoulos, N., Tong, G.J., Hsiao, S.C., Francis, M.B. Dual-surface modified virus capsids for targeted delivery of photodynamic agents to cancer cells. *ACS Nano*. **2010**, *4*, 6014-20.
4. Zhang, J., Spring, H., Schwab, M. Neuroblastoma tumor cell-binding peptides identified through random peptide phage display. *Cancer Lett.* **2001**, *171*, 153-164.
5. Rae, J.M., Creighton, C.J., Meck, J.M., Haddad, B.R., Johnson, M.D. MDA-MB-435 cells are derived from M14 melanoma cells – a loss for breast cancer, but a boon for melanoma research. *Breast Cancer Res. Treat.* **2007,** *104*, 13-19.
6. Tong, G.J., Hsiao, S.C., Carrico, Z.M., Francis, M.B. Viral Capsid DNA Aptamer Conjugates as Multivalent Cell-Targeting Vehicles. *J. Am. Chem. Soc.* **2009**, *131*, 11174-11178.
7. Bates, P.J., Kahlon, J. B., Thomas, S.D., Trent, J.O., Miller, D.M. Antiproliferative activity of G-rich oligeonucleotides correlates with protein binding. *J. Biol. Chem.* **1999**, *274*, 26369-26377.
8. a) Soundararajan, S., Chen, W., Spicer, E.K., Courtenay-Luck, N., Fernandes., D.J. The nucleolin targeting aptamer AS1411 destabilizes *bcl-2* messenger RNA in human breast cancer cells. *Cancer Res.* **2008**, *68*, 2358-2365. b) Bates, P.J., Laber, D.A., Miller, D.M., Thomas, S.D., Trent, J.O. Discovery and development of the G-rich oligonucleotide AS1411 as a novel treatment for cancer. *Exp. Mol Pathol.* **2009**, *86*, 151-164.
9. Ferreira, C.S.M., Matthews, C.S., Missailidis, S. DNA aptamers that bind to MUC1 tumour marker: Design and characterization of MUC1-binding single-stranded DNA aptamers. *Tumor Biol.* **2006**, *27*, 289-301.
10. Li, N., Ebright, J.N., Stovall, G.M., Chen, X., Nguyen, H.H., Singh, A., Syrett, A., Ellington, A.D. Technical and Biological Issues Relevant to Cell Typing with Aptamers. *J. Proteome Res*. **2009,** *8,* 2438-2448.
11. Nord, K., Gunneriusson, E., Ringdahl, J., Stahl, S., Uhlen, M., Nygren, P. Binding proteins selected from combinatorial libraries of an α-helical bacterial receptor domain. *Nat. Biotech.* **1997**, *15*, 772-777.
12. a) Wikman, M., Steffan, A.C., Gunneriusson, E., Tolmachev, V., Adams, G.P., Carlsson, J., Stahl, S. Selection and characterization of HER2/neu-binding affibody ligands. *Protein Eng. Des. Sel.* **2004**, *17*, 455-462. b) Orlova, A., Magnusson, M., Eriksson, T.L.J., Nilsson, M., Larsson, B., Hoiden-Guthenberg, I., Widstrom, C., Carlsson, J., Tolmachev, V., Stahl, S.,

Nilsson, F.Y. Tumor imaging using a picomolar affinity HER2 binding affibody molecule. *Cancer Res.* **2006**, *66*, 4339-4348.

13. Laemmli, U. K. Cleavage of structural proteins during the assembly of the head of bacteriophage T4. *Nature* **1970**, *227*, 680.
14. Qiagen protocol. The QIAexpressionist: A handbook for high-level expression and purification of 6xHis-tagged proteins, 5th Ed. **2003**, Qiagen Inc.
15. Carnazzi, E., Aumelas, A., Barberis, C., Guillon, G., Seyer, R. A new series of photoactivatable and iodinatable linear vasopressin antagonists. *J. Med. Chem.* **1994**, *37*, 1841-1849.
16. a) Witus, L.S. Optimization of protein bioconjugation reactions using combinatorial peptide libraries. Ph.D. dissertation, University of California, Berkeley, Berkeley, CA, 2012. b) Carrico, Z.M. Phage-based bioimaging agents and a selection technique for the directed evolution of proteases. Ph.D. dissertation, University of California, Berkeley, Berkeley, CA, 2011.

Chapter 5: Designed Ankyrin Repeat Proteins for MS2 Targeting

5.1 An introduction to Designed Ankyrin Repeat Proteins (DARPins)

Having observed low selectivity or poor physical characteristics for several targeting groups, we next chose to investigate a class of engineered binding proteins called Designed Ankyrin Repeat Proteins (DARPins). This binding protein was developed by the Pluckthun Group from naturally occurring ankyrin repeat scaffolds, a class of binding protein found in all phyla that is composed of stacked 33 amino acid repeats of stable secondary structure.[1] A consensus AR module was randomized at several positions to form a library of DARPins, from which selective binders were chosen. The selected binders exhibited extremely effective binding characteristics (nanomolar K_d), high levels of expression in *E. coli* culture, as well as high, monomeric solubility and stability. The DARPins do not include native cysteines, meaning we could introduce an engineered cysteine to elaborate as an oxidative coupling partner. DARPins have been developed to bind a wide variety of targets including EGFR, HER2, TNFα, Fc, MBP, EpCAM, and CD4, among others.[2] Of these DARPin variants, the HER2 binding protein was of particular interest to us because of its extremely high affinity (further evolution to 90 pM K_d) and favorable size (~15 kDa).[3] In addition, the favorable physical characteristics and high expression seemed to be particularly beneficial for our MS2 based system's requirements in comparison to previous work with affibodies. Lastly, the HER2 binding DARPin also has been demonstrated to be an effective binder *in vivo*.[4]

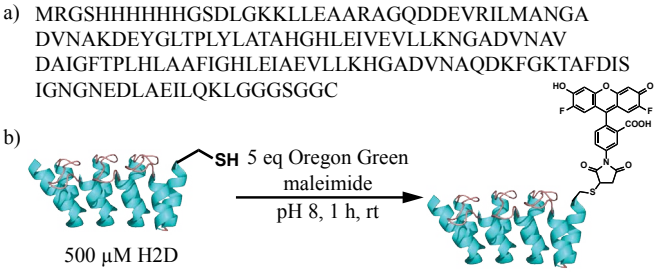

Figure 5-1. a) Amino acid sequence for the expressed α HER2 DARPin containing an N-terminal His_6 tag and unique C-terminal cysteine. b) The unique cysteine can be alkylated using maleimide small molecules, such as the Oregon Green fluorescent dye shown.

We first sought to confirm the selectivity of the HER2 binding DARPin alone to HER2 positive cell lines. We expressed a variant of the published sequence that contained an N-terminal His_6 tag, a C-terminal glycine/serine spacer, and a unique cysteine at the C-terminus. This sequence will hereafter be abbreviated as H2D (Figure 5-1a). H2D was modified at the unique cysteine using Oregon green maleimide, and the fluorescent DARPin (Figure 5-1b) was incubated with HER2 positive SKBR3 cells as well as HER2 negative PC3 cells. As observed by flow cytometry, even incubation at 37 °C resulted in an almost 20-fold greater level of binding to the SKBR3 cell line (Figure 5-2).

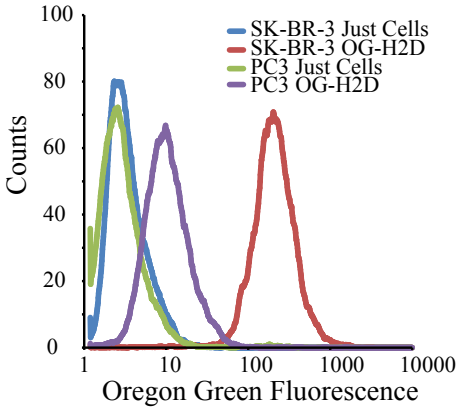

Figure 5-2. Oregon Green labeled αHER2 DARPins (H2D) were incubated with SK-BR-3 (HER2+) and PC3 (HER2-) cells at 1 μM DARPin for 1 h at 37 ºC and analyzed by flow cytometry.

5.2 Oxidative coupling reaction between DARPins and MS2 capsids.

With this encouraging binding result in hand, we next used the oxidative coupling reaction to attach the DARPin to MS2 capsids. First we synthesized phenylene diamine functionalized αHER2 DARPin (PDA-H2D) using cysteine alkylation as we did previously with the affibody (Figure 4-10b). To test the reactivity of the PDA-H2D, we reacted it with aniline-functionalized PEG5K[5] and sodium periodate and analyzed the conjugate by SDS-PAGE (Figure 5-3). Notably, exposure of PDA-DARPin to sodium periodate gave appreciable amounts of DARPin dimer, as observed by gel-shift (Lane 2). However, if the aniline-PEG coupling partner was introduced, a smaller shift was observed, presumably corresponding to PEG-DARPin conjugates (Lane 1), and no DARPin dimer was observed. Lastly, with no periodate present, no addition or dimerization was observed (Lane 3).

Next we reacted the PDA-DARPin with pAF19 MS2 under standard oxidative coupling conditions and purified the reactions with four successive spin concentration steps (Figure 5-4a). The

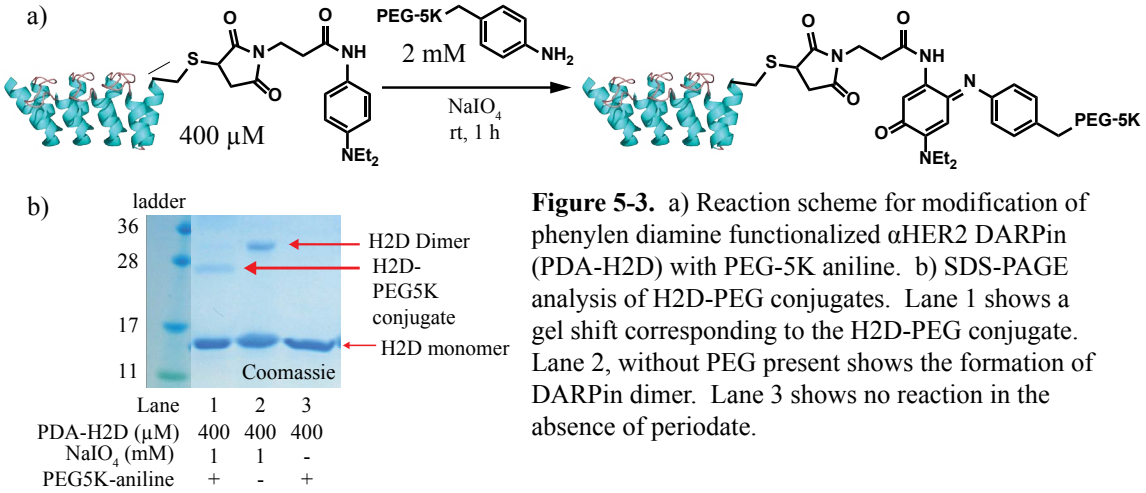

Figure 5-3. a) Reaction scheme for modification of phenylen diamine functionalized αHER2 DARPin (PDA-H2D) with PEG-5K aniline. b) SDS-PAGE analysis of H2D-PEG conjugates. Lane 1 shows a gel shift corresponding to the H2D-PEG conjugate. Lane 2, without PEG present shows the formation of DARPin dimer. Lane 3 shows no reaction in the absence of periodate.

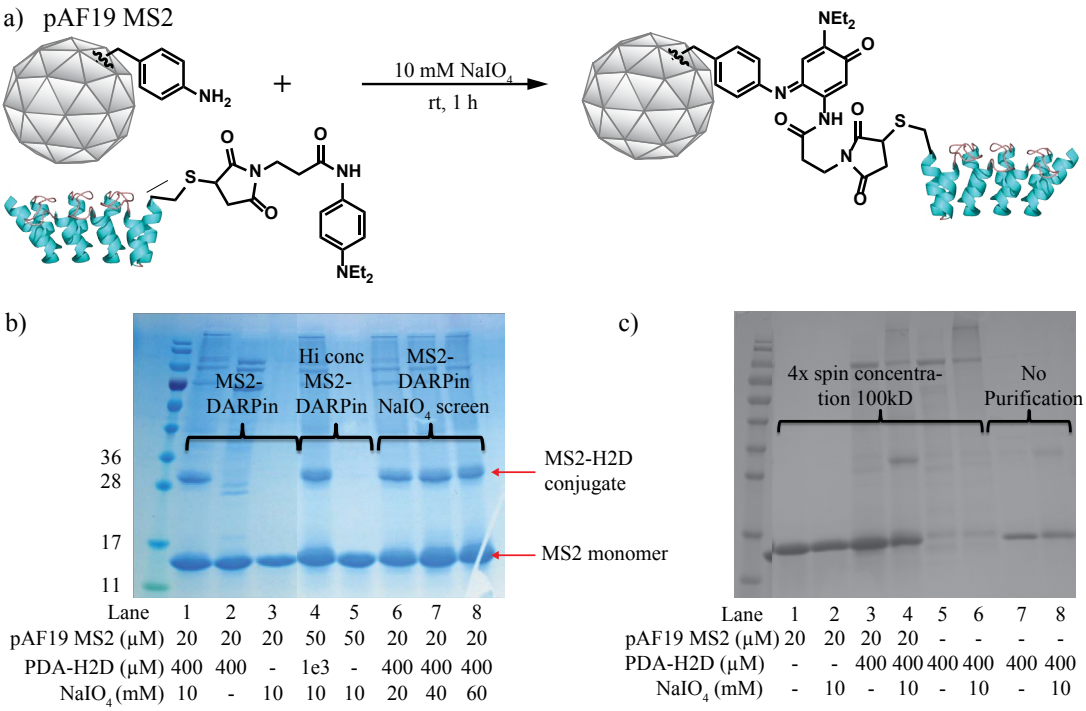

Figure 5-4. a) Reaction scheme for the modification of pAF19 MS2 with PDA-H2D using a $NaIO_4$ mediated oxidative coupling reaction. b-c) MS2-DARPin conjugates were analyzed using SDS-PAGE.

reactions were analyzed using SDS-PAGE, and as expected, a gel shift corresponding to the DARPin addition to the MS2 monomer was observed (Figure 5-4b). In addition, using pAF19 MS2, no MS2 dimers were observed. No reaction occurred without the presence of sodium periodate (Lane 2). A large excess of PDA-H2D reaction partner yielded slightly higher levels of DARPin addition (Lane 4). Varying periodiate concentrations did not, however, cause any appreciable change in reactivity (Lanes 6-8). One problem observed was that the DARPin-dimer ran as a similar band on SDS-PAGE, giving rise to the possibility to confuse DARPin-dimer and MS2-DARPin conjugates.

We sought to clarify whether the higher MW band was indeed the MS2-DARPin conjugate by confirming that the successive spin concentration against 100 kDa membranes would indeed remove the unconjugated DARPin (Figure 5-4c). Since the assembled capsid weighs over 2 megadaltons, the modified capsid can be separated from excess DARPin using this technique. We ran samples containing all combinations of the reaction partners, as well as purified and non-purified samples. Lanes 5 and 6 of Figure 5-4c, which contain only DARPin, show that the spin concentration step indeed removes most of the unreacted DARPin, meaning that the higher molecular weight band in lane 4 indeed corresponds to the MS2-DARPin conjugate. In addition, the location of the dimer band in lane 6 was slightly but noticeably higher than the band in lane 4. The spin concentration is fairly effective in removing unreacted DARPin therefore, though at a slight cost to final recovery of modified capsid.

The next experiment was to test the effect of varying PDA-DARPin concentration. Analysis by SDS-PAGE indeed showed increased modification levels with increasing DARPin reaction partner, up to approximately 30% modification with 1 mM PDA-H2D (Figure 5-5). However, higher equivalents of DARPin (lane 9) resulted in difficulty in purification, so we chose to remain below 20 equivalents of DARPin to streamline the purification.

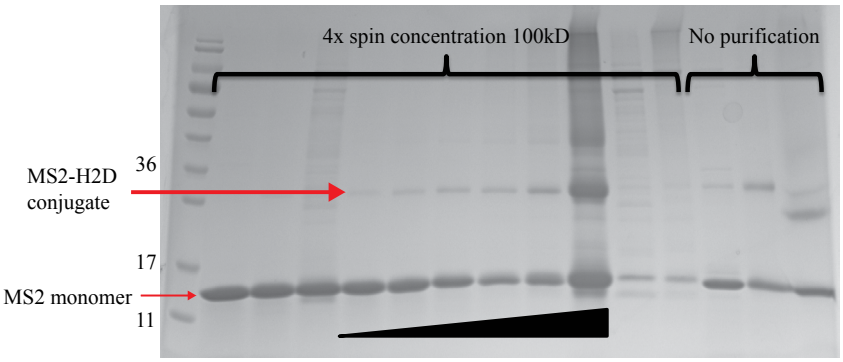

Lane	1	2	3	4	5	6	7	8	9	10	11	12	13	14
pAF19 MS2 (μM)	20	20	20	20	20	20	20	20	20	-	-	-	-	-
PDA-H2D (μM)	-	-	400	20	40	100	200	400	1000	400	400	400	400	20
$NaIO_4$ (mM)	-	10	-	10	10	10	10	10	10	-	10	-	10	10
														+ 400 μM PEG-5K aniline

Figure 5-5. SDS-PAGE analysis of MS2-DARPin conjugates, screening for PDA-H2D concentration. Increasing levels of modification were observed with increasing PDA-H2D concentration.

We next used fluorescent MS2 capsids to construct dual modified MS2 using the new DARPin targeting group (Figure 5-6a). Once again, we used Oregon green modified N87C MS2 and chemically incorporated anilines using isatoic anhydride. However, upon reaction with PDA-H2D, it was difficult to assess whether the high molecular weight band was MS2 dimer or MS2-DARPin conjugate (Figure 5-6b). A reaction with PEG5K phenylene diamine confirmed that the

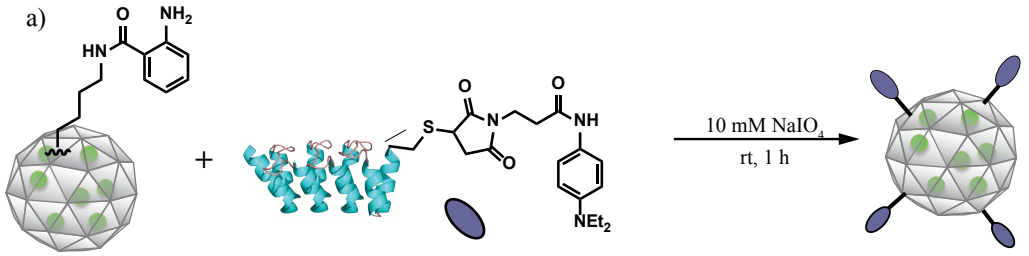

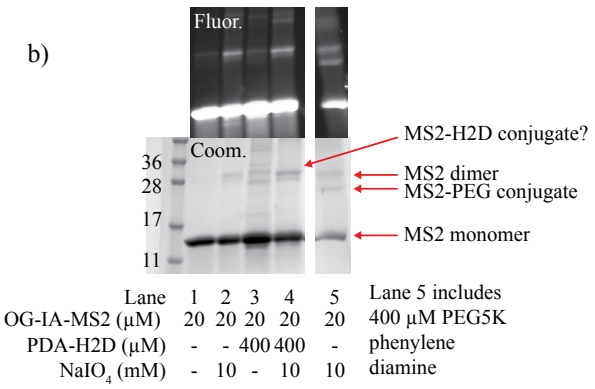

Lane	1	2	3	4	5	
OG-IA-MS2 (μM)	20	20	20	20	20	Lane 5 includes
PDA-H2D (μM)	-	-	400	400	-	400 μM PEG5K
$NaIO_4$ (mM)	-	10	-	10	10	phenylene diamine

Figure 5-6. a) Reaction scheme for the dual modification of N87C MS2 capsids. MS2 capsids were modified with Oregon Green maleimide and isatoic anhydride, as shown in Chapter 4. These capsids were then reacted with PDA-H2D in the present of $NaIO_4$. b) MS2 dual conjugates were analyzed using SDS-PAGE. It was difficult to differentiate between MS2 dimers and MS2-H2D conjugates based on their electrophoretic mobility on SDS-PAGE.

chemically incorporated anilines on MS2 were indeed reactive, and noticeably, both PEG-MS2 conjugate, as well as MS2 dimer are observable (Figure 5-6b, Lane 5). At this point, the difficulty associated with MS2 dimer formation with chemically incorporated anilines proved to be such an obstacle that we sought alternative methods of external MS2 modification.

5.3 A new oxidative coupling reaction for MS2 modification.

5.4 Optimization of MS2 soluble expression.

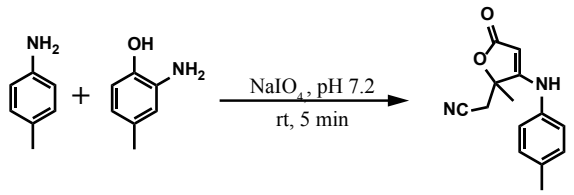

Figure 5-7. An accelerated oxidative coupling reaction between anilines and *ortho*-aminophenols with $NaIO_4$ as oxidant.

One such solution involved a new oxidative coupling reaction that had been recently developed and optimized by Chris Behrens in the group (Figure 5-7).[6] In this variant of the oxidative coupling, sodium periodate is still used as the oxidant with an aniline reactive group. However, instead of a substituted phenylene diamine reactive partner, a *para*-substituted *ortho*-aminophenol functionality is used. This reaction proceeds much faster than the phenylene diamine version of the oxidative coupling and has in fact been used by our group for radiochemistry applications with short-lived isotopes. Another potential benefit of this reaction is that native tyrosine residues can be chemically converted to *ortho*-aminophenols via tyrosine diazotization or nitration, followed by reduction to the aminophenol.

To exploit this, we therefore sought to substitute a tyrosine residue at position 19 and upon chemical elaboration, perform the new oxidative coupling. This pathway would be beneficial because this second mutation (after the N87C mutation for interior modification), being a native amino acid, would result in higher dual-mutant yields compared to the extremely low yields of the pAF19 N87C MS2 mutant due to artificial amino acid incorporation.

We therefore expressed several dual mutants of MS2, containing the T19Y mutation and several interior cysteine mutations. All of these dual mutants expressed well in *E. coli*, but showed no protein recovery upon purification. Searching for the protein revealed that it resided almost com-

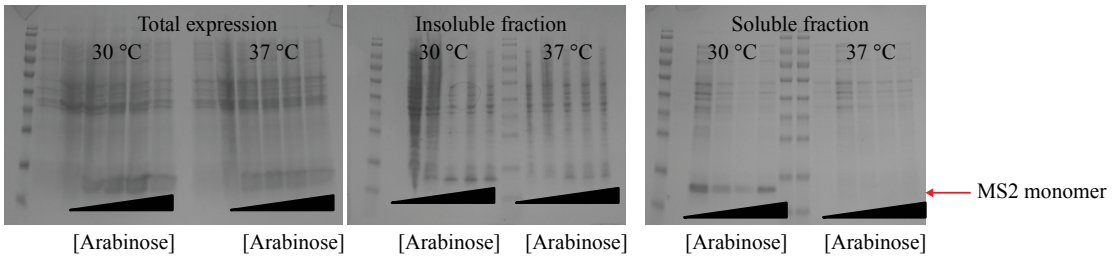

Figure 5-8. T19Y MS2 expression as analyzed by SDS-PAGE. MS2 only appears in the soluble fraction when protein expression is induced at 30 °C.

pletely in the insoluble fraction, which could be recovered by lysing the cells under denaturing conditions. However, upon buffer exchange back to phosphate buffer, the MS2 immediately precipitated. To combat the solubility problems, we carried out small scale expression screens with varying arabinose concentration and at 30 °C. Upon expression at 30 °C, an appreciable amount of MS2 dual mutant resided in the soluble fraction, compared to none at 37 °C. Little variation due to inducer concentration was found (Figure 5-8).

Due to this success in increasing the MS2 dual mutant yield, we began to consider whether the T19pAF N87C MS2 mutant would benefit from decreasing expression temperature as well, since this mutant differs from the T19Y tyrosine mutant by only a single atom. Much to our delight, expression of the *p*-aminophenylalanine containing dual mutant at 30 °C indeed resulted in much higher recovery of MS2 capsid. Further optimization also led us to utilize a PEG precipitation after the DEAE column first pass purification, instead of the ammonium sulfate precipitation in the original protocol.

With the T19pAF N87C MS2 dual mutant in hand, we decided to couple it with the new aminophenol based oxidative coupling due to the speed of the reaction. Prolonged exposure to sodium periodate has not seemed to affect most native proteins adversely except for possible cysteine oxidation. However, periodate could potentially interact with our cargo molecules if they were

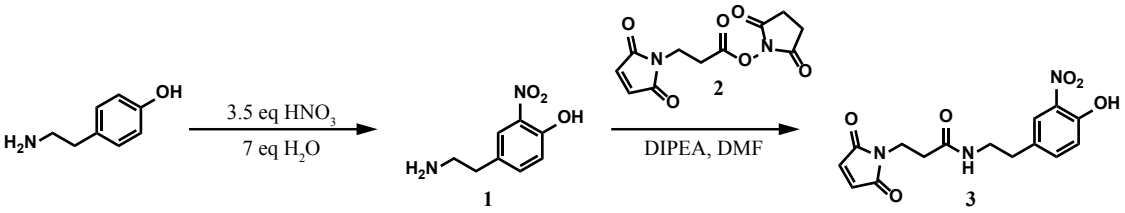

Figure 5-9. Synthesis of an *ortho*-aminophenol containing maleimide.

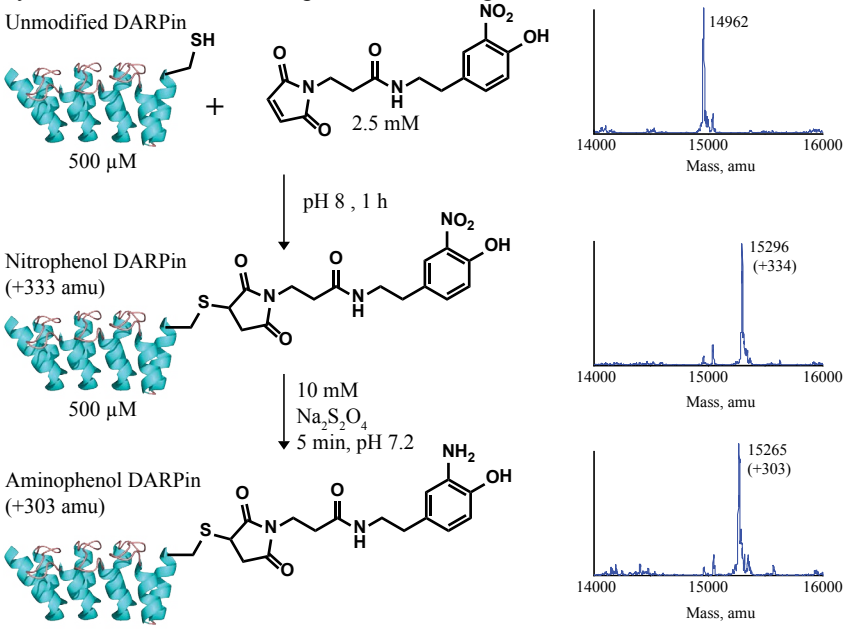

Figure 5-10. Modification of a αHER2 DARPin with **3** and subsequent dithionite reduction to the aminophenol as confirmed by LC-ESI-MS.

attached to the capsid first (to avoid cysteine oxidation). We therefore synthesized an aminophenol maleimide small molecule linker (Figure 5-9). The first step was the nitration of tyramine, which proceeded with excess nitric acid in water, immediately precipitating out nitrotyramine.[7] Nitrotyramine is slightly soluble in CH_2Cl_2 and can be reacted with **2** to afford maleimide/nitrophenol linker **3**. We decided to reduce the nitro group after cysteine modification in order to avoid possible polymerization of the aminophenol/maleimide. Cysteine modification of H2D followed by nitro reduction using sodium dithionite proceeded with high yield, resulting in an aminophenol functionalized DARPin (or APH2D, Figure 5-10), which could then be attached to MS2.

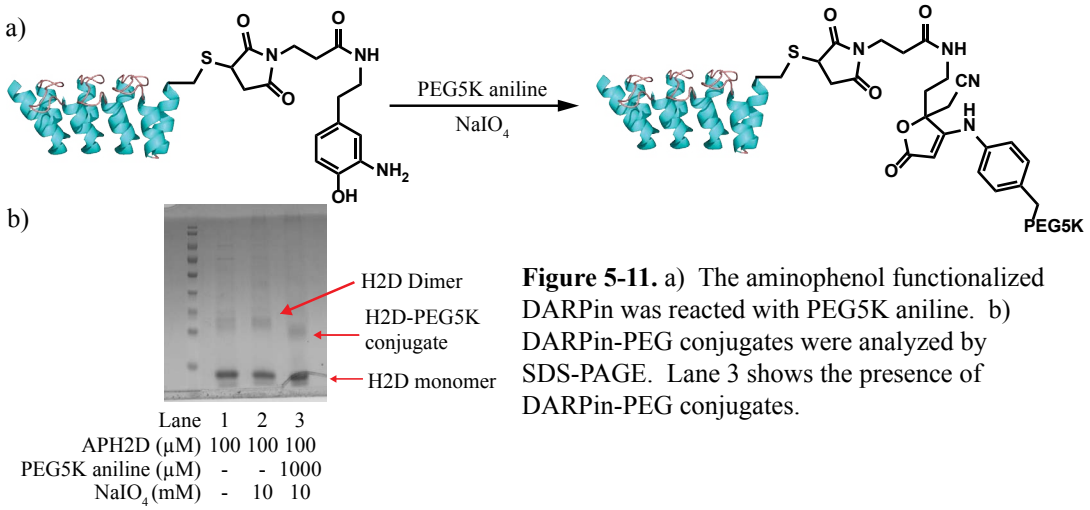

Figure 5-11. a) The aminophenol functionalized DARPin was reacted with PEG5K aniline. b) DARPin-PEG conjugates were analyzed by SDS-PAGE. Lane 3 shows the presence of DARPin-PEG conjugates.

First we tested the reactivity of the aminophenol functionalized DARPin. We reacted the APH2D with PEG5K aniline and looked for a gel shift by SDS-PAGE (Figure 5-11). Again, we observed small amounts of DARPin dimer and a lower shift corresponding to PEG addition to the DARPin, though at lower levels than expected (Lane 3). Still, we took on APH2D to react with Oregon Green functionalized pAF19 N87C MS2 (Figure 5-12). Gratifyingly, a prominent

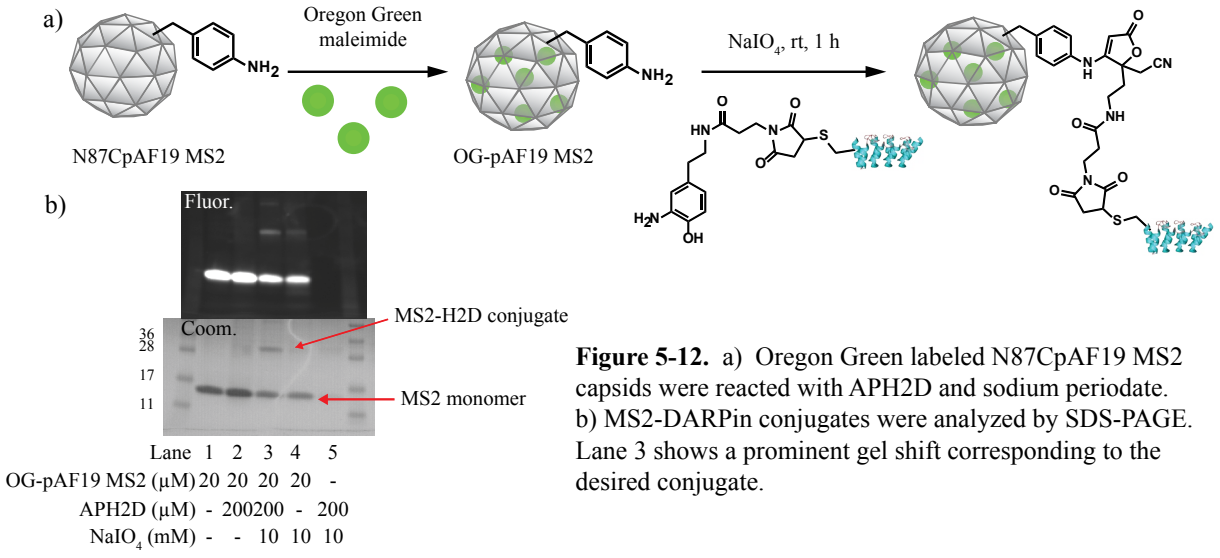

Figure 5-12. a) Oregon Green labeled N87CpAF19 MS2 capsids were reacted with APH2D and sodium periodate. b) MS2-DARPin conjugates were analyzed by SDS-PAGE. Lane 3 shows a prominent gel shift corresponding to the desired conjugate.

band appeared only in the lane containing both MS2 and APH2D as well as $NaIO_4$, indicating that this higher molecular weight band was most likely not MS2 dimer (Lane 3). Small amounts of MS2 dimer were observed in the fluorescence image of the gel, but not at comparable levels. However, with these dual-mutant capsids, the usual spin concentration purification procedure proved ineffective and resulted in large losses of protein. Further efforts at purification will be detailed below.

We continued to characterize the conjugates and to confirm that the top band was not simply the MS2 dimer. First, SEC analysis gave a shorter retention time for modified capsids, as expected due the increased diameter of the modified particles. To confirm, we synthesized the above maleimide/nitrophenol linker using a PEG based spacer, which was expected to give a larger gel shift then the short alkyl linker. Compound **4** was synthesized as in a similar fashion to the shorter alkyl linker and after purification by RP-HPLC, was used to modify H2D (Figure 5-13). The same dithionite reduction as with the alkyl linker could be used to access the reactive aminophenol. The oxidative coupling was carried out using standard conditions and followed by SDS-PAGE analysis, this time comparing the gel shift with the previous alkyl linker modified DARPin. While the PEG-DARPin conjugate appeared to contain residual linker, which also modified the MS2 capsid, we happily observed a larger gel shift compared to that occurring with the alkyl linker, as well as the small gel shift corresponding to addition of the small PEG molecule. (Figure 5-13b) We could further purify the PEG-APH2D molecule using 15 spin concentration cycles to reduce the amount of small PEG conjugation. This experiment showed that it was indeed AP-DARPin being attached to the MS2 capsids. However, unreacted PEG-DARPin proved to be even more difficult to remove from the capsids, so we did not pursue it further.

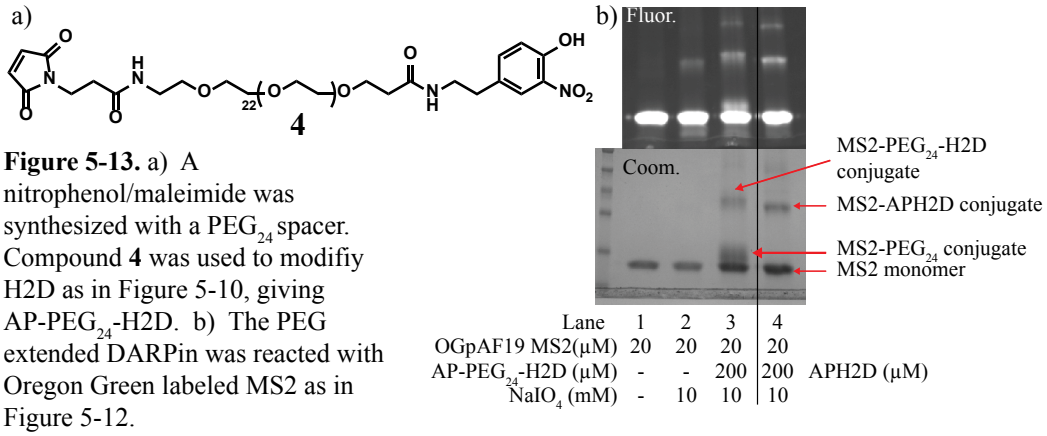

Figure 5-13. a) A nitrophenol/maleimide was synthesized with a PEG_{24} spacer. Compound **4** was used to modifiy H2D as in Figure 5-10, giving AP-PEG_{24}-H2D. b) The PEG extended DARPin was reacted with Oregon Green labeled MS2 as in Figure 5-12.

5.5 DARPin-MS2 optimization and purification.

Several purification strategies were pursued to separate unreacted DARPin from intact capsids and recover useful amounts of modified capsid. Variables tested included oxidation time, oxidant concentration, quencher, quencher concentration, order of oxidation, as well as spin concentration speed and conditioning. In general, we could assay for remaining MS2 by measuring Oregon Green absorbance and determine the capsid assembly state using SEC-HPLC. Through these experiments, it was found that fresh $NaIO_4$ and TCEP for quenching were vital to ensure capsid stability upon spin concentration. We also packed small S300 resin columns, both using gravity and centrifugation, that proved effective for first pass purification steps. In addition,

it was observed that the modified capsids remained intact even upon precipitation using 40% ammonium sulfate. Eventually, we were able to purchase a SEC-HPLC column, a Biosep 4K, that proved particularly effective in separating monomeric proteins from the assembled capsid. Several of these purification strategies were used interchangeably in the following experiments.

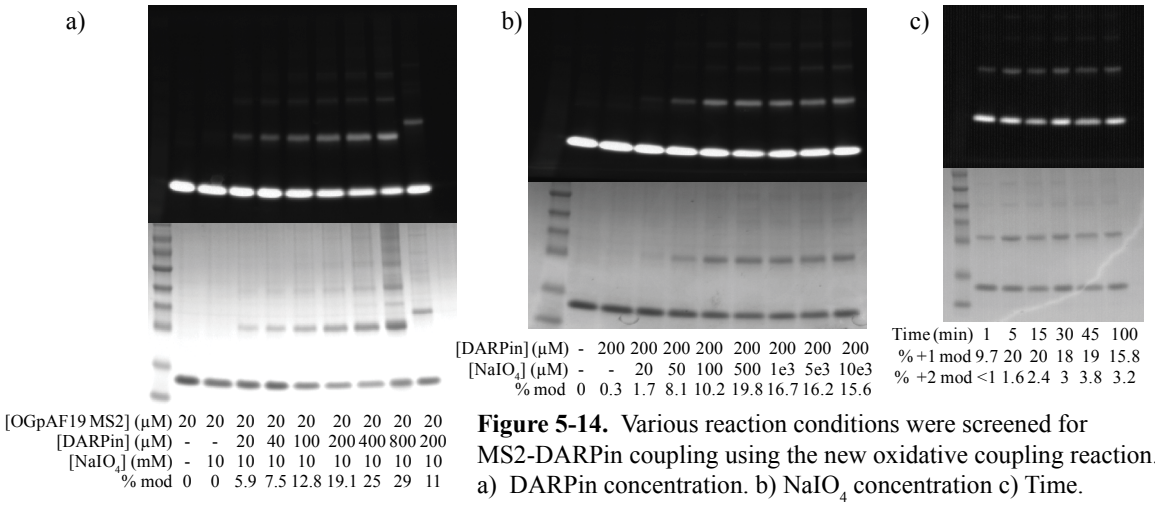

Figure 5-14. Various reaction conditions were screened for MS2-DARPin coupling using the new oxidative coupling reaction. a) DARPin concentration. b) $NaIO_4$ concentration c) Time.

With a purification strategy in hand, we also sought to optimize the reaction conditions for protein-protein coupling using the new oxidative coupling reaction (Figure 5-14). We first screened the concentration of APH2D and saw that modification increased with increasing APH2D concentration. However, purification again grew increasingly difficult with more equivalents of DARPin. The same gel has the last lane showing a reaction with an 18 kDa non-binding control DARPin that we had also expressed to demonstrate the difference in gel shift between the two DARPins when added to MS2. Next, we also tested the reaction time and observed that the reaction was complete in five minutes, and actually low levels of double modification occurred at longer reaction times. Lastly, we also screened oxidant concentration and saw that the modification level maximized with 500 μM $NaIO_4$.

5.6 MS2-DARPin cell binding experiments

With optimized reaction and purification conditions, we began to test the binding efficiency of DARPin-MS2 conjugates to HER2 positive cell lines. We chose to modify capsids to ~20-25% DARPin modification for initial cell experiments. Cells were incubated with varying concentrations of MS2 capsids containing fluorescent dyes on the interior and targeting DARPins on the exterior surface. In general, background binding was the lowest when incubated at 4 °C; however, even at 37 °C, DARPin-MS2 conjugates showed rather selective binding to HER2+ cell lines compared to negative cell lines, and also compared to non-binding control DARPins (Figure 5-15). Cells were exposed to the agents either while adhered to plate surfaces or while suspended in 1% FBS media. The highest selectivity in binding was observed on suspended cells. After exposure, the cells were washed with cold PBS and analyzed using flow cytometry. A time course experiment showed that when suspended SKBR3 cells were incubated at 4 °C, binding plateaued after 15 minutes (Figure 5-16). Fluorescence microscopy experiments showed uptake

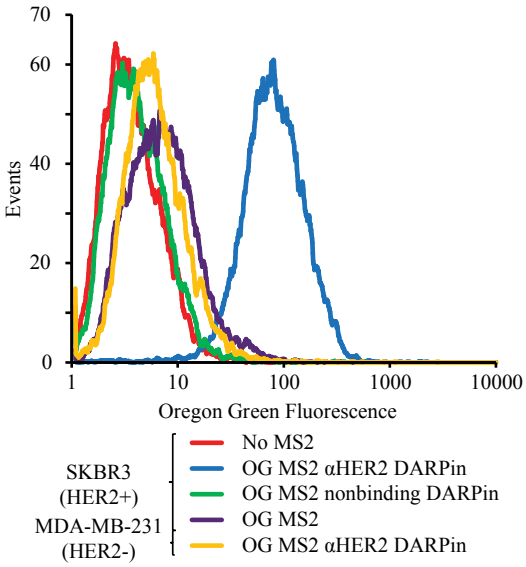

Figure 5-15. HER2 targeted fluorescent MS2 capsids were incubated at 4 °C with suspended HER2+ and HER2- cell lines and analyzed using flow cytometry. The targeted capsids only bound the HER2+ cell line.

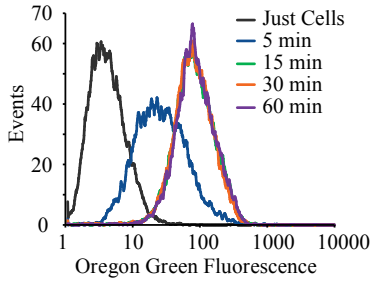

Figure 5-16. Time course analysis of OG-H2D-MS2 binding to SKBR3 (HER2+) cell lines using flow cytometry.

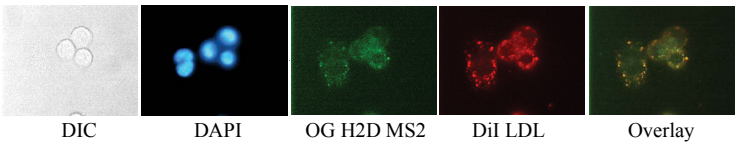

Figure 5-17. Fluorescence microscopy experiments on SKBR3 cells show uptake by the HER2+ SKBR3 cell line and colocalization with LDL.

of modified capsids and also apparent co-localization with DiI-LDL (Figure 5-17), although further experiments using confocal microscopy are needed to confirm this uptake pathway.

We next tested the binding of H2D-MS2 to a variety of cancer cell lines to test the generality of the targeting (Figure 5-18). In general, agent binding correlated well with the reported HER2 expression level of the cell line tested. In many cases, non-specific binding of MS2 alone was greater than the other controls. In all cases it was observed that binding of the individual DARPin alone gave much higher fluorescent signal compared to binding of the MS2-DARPin conjugates. Since the agents had been normalized to DARPin concentration (considering ~20% capsid modification), it had been expected that the MS2-DARPin conjugates would have given higher signal due to the presence of more dyes per DARPin in these systems.

5.7 Improving MS2-DARPin fluorescence signal.

Our next goal was both to increase the fluorescence signal of MS2 capsids and also explain the discrepancy between the dye brightness on monomeric DARPins and inside MS2 capsids. The first step was to simply use higher quality fluorescent dyes, such as the Alexa Fluor or Dylight series from Invitrogen and Thermo-Scientific, respectively. We eventually settled on Dylight 650 as our main dye due to lower cost, molecular weight, and brightness, although we also occasion-

a)

Cell Line	Jurkat	L3.6	MCF7 Cl 18	MDA-MB-453	SK-BR-3	MDA-MB-231	HCC1954	MCF7
Reported HER2 expression level	-	-	++	+++	+++	+	+++	+
Cells only	3.6	3	2.7	2.6	6	5.4	4.3	5.1
2 μM H2D-MS2	10.1	4	30.8	14.6	19.8	7.6	19.3	14.3
2 μM e35d-MS2	4.9	3.1	2.7	2.9	6.5	6	4.6	5.8
400 nM H2D	6	25.5	184.4	82.8	119.4	13.5	504.6	14.1
400 nM e35d	4.5	3.7	3.2	3	6.7	7.9	5.8	6.7
2 μM MS2	12.2	4.9	3.6	3.4	7.1	8.9	6.9	14.7

b)

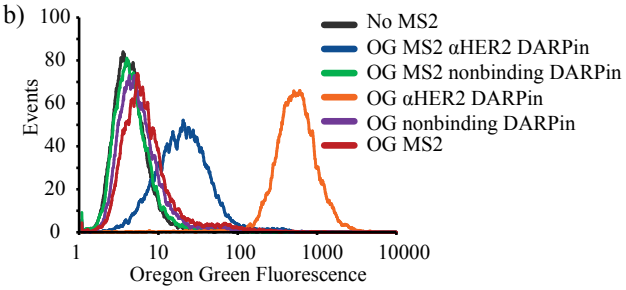

Figure 5-18. a) HER2-binding DARPin-MS2 was compared to various controls and DARPin alone in binding a variety of cell lines. b) Flow cytometry histograms are shown for binding to HER2+ HCC1954 cells. Agents are normalized for DARPin concentration.

ally used Alex Fluor 649. The use of these dyes dramatically increased the fluorescent signal from the labeled capsids.

Two other modifications we attempted addressed the possibility of worse binding of the DARPins due to attachment to the capsid. The first experiment was to shift the location of the unique cysteine used for bioconjugation. The initial location had been at the C-terminus; however, inspecting the structure showed that the C-terminus is at the side of the DARPin binding domain, and this could potentially lead to difficulty in accessing the binding site of the DARPin upon attachment to MS2. We therefore made three mutants of the DARPin: K68C, E64C, E61C. In all three the former cysteine was changed to a W residue so that the introduced sulfhydryl group could be selectively modified. These mutants all moved the cysteine to the back of the DARPin, so that upon bioconjugation to the MS2 capsid, the binding site would be more revealed. The second modification was to the linker. We decided to lengthen the linker using a PEG spacer, as detailed previously, in order to increase the space between the capsid and DARPin. This was in hopes of giving the DARPin more flexibility to reveal its binding site. Both of the above modifications were carried out, and the resulting DARPins were attached to MS2 successfully. However, there was no detectable improvement in binding (as determined by single sample flow cytometry experiments) with any of the above modifications to the system. We thus continued to use the original C-terminal cysteine version of the DARPin.

The use of Dylight 650 as the fluorescent tag did increase the signal range available, clearly revealing that the dyes on the interior surface of MS2 are indeed quenched. We were able to measure dye absorbance and fluorescence and noticed a dramatic difference in fluorescence per absorbance (a type of brightness calculation) between dye labeled DARPin and dye-labeled MS2, as shown in Figure 5-19. While we had always suspected that dyes inside MS2 would quench, due to the close proximity of adjacent N87C groups at the dimer interface (Figure 3-1b), we had never calculated the extent to which the dyes were quenched. To systematically investigate these effects, we created a complete set of dye-modified capsids containing varying levels of dye modification, from ~1 dye/capsid to >100 dyes/capsid. For each of these samples we measured protein absorbance, and dye absorbance and fluorescence. We then also calculated the same

		Dye-DARPin	MS2 (no $NaIO_4$)	H2D-MS2 (after $NaIO_4$)
1	A649	925	939	580
2	Flourescence (649/670)	36.3	3.81	3.14
3	Fl/A649*1000	39.24	4.06	5.41

Figure 5-19. Dye quenching was examined using absorbance and fluorescence measurements. The MS2 and DARPin were labeled with a Dylight 650 dye. Row 1 shows the absorbance at 649 nm and row 2 shows the fluorescence with a 649/670 excitation/emission. Row 3 is a calculated "brightness" value, showing the relative brightness of the dyes on the monomeric DARPin, compared to inside the MS2 capsids.

"brightness" value as in Figure 5-19 and plotted all of these values against the number of dyes/capsid. As shown in Figure 5-20a, the dye fluorescence (green trace) changed remarkably little upon the addition of more dyes per capsid. In fact, peak fluorescence occured at only ~15% dye modification, after which quenching dominated. In contrast, analysis of the dye-labeled monomer DARPins showed no such plateau, as expected (Figure 5-20b). This knowledge allowed us to use much less dye in modifying MS2 capsids in the future and to maximize dye brightness.

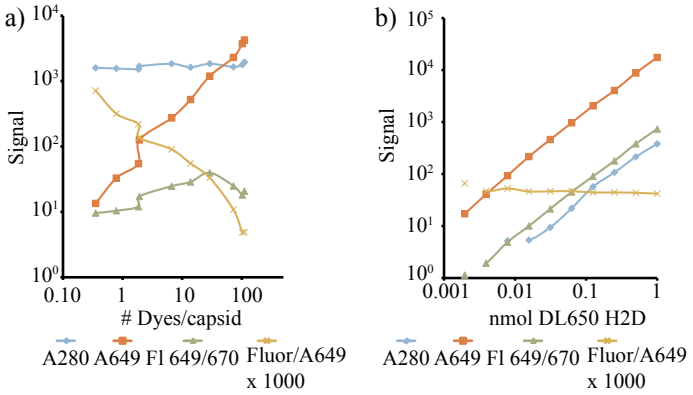

Figure 5-20. Measurement of DL650 absorbance and fluorescence for a) MS2 capsids with varying levels of dye modification and b) varying amounts of fully dye-modified DARPins. Protein absorbance at 280 nm is also measured and a calculated brightness value (yellow traces) is also shown.

5.8 Construction of binding curves for analysis of MS2-DARPin cell binding.

As we were attempting to determine improvements in binding from the DARPin mutants and PEG linker using flow cytometry, we discovered that it was extremely challenging to compare samples across experiments due to the variance in binding due to agent concentration, differing saturation points, the logarithmic nature of the binding behavior and data, and simple day to

day instrument calibration issues. We therefore decided to approach DARPin binding measurements by constructing binding curves, plotting flow cytometric mean fluorescence intensity versus agent concentration. This would allow us to measure the plateau level of agent binding, and also calculate K_d values for the binding. Using this technique, we could determine the K_d for each agent tested, as shown in Figure 5-21. While monomeric DARPin gave a K_d value of 35 nM, the targeted capsid gave a much lower K_d of 5.4 nM, demonstrating the power of attaching multiple targeting groups to the MS2 capsid.

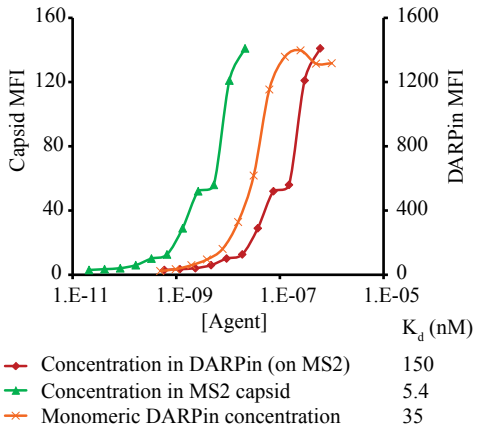

Figure 5-21. Binding curves and calculated K_d values for agent binding to HCC1954 cells. Curves and values for both MS2-DARPin conjugates and monomeric DARPins were determined. In addition, MS2-DARPin conjugate concentration was calculated using both DARPin concentration as well as capsid concentration.

In the next experiment, we tested a panel of MS2-DARPin conjugates that contained varying numbers of DARPins per MS2 capsid, from 9-45 copies. These capsids were produced by varying the equivalents of AP-H2D in the oxidative coupling reaction and quantification by SDS-PAGE densitometry measurements. The capsids had been fluorescently tagged previously and were incubated with HCC1954 cells. We were able to plot binding curves and calculate the binding constant first by normalizing to capsid concentration (Figure 5-22a). As expected, as the number of DARPins per capsid increased, the binding of the capsids to HER2+ cells improved, demonstrating the effects of having multiple targeting groups on a single capsid. Secondly, we were also able to plot binding curves by normalizing to DARPin concentration, given the varying number of DARPins/capsid. These curves showed that on a per DARPin basis, binding is actually worse for the DARPins attached to MS2 when compared to the binding curve of a monomeric DARPin (Figure 5-22b).

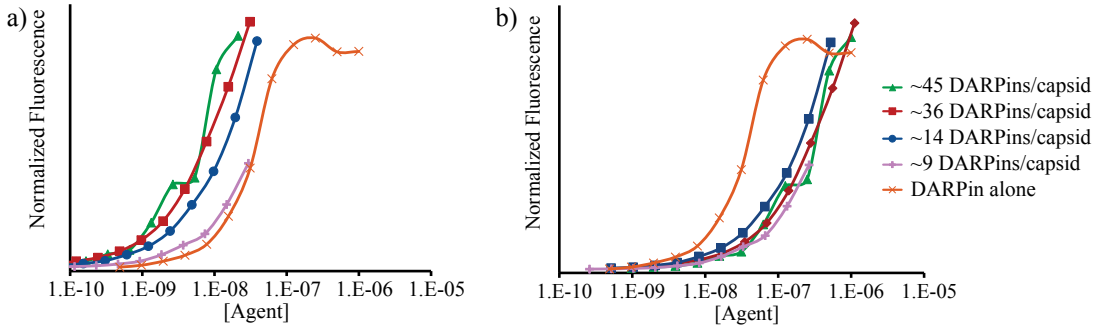

Figure 5-22. MS2 capsids with varying levels of HER2 DARPin modification were exposed to HER2+ HCC1954 cells at various concentrations and binding curves were constructed. a) Agent concentration was calculated using the concentration of intact MS2 capsids. b) Agent concentration was calculated using the concentration of DARPin.

5.9 Implications for future work.

These binding constants have important implications for potential drug delivery applications, such as constructing dual modified MS2 capsids with taxol on the interior and H2D on the exterior. Since there are up to 180 copies of the drug per capsid, the concentration of drug molecule at the K_d of H2D-MS2 capsids extremely high, possibly ~500 nM, which is markedly higher than the IC_{50} of taxol. In fact, while we were able to construct taxol-MS2-DARPin dual conjugates, when we exposed them to cells, even at low concentrations of capsid (but high taxol concentrations), we saw universal cytotoxicity, unable to differentiate between HER2+ and – cell lines. Furthermore, we saw no difference between targeted and non-binding DARPins. When we went below the K_d of the capsid to administer lower doses of drug, we once again saw no difference between + and – cell lines, since at these low concentrations, the DARPin-MS2 conjugates no longer targeted the desired cells. We have since performed preliminary experiments attaching doxorubicin to the capsids through an acid-sensitive hydrazone bond, in hopes of achieving a more specific release, but have not yet been able to achieve selective cell death.

In collaboration with Chris Behrens[8] and Michelle Farkas, we have also begun preliminary work in preparation for *in viv*o mouse experiments with these targeted capsids. We have exploited the modularity of the MS2-based system to easily attach near-IR dyes or PET imaging agents to the interior of the capsid for optical and nuclear imaging purposes, followed by the attachment of targeting DARPins to the exterior. With the known success of the DARPin class of binding proteins for *in vitro* selective binding, we can also envision constructing MS2-based systems using the oxidative coupling reaction and any of the other reported DARPins to bind alternative targets.

5.10 Materials and methods.

General Procedures and Materials

Unless otherwise noted, all chemicals were obtained from commercial sources and used without further purification. Analytical thin layer chromatography (TLC) was performed on EM Reagent 0.25 mm silica gel 60-F_{254} plates with visualization by ultraviolet (UV) irradiation at 254 nm and/or staining with potassium permanganate. Purifications by flash chromatography were performed using EM silica gel 60 (230-400 mesh). The eluting system for each purification was determined by TLC analysis. Chromatography solvents were used without distillation. All organic solvents were removed under reduced pressure using a rotary evaporator. Water (ddH_2O) used in biological procedures or as a reaction solvent was deionized using a NANOpure™ purification system (Barnstead, USA) purchased from Aldrich. All cell culture reagents were obtained from Gibco/Invitrogen Corp (Carlsbad, CA) unless otherwise noted.

Instrumentation and Sample Analysis Preparations

NMR. ^{1}H and ^{13}C spectra were measured with a Bruker AV-500 (500 MHz), or a Bruker DRX-500 (500 MHz) spectrometer, as noted. ^{1}H NMR chemical shifts are reported as δ in units of parts per million (ppm) relative to $CDCl_3$ (δ 7.26, singlet), or methanol-d_4 (δ 3.31, pentet). Multiplicities are reported as follows: s (singlet), d (doublet), t (triplet), or m (multiplet). Coupling constants are reported as a *J* value in Hertz (Hz). The number of protons (n) for a given

resonance is indicated as nH, and is based on spectral integration values. ^{13}C NMR chemical shifts are reported as δ in units of parts per million (ppm) relative to $CDCl_3$ (δ 77.2, triplet), or methanol-d_4 (δ 49.00, septet).

Mass Spectrometry. High resolution Electrospray (ESI) and Fast Atom Bombardment (FAB^+) mass spectra were obtained at the UC Berkeley Mass Spectrometry Facility. Electrospray LC/MS analysis was performed using an API 150EX system (Applied Biosystems, USA) equipped with a Turbospray source and an Agilent 1100 series LC pump. Protein chromatography was performed using either a Phenomenex Jupiter™ 300 5μ C5 300 Å reversed-phase column (2.0 mm x 150 mm), Phenomenex Jupiter™ 300 5μ C18 300 Å reversed-phase column (2.0 mm x 150 mm), or Dionex Proswift RP-4H reversed phase column (1mm x 50 mm) with a MeCN:ddH_2O gradient mobile phase containing 0.1% formic acid (250 μL/min). Protein mass reconstruction was performed on the charge ladder with Analyst software (version 1.3.1, Applied Biosystems). MALDI-TOF analysis was performed on a Voyager-DE instrument (Applied Biosystems), and all spectra were analyzed using Data Explorer software. The matrix solution was a 10 mg/mL solution of sinapic acid in in 50% acetonitrile, 50% water, 0.1 % TFA.

High Perfomance Liquid Chromatography. HPLC was performed on an Agilent 1100 Series HPLC System (Agilent Technologies, USA). Size exclusion chromatography was accomplished on an Agilent Zorbax® GF-250 with isocratic (0.5 mL/min) flow or a Phenomenex PolySep-GFC-P 5000 (PS5K) column (300 x 7.8 mm, flow rate 1.0 mL/min) or a Phenomenex BioSEP-4000 (BS4K) column (300 x 7.8 mm, flow rate, 1.0 mL/min) using an aqueous mobile phase (10 mM Na_2HPO_4, pH 7.2) . Reversed-phase liquid chromatography on protein samples was accomplished on a Agilent Poroshell 300 SB-C18 column (2.1 x 75 mm) using a MeCN:ddH_2O gradient mobile phase containing 0.1% trifluoroacetic acid. Semi-preparatory scale purification was performed using a Agilent Zorbax 300 SB-C18 column (9.4 mm x 25 cm). Sample analysis for all HPLC experiments was achieved with an inline diode array detector (DAD) and an inline fluorescence detector (FLD).

Gel Analyses. Sodium dodecyl sulfate-poly(acrylamide) gel electrophoresis (SDS-PAGE) was accomplished on a Mini-Protean apparatus from Bio-Rad (Hercules, CA) with 10-20% gradient polyacrylamide gels (Bio-Rad, CA), following the protocol of Laemmli.[9] All electrophoresis protein samples were mixed with SDS loading buffer in the presence of dithiothreitol (DTT) and heated to 100 °C for 10 min to ensure reduction of disulfide bonds and complete denaturation unless otherwise noted. Commercially available molecular mass markers (Bio-Rad) were applied to at least one lane of each gel for calculation of the apparent molecular masses. Gel imaging was performed on an EpiChem3 Darkroom system (UVP, USA).

Centrifugations were conducted with an Allegra 64R Tabletop Centrifuge (Beckman Coulter, Inc., USA). General desalting and removal of other small molecules of biological samples were achieved using NAP-5 gel filtration columns (GE Healthcare). Protein samples were concentrated by way of centrifugal ultrafiltration using Amicon Ultra-4 or Ultra-15 100 kDa molecular weight cut off (MWCO) centrifugal filter units (Millipore), or Amicon Microcon 10 kDa and 100 kDa MWCO (Millipore) centrifugal filter units.

N87C MS2 production.

N87C MS2 was produced as in Chapter 4.

N87C pAF19 MS2 production.

N87C T19pAF MS2 was produced as previously described with a few modifications.[10] Expression was carried out at 30 °C rather than 37 °C, as previously done. In addition, instead of an ammonium sulfate precipitation step after pooling of MS2-containing DEAE fractions, the protein was isolated via PEG precipitation as described for native MS2 isolation.

DARPin production (H2D and non-binding e35d). The genes for the HER2 DARPin and non-binding (e35d) DARPin were optimized and purchased from DNA 2.0 and received in a pJ-express *E.coli* expression plasmid under control of a T5 promoter with ampicillin resistance. The optimized sequences are shown below. BL21(DE3) cells were transformed with the purchased plasmid. All cells used for DARPin cloning were under ampicillin antibiotic control and grown in sterile LB with 100 mg/L ampicillin or LB-agar-amp plates. The successfully transformed colonies were used to grow 5 mL overnight starter cultures in sterile LB. One starter culture was added to 1 L sterile LB with 100 mg/L solid ampicillin and cultures were grown for 3-6 h and allowed to reach log phase growth (OD_{600}=0.7). Upon reaching log-phase growth, protein expression was induced using 0.6 mM IPTG. The protein was expressed for 3-18 h and then the cells centrifuged and pelleted. Cell pellets were centrifuged and frozen at -80 °C.

HER2 DARPin sequence.

ATG CGC GGC AGC CAC CAC CAT CAC CAT CAC GGC AGC GAC CTG GGT

Met Arg Gly Ser His His His His His His Gly Ser Asp Leu Gly

AAA AAG CTG CTG GAG GCA GCG CGT GCG GGT CAA GAT GAC GAA GTT

Lys Lys Leu Leu Glu Ala Ala Arg Ala Gly Gln Asp Asp Glu Val

CGT ATC CTG ATG GCG AAC GGT GCG GAT GTG AAT GCC AAA GAT GAG

Arg Ile Leu Met Ala Asn Gly Ala Asp Val Asn Ala Lys Asp Glu

TAT GGT CTG ACG CCG CTG TAC TTG GCG ACC GCG CAC GGT CAT CTG

Tyr Gly Leu Thr Pro Leu Tyr Leu Ala Thr Ala His Gly His Leu

GAA ATT GTC GAG GTT CTG TTG AAA AAT GGT GCT GAC GTC AAC GCC

Glu Ile Val Glu Val Leu Leu Lys Asn Gly Ala Asp Val Asn Ala

GTG GAC GCG ATT GGT TTC ACC CCG CTG CAC CTG GCA GCT TTT ATC

Val Asp Ala Ile Gly Phe Thr Pro Leu His Leu Ala Ala Phe Ile

GGT CAC CTG GAA ATC GCG GAA GTG CTG CTG AAG CAT GGC GCA GAT

Gly His Leu Glu Ile Ala Glu Val Leu Leu Lys His Gly Ala Asp

GTC AAT GCC CAG GAC AAG TTT GGC AAA ACT GCG TTC GAC ATC AGC

Val Asn Ala Gln Asp Lys Phe Gly Lys Thr Ala Phe Asp Ile Ser

ATT GGT AAC GGC AAC GAG GAT CTG GCA GAG ATT TTG CAG AAG CTG

Ile Gly Asn Gly Asn Glu Asp Leu Ala Glu Ile Leu Gln Lys Leu

GGC GGT GGC TCC GGT GGT TGC TGA

Gly Gly Gly Ser Gly Gly Cys End

E35D DARPin sequence.

ATG CGC GGC AGC CAC CAT CAC CAC CAT CAC GGC AGC GAC CTG GGT

Met Arg Gly Ser His His His His His His Gly Ser Asp Leu Gly

AAA AAG CTG CTG GAG GCA GCG CGT GCG GGT CAG GAT GAT GAA GTT

Lys Lys Leu Leu Glu Ala Ala Arg Ala Gly Gln Asp Asp Glu Val

CGT ATC CTG ATG GCT AAT GGC GCG GAT GTT AAC GCT ACG GAC AAC

Arg Ile Leu Met Ala Asn Gly Ala Asp Val Asn Ala Thr Asp Asn

GAC GGT TAC ACC CCG TTG CAC TTG GCG GCG AGC AAC GGT CAC CTG

Asp Gly Tyr Thr Pro Leu His Leu Ala Ala Ser Asn Gly His Leu

GAA ATC GTG GAA GTC CTG CTG AAG AAC GGT GCA GAC GTG AAC GCC

Glu Ile Val Glu Val Leu Leu Lys Asn Gly Ala Asp Val Asn Ala

TCC GAC CTG ACG GGC ATC ACC CCG CTG CAT CTG GCA GCG GCG ACC

Ser Asp Leu Thr Gly Ile Thr Pro Leu His Leu Ala Ala Ala Thr

GGC CAT CTG GAA ATT GTC GAG GTT CTG CTG AAA CAT GGT GCG GAC

Gly His Leu Glu Ile Val Glu Val Leu Leu Lys His Gly Ala Asp

GTG AAT GCG TAT GAC AAT GAT GGT CAC ACT CCG CTG CAC CTG GCA

Val Asn Ala Tyr Asp Asn Asp Gly His Thr Pro Leu His Leu Ala

GCC AAG TAC GGC CAC TTG GAG ATT GTT GAG GTG CTG CTG AAG CAT

Ala Lys Tyr Gly His Leu Glu Ile Val Glu Val Leu Leu Lys His

GGC GCC GAT GTC AAC GCC CAG GAC AAA TTC GGC AAA ACC GCA TTT

Gly Ala Asp Val Asn Ala Gln Asp Lys Phe Gly Lys Thr Ala Phe

GAC ATT AGC ATC GAT AAT GGT AAT GAG GAT TTG GCT GAG ATT CTG

Asp Ile Ser Ile Asp Asn Gly Asn Glu Asp Leu Ala Glu Ile Leu

CAA GGT GGT GGT TCT GGT GGT TGC TAG

Gln Gly Gly Gly Ser Gly Gly Cys End

DARPin purification. DARPin cell pellets were purified according to the procedure outlined in the following reference for purification under native conditions.[11] Buffer composition is described in the above reference. A cell pellet was thawed and suspended in 20 mL lysis buffer. Following sonication for 1 minute, the cells were centrifuged and the supernatant was isolated and to it was added 4 mL 50% Ni-NTA agarose (Qiagen). The slurry was allowed to spin on a rotary shaker for 1 h at 4 °C. The agarose with protein bound was washed with 3x 10 mL portions of wash buffer containing 20 mM imidazole. The purified protein was then eluted using 10 mL elution buffer containing 150 mM imidazole. The eluent was concentrated using 100 k MWCO spin concentrators and using NAP-25 gel filtration columns.

3-(2,5-dioxo-2,5-dihydro-1*H*-pyrrol-1-yl)-*N*-(4-hydroxy-3-nitrophenethyl)propanamide (3). To a solution of nitrotyramine (77 mg, 425 µmol) at 0.1 M in DMF was added **2** (1 eq.,146 mg), and DIPEA (2 eq., 148 µL) and the reaction stirred for 2 h. The solvent was removed under vacuum and the residue resuspended in ~300 µL CH_2Cl_2, washed with two portions of saturated sodium bisulfite solution and brine and the solvent removed under reduced pressure. The crude material was purified using flash chromatography (6:4 - 95:5 ethyl acetate:hexanes), yielding a pale yellow, flaky solid (59 %). ^{1}H NMR(500 MHz, $CDCl_3$): δ, 2.50 (t, 2H, J=7 Hz), 2.81 (t, 2H, J=7 Hz), 3.48 (t, 2H, J=7 Hz), 3.81 (t, 2H, J=7 Hz), 5.67 (s, 1H), 6.70 (s, 2H), 7.11 (d, 1H, J=9 Hz), 7.44 (d, 1H, J=9 Hz), 7.93 (s, 1H), 10.49 (s, 1H).

Typical MS2 modification with fluorescent dye maleimides. To a solution of N87C MS2 (100 nmol, 200 µL, 500 µM in 100 mM pH 7.2 phosphate buffer) was added Oregon Green maleimide (200 nmol, 10 µL, 20 mM in DMSO). The reaction mixture was incubated at rt for 1 h, followed by purification by size exclusion chromatography (NAP-5) and several spin concentration cycles until the flow-through was colorless. Longer reaction times and/or higher buffer pH led to detectable double modification. Dye-labeled MS2 monomers were characterized using LC-MS and the expected mass addition was observed.

Typical procedure for the modification of DARPin cysteine with 3. This procedure was

analogous to that with the affibody protein described in Chapter 4.

Typical procedure for the reduction of nitrophenol functionalized DARPin. To a solution of nitrophenol-functionalized DARPin (1 μmol, 500 μM) in 100 mM pH 7 phosphate buffer was added sodium dithionite (100 mM stock solution in water) to a final concentration of 10 mM. The reaction was allowed to proceed at room temperature for 5 min and then purified by gel filtration (NAP) column and subsequent spin concentration against 3 kDa MWCO spin concentrators.

Typical procedure for the modification of aniline-MS2 with phenylene-diamine functionalized targeting group. This procedure was analogous to that with the affibody described in Chapter 4.

Typical procedure for the modification of aniline-MS2 with aminophenol functionalized targeting group. An Eppendorf tube was charged with either pAF19 MS2 or N87C pAF19 MS2 (20 μM) (with the interior cysteine first modified with maleimide reagents), aminophenol-containing targeting group (0.02-1 mM), and $NaIO_4$ (2-10 mM). The reaction is carried out in 10 mM pH 7.0 phosphate buffer. The reaction was briefly vortexed and allowed to react at rt for 5 min - 1 h. After an hour, for a 50 μL reaction, the reaction was quenched by the addition of 5 μL of pH 7, 500 mM tris(2-carboxyethyl)phosphine hydrochloride (TCEP). For purification, the sample was first buffer exchanged by gel filtration (NAP) into the desired buffer. The excess targeting group was then removed by successive centrifugal filtration using 100 kDa molecular weight cutoff filters (Millipore).

Cell culture. Immortalized human breast cancer cells were maintained according to ATCC guidelines. MCF-7, MCF-7 Clone 18, SKBR3. MDA-MB-231, MDA-MB-453, Jurkat, L3.6, HCC1954 cells were from the Tissue Culture Facility, Department of Molecular & Cell Biology, UC Berkeley, and were grown in DMEM supplemented with 10% FBS.

Flow cytometry of cells exposed to fluorescent capsids. Flow cytometry analysis was acquired on a FACSCalibur flow cytometer (BD Biosciences, USA) using a standard 488 Ar laser. Data were collected for at least 10,000 live cells for all experiments. Cells ($1x10^6$ cells in 100 μL) were treated with fluorescent capsids in culture media or 1% FBS and incubated either on ice or at 37 ºC for 30-60 min in Eppendorf tubes or multi-well plates. After incubation, the cells were washed twice with 1% FBS, suspended in 500 μL 1% FBS, and then analyzed on the flow cytometer.

5.11 References.

1. a) Binz, H.K., Stumpp, M.T., Forrer, P., Amstutz, P., Pluckthun, A. Designing repeat proteins: Well-expressed, soluble and stable proteins from combinatorial libraries of consensus ankyrin repeat proteins. *J. Mol. Biol.* **2003**, *332*, 489-503. b) Binz, H.K., Amstutz, P., Kohl, A., Stumpp, M.T., Briand, C., Forrer, P., Grutter, M.G., Pluckthun, A. High-affinity binders selected from designed ankyrin repeat protein libraries. *Nat. Biotech*. **2004**, *22*, 575-582.

2. Stumpp, M.T., Binz, H.K., Amstutz, P. DARPins: A new generation of protein therapeutics. *Drug Discov. Today* **2008**, *13*, 695-701.

3. a) Zahnd, C., Pecorari, F., Straumann, N., Wyler, E., Pluckthun, A. Selection and characterization of HER2 binding-designed ankyrin repeat proteins. *J. Biol. Chem.* **2006**, *281*, 35167-35175. b) Zahnd, C., Wyler, E., Schwenk, J.M., Steiner, D., Lawrence, M.C., McKern, N.M., Pecorari, F., Ward, C.W., Joos, T.O., Pluckthun, A. A designed ankyrin repeat protein evolved to picomolar affinity to HER2. *J. Mol. Biol.* **2007**, *369*, 1015-1028.

4. Zahnd, C., Kawe, M., Stumpp, M.T., de Pasquale, C., Tamaskovic, R., Nagy-Davidescu, G., Schibli, R., Binz, H.K., Waibel, R., Pluckthun, A. Efficient tumor targeting with high-affinity designed ankyrin repeat proteins: Effects of affinity and molecular size. *Cancer Res.* **2010**. *70*, 1595-1605.

5. PEG5K was synthesized by Chris Behrens.

6. Behrens, C.R., Hooker, J.M., Obermeyer, A.C., Romanini, D.W., Katz, E.M., Francis, M.B. Rapid Chemoselective Bioconjugation Through the Oxidative Coupling of Anilines and Aminophenols. *J. Am. Chem. Soc.* **2011**, *133*,16398-401.

7. Waser, E., Sommer, H. Untersuchungen in der Phenylalanin-Reihe II. Synthese des 3,4-Dioxy-phenylathylamins. *Helv. Chim. Acta* **1923**, 54-61.

8. Behrens, C.R. Oxidative coupling of ortho-aminophenols and anilines for the application of labeling proteins with fluorine-18. Ph.D. dissertation, University of California, Berkeley, Berkeley, CA, 2012.

9. Laemmli, U. K. Cleavage of structural proteins during the assembly of the head of bacteriophage T4. *Nature* **1970**, *227*, 680.

10. Tong, G.J., Hsiao, S.C., Carrico, Z.M., Francis, M.B. Viral Capsid DNA Aptamer Conjugates as Multivalent Cell-Targeting Vehicles. *J. Am. Chem. Soc.* **2009**, *131*, 11174-11178.

11. Qiagen protocol. The QIAexpressionist: A handbook for high-level expression and purification of 6xHis-tagged proteins, 5th Ed. **2003**, Qiagen Inc.